THE ROLE OF NF-κB AND HISTONE DEACETYLASE IN GENE REGULATION

JOANNE CHRISTABELLE

CHEW SOO FEN

NATIONAL UNIVERSITY OF SINGAPORE

2008

THE ROLE OF NF-κB AND HISTONE DEACETYLASE IN GENE REGULATION

JOANNE CHRISTABELLE

CHEW SOO FEN

(BSc. (Hons.), THE UNIVERSITY OF MELBOURNE)

A THESIS SUBMITTED FOR

THE DEGREE OF DOCTOR OF PHILOSOPHY

INSTITUTE OF MOLECULAR AND CELL BIOLOGY

NATIONAL UNIVERSITY OF SINGAPORE

ACKNOWLEDGEMENTS

First of all, I would like to show my appreciation and gratitude to my PhD supervisor Assistant Professor Vinay Tergaonkar for his guidance, scientific discussions, and suggestions in the NF-κB and WIP1 project, which makes the completion of the later years of my PhD journey possible. I would also like to express my heartfelt thanks to my PhD supervisory committee members Dr. Li Bao Jie, Dr. Dimitry Bulavin and Dr. Stephen Ogg for their support and valuable suggestions during the yearly supervisory committee meetings. I would also like to thank Professor Alan Porter for the training I have received for the first few years of my PhD, for in his laboratory, I learnt the basic techniques of doing bench work while working on the histone deacetylase (HDAC) inhibitor project.

Sincere thanks to my collaborators from BD laboratory, Dr. Dmitry Bulavin, Dr. Sheeram Sathyavageeswaran, and Dr. Esther Wong for all the cell lines and reagents, and constructive suggestions that they have given me for the completion of the NF-κB and WIP1 project, and also not forgetting members of BD lab who have been very helpful. I would also like to express my thanks to Dr. Yu Qiang at the Genome Institute of Singapore (GIS) for the guidance and supervision I received in doing the microarray screening of the genes regulated by the HDAC inhibitor.

I would like to express my appreciation to members of VT laboratory and members of AGP laboratory for their companionship during my PhD years. I would also

like to thank especially Dr. Wong Siew Cheng, and Dr. Yu Xianwen who without cease, encouraged and supported me during these PhD years.

Finally, I would like to thank God, and my family who have stood by me, constantly supported, and encouraged me. Without them, this thesis would be difficult to complete.

TABLE OF CONTENTS

ACKNOWLEDGEMENTS……. i

TABLE OF CONTENTS……. iii

SUMMARY……... vii

LIST OF TABLES…… x

LIST OF FIGURES……... xi

LIST OF ABBREVIATIONS…….. xiii

CHAPTER 1 Introduction

1.1 Apoptosis in cancer.....1

1.2 Mechanism of apoptosis..... 2

1.3 Transcription factor NF-κB……...7

1.4 NF-κB in inflammatory diseases and cancer.....11

1.5 NF-κB signaling pathway

1.5.1 Signaling to NF-κB through the classical or “canonical” pathway.....12

1.5.2 Signaling to NF-κB through the alternative or “non-canonical” pathway……...20

1.5.3 Signaling to NF-κB through cell stress.....20

1.6 Regulation of NF-κB transcriptional activation by post-translation modification

1.6.1 Protein kinases as positive regulators.....21

1.6.2 Protein phosphatases as negative regulators.....26

1.7 Involvement of chromatin remodeling in transcriptional control of NF-κB target genes

1.7.1 Chromatin remodeling- histone acetylation and histone deacetylation..... 28

1.7.2 p38 MAPK marks histones of NF-κB target genes.....32

1.7.3 p65 acetylation by p300 and CBP co-activators.....34

1.8 Objectives of study..... 36

CHAPTER 2 Material and methods

2.1 Table 1: List of antibodies..... 37

2.2 List of primers..... 41

2.3 RNA/DNA methodology

2.3.1 RNA isolation..... 44

2.3.2 First strand cDNA synthesis..... 45

2.3.3 Mini-preparation of plamid DNA..... 46

2.3.4 Maxi-preparation of plasmid DNA..... 46

2.3.5 Sybr green real-time PCR..... 48

2.3.6 Quantitect sybr green real-time PCR..... 49

2.3.7 Agarose gel electrophoresis..... 50

2.3.8 DNA sequencing.....51

2.3.9 One-step RT-PCR..... 52

2.4 Protein methodology

2.4.1 Protein concentration determination by Bradford assay..... 53

2.4.2 Protein isolation from mouse tissue.....54

2.4.3 Western blotting.....54

2.4.4 Immunoprecipitation.....55

2.4.5 Transient transfection methods

2.4.5.1 Lipofectamine 2000 transfection for plasmid DNA..... 56

2.4.5.2 Lipofectamine 2000 transfection for siRNA oligonucleotides..... 57

2.4.6 Nuclear extraction..... 58

2.5 Mammalian cell culture and assays

2.5.1 Cell culture and drug treatments…….. 60

2.5.2 Apoptosis assay- Propidium Iodide (PI) staining..... 60

2.5.3 Cell proliferation assay- Wst-1..... 61

2.5.4 Sytox-hoechst cell staining..... 61

2.5.5 Luciferase reporter gene assay..... 61

2.5.6 *In vitro* phosphatase assay..... 62

2.6 Microarray hybridization and data analysis

2.6.1 Sample (probe) labeling by reverse transcription..... 63

2.6.2 Probe purification..... 65

2.6.3 Microarray hybridization

2.6.3.1 Pre-hybridization..... 66

2.6.3.2 Hybridization..... 66

2.6.4 Data analysis..... 67

CHAPTER 3 WIP1 phosphatase negatively regulates p65 transcriptional activity

3.1 Introduction..... 68

3.2 Mice lacking WIP1 show increased activation of NF-κB and phosphorylation of p65 on serine 536..... 72

3.3 Overexpression of WIP1 reduces p65 transcriptional activity..... 75

3.4 WIP1 regulates NF-κB activation and phosphorylation of p65 on serine 536……..... 79

3.5 NF-κB target genes are regulated in a p38 MAPK dependent and independent manner..... 87

3.6 PP2A phosphatase does not synergize with WIP1 in regulating NF-κB dependent transcription..... 96

3.7 WIP1 dephosphorylates p65 directly on serine 536..... 102

3.8 Discussion..... 105

3.9 Conclusion and future directions..... 111

3.10 Perspective..... 115

CHAPTER 4 Microarray studies and functional analysis of genes regulated by the HDAC inhibitor-Trichostatin A (TSA)

4.1 Introduction……...117

4.2 Concentration and time course studies of TSA treatment on HCT116, Jurkat and U937 human cancer cells…….. 120

4.3 Microarray analysis of genome wide effects in gene expression in response to TSA treatment……. 127

4.4 TSA inducible genes…… 129

4.5 TSA repressed genes…….134

4.6 Role of Clusterin in TSA induced apoptosis…….142

4.7 Discussion…….…… 151

4.8 Conclusion and future directions…….. 157

4.9 Perspective.……... 161

REFERENCES……..164

PUBLICATION LIST……...193

SUMMARY

Post-translational modifications of NF-κB via phosphorylations enhance the transactivation potential of NF-κB. Much is known about the kinases that phosphorylate NF-κB, but little is known about the phosphatases that dephosphorylate NF-κB. Here, we report the regulation of NF-κB by the WIP1 phosphatase and its role in inflammation. Overexpression of WIP1 in HeLa cervical cancer and Saos-2 osteoscarcoma cells results in decreased NF-κB activation in a manner dependent on the dosage of WIP1. Overexpression of WIP1 could also repress the expression of endogenous NF-κB target genes in response to inflammatory stimuli. Conversely, knockdown of WIP1 results in increased NF-κB transcriptional function.

To investigate the molecular mechanism by which WIP1 regulates NF-κB function, we investigated whether WIP1 can dephosphorylate any component of the NF-κB signaling cascade. Using *in vitro* and *in vivo* experiments, we demonstrate that WIP1 is a direct phosphatase on serine 536 of the p65 subunit of NF-κB. The phoshorylation of p65 on serine 536, is known to be critical for the transactivation function of p65 since the phosphorylation of p65 is required for the recruitment of transcriptional co-activator p300 to aid in full transcriptional activity of p65.

Since WIP1 can dephosphorylate p38 mitogen-activated protein kinase (MAPK), and p38 MAPK is known to regulate p65 through direct/indirect phosphorylation, we investigated the possibility of WIP1 affecting NF-κB through p38 MAPK. The addition of a specific p38 MAPK inhibitor (SB202190) did not decrease the

phosphorylation status of p65 on serine 536, nor did it affect the expression of a subset of NF-κB target genes in HeLa WIP1siRNA cells. We thus propose that WIP1 is part of the NF-κB signaling pathway, and has a role in negatively regulating a subset of NF-κB target genes in a p38 MAPK independent manner.

Post-translational modification of the histones surrounding NF-κB target genes has a key role in modulating cancer and inflammation. Chromatin remodeling must happen for the accessibility of transcription factors and the replication machinery to gene promoters of the cell. Inappropriate expression of genes due to altered chromatin structure has been implicated in tumourigenesis. Inhibiting the activity of histone deacetylases (HDACs) using HDAC inhibitors, can induce histone hyperacetylation, reactivate transcriptionally silenced genes, resulting in cell cycle arrest and apoptosis. The growth and survival of tumour cells are inhibited, while leaving untransformed cells relatively intact.

Through microarray analysis, we identified several mRNA of NF-κB associated genes in inflammation, for example, lymphotoxin β receptor (LTβR), interleukin-2 receptor (IL-2R), NF-κB1, and adaptor protein interleukin-1 receptor-associated kinase 1 (IRAK1), to be down-regulated when human cancer cells are treated with HDAC inhibitor, trichostatin A (TSA). We also identified genes involved in apoptosis, of particular interest, clusterin, which has a proapoptotic role via relief of histone deacetylase inhibition. Therefore, we propose HDAC inhibitors are good therapeutics for treatment of cancer, and malignancies associated with inflammation because they can

regulate NF-κB associated genes in inflammation through chromatin remodeling. By reducing cytokine expression, HDAC inhibitor can inhibit tumour growth.

LIST OF TABLES

Table 1 List of antibodies.....37

Table 2 Function of clusterin in different cell types……. 156

LIST OF FIGURES

Figure 1.1 The extrinsic and intrinsic pathways of caspase activation and apoptosis..... 5

Figure 1.2 The family of mammalian NF-κB/REL proteins.....10

Figure 1.3 The family of mammalian IκB proteins.....18

Figure 1.4 Activation of the NF-κB pathway.....19

Figure 1.5 Multiple kinases phosphorylate p65 at various sites induced by distinct stimuli.....25

Figure 1.6 Chromatin remodeling regulates transcriptional activity.....31

Figure 3.1 WIP1 in cell cycle regulation and apoptosis.....71

Figure 3.2 Mice lacking WIP1 show increased activation of NF-κB and phosphorylation of p65 on serine 536.....73

Figure 3.3 Overexpression of WIP1 reduces p65 transcriptional activity.....77

Figure 3.4.1 WIP1 regulates NF-κB activation and phosphorylation of p65 on serine 536.....81

Figure 3.4.2 Knock down of WIP1 increases activation and phosphorylation on serine 536 of p65.....84

Figure 3.5.1 NF-κB target genes are regulated in a p38 MAPK dependent and p38 MAPK independent manner.....89

Figure 3.5.2 NF-κB target gene independent of p38 MAPK regulation.....93

Figure 3.6 PP2A does not synergize with WIP1 to regulate NF-κB dependent transcription.....98

Figure 3.7 WIP1 dephosphorylates p65 directly on serine 536.....103

Figure 3.8 Model of WIP1 phosphatase modulating the NF-κB signaling pathway.....110

Figure 3.9 Phosphorylation sites on p65.....114

Figure 4.2.1 Concentration studies of TSA treatment on HCT116, Jurkat and U937 cells……..121

Figure 4.2.2 Sytox-hoechst staining of HCT116, Jurkat and U937 cells treated with 1 μM TSA for 24 hours……....123

Figure 4.2.3 Time course studies of TSA treatment on HCT116, Jurkat and U937 cells……125

Figure 4.3 Microarray analysis of genome wide effects in gene expression in response to TSA treatment……...…….....128

Figure 4.4 TSA inducible genes……130

Figure 4.5.1 TSA repressed genes……135

Figure 4.5.2 TSA repressed genes that are in the NF-κB signaling pathway……...139

Figure 4.6.1 Secretory clusterin has a proapoptotic role in TSA induced apoptosis...145

Figure 4.6.2 Increased clusterin expression is dependent on HDAC regulation…….148

LIST OF ABBREVIATIONS

aa	Amino acid
AKT1	V-AKT murine thyoma viral oncogene homolog 1
ATP	Adenosine triphosphate
BAFF	B-cell activating factor
BSA	Bovine serum albumin
cDNA	Complementary DNA
CHOP	C/EBP-homologous protein
CKII	Casein kinase II
CSF	Colony-stimulating factor
CTP	Cytosine triphosphate
DEPC	Diethyl pyrocarbonate
DMSO	Dimethyl sulfoxide
DNA	Deoxyribonucleic acid
DTT	Dithiothreitol
dNTP	Deoxyribonucleotide triphosphate
dUTP	Deoxyuridine triphosphate
DMEM	Dulbecco's modified eagle's medium
DMBA/TPA	7, 12-dimethylbenz (a) anthracene/12-O-tetradecaroylphorbol-13-acetate
ECL	Enhanced chemiluminescence
EDTA	Ethylenediamine tetraacetic acid
EGTA	Ethyleneglycol tetraacetic acid
FADD	Fas-associated via death domain
FCS	Fetal calf serum

Gly	Glycine
GTP	Guanine triphosphate
HEPES	Hydroxyethylpiperazine ethanesulfonic acid
h	Hour
hr	Hour
IL-1	Interleukin-1
IKK	IkappaB kinase
IP	Immunoprecipitation
KCl	Potassium chloride
L	Liter
LB	Liquid broth
M	Molar
Mg	Milligram
$MgCl_2$	Magnesium chloride
Min	Minute
ml	Milliliter
mM	Millimolar
µM	Micromolar
µg	Microgram
µl	Microliter
NaCl	Sodium chloride
NaF	Sodium flouride
NaOH	Sodium hydroxide
NaV	Sodium vanadate
ND	Not detected

NES	Nuclear export sequence
ng	Nanogram
NLS	Nuclear localization sequence
NP40	Nonidet P-40
PAGE	Polyacrylamide gel electrophoresis
PBST	Phosphate buffered saline with Tween 20
PCR	Polymerase chain reaction
PI	Propidium iodide
ρmol	Picomole
PNAd	Peripheral lymph node addressin
PVDF	Polyvinylidene fluoride
Rbx1	Ring-box 1
RNA	Ribonucleic acid
RNAi	RNA interference
RPMI	Roswell park memorial institute medium
RT-PCR	Reverse transcription polymerase chain reaction
Rpm	Revolutions per minute
S.D.	Standard deviation
SDS	Sodium dodecyl sulfate
Sec	Second
siRNA	Small interfering RNA
Skp1	S-phase kinase-associated protein 1
SSC	Saline-sodium citrate
TBST	Tris buffered saline with Tween 20
Thr	Threonine

TNF	Tumour necrosis factor
Trail	TNF-related apoptosis-inducing ligand
Tris	Tris (hydroxymethyl) aminomethane
Tris-HCl	Tris (hydroxymethyl) aminomethane-Hydrogen chloride
TTP	Thymine triphosphate
Tyr	Tyrosine
U/µl	Units per microliter
UV	Ultra violet
VEGF	Vascular endothelial growth factor
V/V	Volume per volume
WT	Wild type
W/V	Weight per volume

Chapter 1
Introduction

1.1 Apoptosis in cancer

Intensive research effort has been focused on understanding cancer biology and cancer genetics that drive the progressive transformation of normal human cells into highly malignant cancer cells. The tumourigenic process of a normal cell to a cancer cell has been described into three phases: 1) tumour initiation, 2) tumour promotion, 3) tumour invasion and metastasis (Karin and Greten, 2005). In the first phase of tumourigenesis, the DNA of a normal cell becomes mutated by physical and chemical carcinogens, leading to the activation of oncogenes or the inactivation of the tumour suppressor genes, where the normal cell eventually develop into a cancerous cell. In the second phase of tumour promotion, inflammatory cytokines such as interleukin-1 (IL-1) and tumour necrosis factor (TNF) has been observed to promote the proliferation and clonal expansion of initiated cancerous cells. In the final phase of tumourigenesis, the tumour increase in size (or growth), and acquire more mutations, leading to a more malignant phenotype.

The ability of cancer cells to expand in numbers is not only determined by the rate of proliferation, but dependent on the rate of elimination of cancerous cells by apoptosis. Apoptosis or "physiological cell death" was described by its morphological characteristics, such as cell shrinkage, membrane blebbing, chromatin condensation and nuclear fragmentation which are engulfed by phagocytic cells (Wyllie *et al*., 1980). A variety of signals that can trigger apoptosis in cells include growth/survival factor depletion, hypoxia, UV radiation, and DNA damage (cell-cycle checkpoint defects) and chemotherapeutic drugs (Lowe and Lin, 2000).

Like metabolism or development, the inherent apoptotic program can be disrupted by genetic mutations in cancer-related genes that disrupt or promote apoptosis. These genes were classified as oncogenes with dominant gain of function or tumour suppressor genes with recessive loss of function in tumour development. One example of such loss of function of a tumour suppressor gene is p53, which is often found to be mutated or deleted in cancer. The antiproliferative effect of p53 in response to cellular stresses is exhibited in cell cycle progression. p53 prevents a damaged cell from dividing before completion of DNA repair, and prevent the cell from becoming cancerous (Lane, 2005). The importance of p53 proapoptotic function is demonstrated in mouse thymocytes where the presence of p53 in these thymocytes induced cell death in response to radiation (Lowe *et al*., 1993). On the other end of the spectrum, the gain of function of the oncogene Bcl2 promote cancer. Its antiapoptotic effect was shown in transgenic mice, whereby the overexpression of Bcl2 promoted extended B cell survival and lymphoproliferation (McDonnell *et al*., 1989). Given the above examples of how oncogenic or tumour suppressor genes can disrupt the process of apoptosis, the loss of apoptotic program in cells can promote tumour progression, invasion and metastasis.

1.2 Mechanism of apoptosis

Despite the cellular diversity of our body, all cells appear to activate the basic apoptotic program upon external trigger. Two major pathways have been indentified, namely the “extrinsic” and the “intrinsic” pathways (Figure 1.1). The extrinsic pathway is triggered through the ligation of specific cell-death surface receptors (TNF, TRAIL and FasL), whereas the intrinsic pathway is dependent on mitochondrial membrane permeabilization which releases apoptogenic factors into the intermembrane space of the

cytoplasm. The eventual consequences of both pathways are similar as they both converge on the activation of key effectors of apoptosis-the caspases. Once activated, caspases cleave cellular substrates (Luthi and Martin, 2007), including lamins, kinases, and proteins involved in DNA replication, cell survival and mRNA splicing, resulting in morphological cell death known as apoptosis. Generally, it is believed that the "extrinsic" pathway is activated by immune-mediated signals, while the "intrinsic" pathway is engaged by cellular stresses.

Regulators of apoptosis exist in the mammalian cells to switch cells to the "death mode" or to remain alive in the event of cancer. The B-cell CLL/lymphoma 2 (Bcl2) family constitutes a major family of cell death regulators which have either proapoptotic or antiapoptotic effects. The proapoptotic members of Bcl2 family such as Bcl2-associated X protein (Bax), Bcl2 antagonist killer 1 (Bak), and BH3-interacting domain death agonist (Bid) promote cytochrome-c release from the mitochondria while the overexpression of the antiapoptotic molecule Bcl2 block cytochrome-c release (Yang *et al*., 1997). The release of cytochrome c from the mitochondria is necessary in the formation of the apoptotic protease activating factor 1(Apaf-1)/cytochrome-c complex (Li *et al*., 1997), which mediates the activation of initiator caspase-9. Activated caspase-9 cleaves procaspase-3 to activated caspase-3 which is responsible for the cleavage of DNA, and the morphological changes observed in cells undergoing apoptosis. It was proposed that the Bcl2 family of proteins can in turn regulate each other by binding to one another. The antiapoptotic proteins Bcl2, Bcl2-related protein, long isoform, included (Bcl-XL), Bcl2-like2 (BcL-W), myeloid cell leukemia 1 (Mcl-1) and Bcl2-related protein A1 (A1) act on the outer mitochondrial membrane by neutralizing the killer proteins Bax

and Bak, and following death triggers, Bax and Bak are liberated from Bcl-2 mediated inhibition by BH3-only proteins like Bcl2-interacting protein Bim (Bim), Bid, Bcl2 antagonist of cell death (Bad), Puma, Noxa, Bcl2-modifying factor (Bmf), harakiri (Hrk), and Bcl2-interacting killer (Bik) (Willis *et al*., 2007; Letai *et al.,* 2002). The details of how this Bcl-2 family of proteins function and how their dynamics influence cell fate is unclear, and an area of intense debate.

Activation of apoptosis does not always lead to cell death. Inhibitor of Apoptosis (IAP) is another group of regulatory proteins that are able to bind to and inhibit caspases. The mammalian IAP, inhibitor of apoptosis, X-linked (XIAP) is a potent physiological inhibitor of caspase-3, caspase-7 and capase-9, and its capability to bind to caspase-3 and 7 lies in the baculoviral IAP repeat 2 (BIR2) domain, while its BIR3 domain binds to caspase-9, which occludes substrate entry on the caspases and hence the inhibition of the caspase's catalytic activity (Silke *et al*., 2002). Cells that are fated to die overcome the IAP-mediated inhibition through a specialized group of IAP antagonists, Second mitochondria-derived activator of caspase (Smac) or Direct IAP-binding protein with low pI (DIABLO), that are released into the cytosol, alongside with apoptogenic factors like cytochrome-c upon death stimuli. When Smac/DIABLO is released into the cytosol, promotes apoptosis by binding to XIAP, and remove the inhibitory effect of XIAP on caspase-3 and caspase-9, thus liberating caspases to execute apoptosis (Verhagen *et al*., 2000). Smac/DIABLO can therefore circumvent the effect of IAPs and are good therapeutic targets in cancer.

Figure 1.1

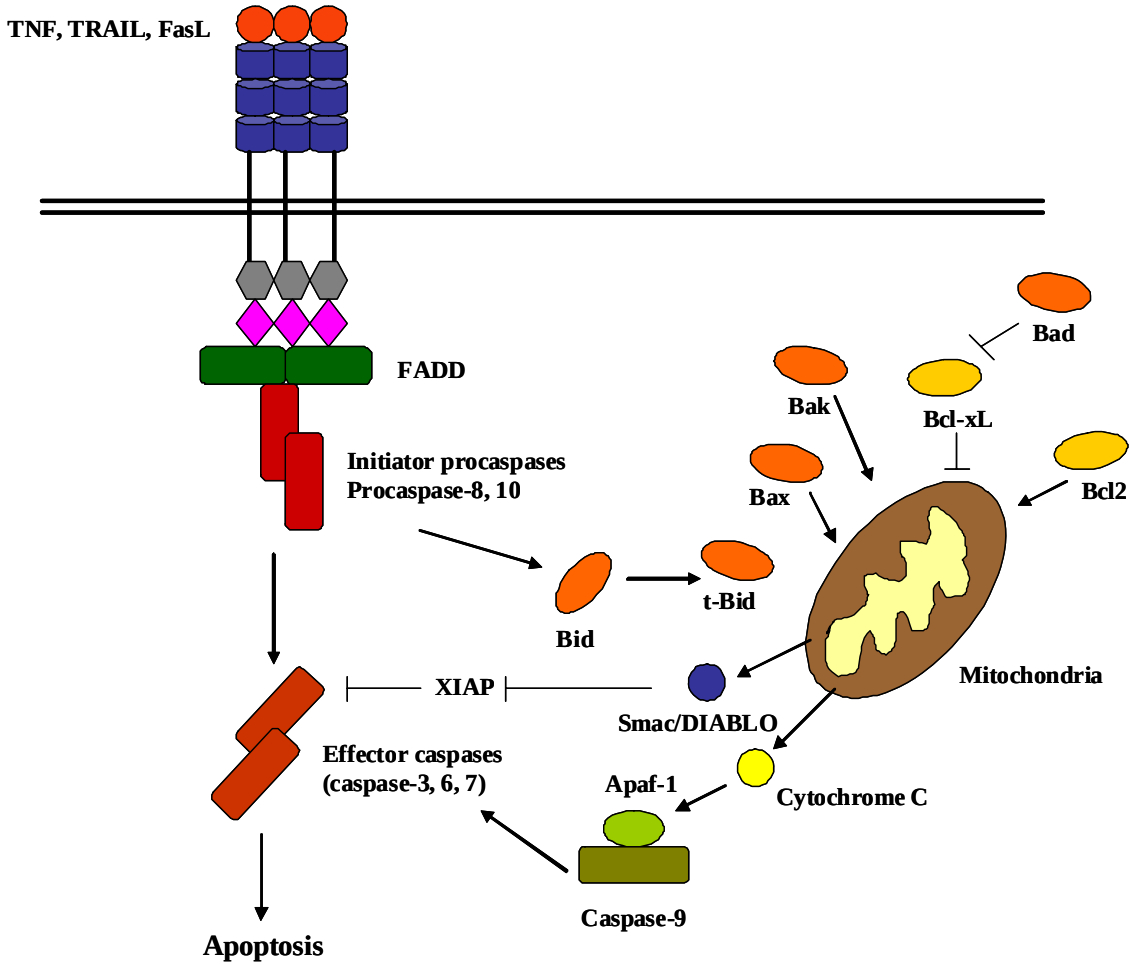
TNF, TRAIL, FasL
FADD
Initiator procaspases
Procaspase-8, 10
Bid
t-Bid
Bad
Bak
Bcl-xL
Bax
Bcl2
Mitochondria
XIAP
Smac/DIABLO
Effector caspases
(caspase-3, 6, 7)
Apaf-1
Cytochrome C
Caspase-9
Apoptosis

Figure 1.1: The extrinsic and intrinsic pathways of caspase activation and apoptosis

The extrinsic pathway involves oligomerization of death receptors by their ligands, resulting in the recruitment and activation of initiator caspases which directly execute apoptosis by cleaving Bid which then translocate to the mitochondria to initiate the intrinsic pathway, or the cleavage and activation of caspase-3. The intrinsic pathway is activated by the proapoptotic Bcl2 family of proteins which triggers mitochondrial release of apoptogenic factors like cytochrome-c into the cytosol, necessary in the formation of the Apaf-1/cytochrome-c complex which mediates the activation of caspase-9.

1.3 Transcription factor NF-κB

Transcription factors influence cells' decision to undergo apoptosis by activating the transcription of genes involved in apoptosis. Nuclear factor kappa B (NF-κB) is one such transcription factor believed to have an antiapoptotic effect in cancer cells, while tumor suppressor p53 is another transcription factor which has a proapoptotic effect. The transcriptional targets of p53 include the Bcl2 family of proapoptotic proteins such as p53-upregulated modulator of apoptosis (PUMA) and NOXA (for "damage"), which function by inducing the loss of inner mitochondrial membrane potential, leading to the release of cytochrome-c and apoptogenic factors and the activation of the caspase cascade that results in apoptotic cell death (Villunger *et al*., 2003). NF-κB acts in opposition to p53, and has a proliferative effect in cells by activating the expression of antiapoptotic genes like Bcl-XL, cIAP1, cIAP2 and XIAP (Pahl, 1999). NF-κB and p53 play pivotal role in deciding cell fate because NF-κB mediated upregulation of antiapoptotic gene targets can antagonize the proapoptotic function of p53 (Tergaonkar and Perkins, 2007).

NF-κB is discovered by Sen and Baltimore to be a protein that binds to specific DNA sequences (5'-GGGACTTTCC-3') also known as κB sites, of the immunoglobulin kappa light chain gene in mature B and plasma cells (Sen and Baltimore, 1986). NF-κB was shown to exist and expressed in many cell types. In the majority of cell types, NF-κB exists in the cytoplasm as a complex with inhibitor of kappa light chain gene enhancer in B cells (IκB) in quiescent cells. Mammalian cells express 5 members of the NF-κB members of protein (Figure 1.2), RELA, RELB, c-REL, p105 and p100 (Hayden and Ghosh, 2008). The REL members can form hetero and homodimers among themselves except RELB, and by far the p65/p50 heterodimers is the most stable heterodimer seen in

all cell types. The REL members all contain a REL homology domain (RHD), in it which lies the DNA binding, dimerization and IκB binding domain. Of the five members, only RELA, RELB and c-REL has a transcription activation domain (TAD) necessary for gene expression. Both the RHD and TAD domain undergo post-translational modification that affect NF-κB transcription.

The p100 and p105 function as inhibitors of NF-κB as they interact with other REL members, and they reside exclusively in the cytoplasm, and prevent NF-κB into the nucleus to activate transcription. p100 and p105 are processed through distinct mechanism to p52 and p50 respectively (Lin *et al*., 1998; Xiao *et al*., 2001). p50 and p52 form hetero or homodimers, bind to κB consensus sites on DNA, and hence may act as transcriptional co-repressors, unless they form heterodimers with any of the TAD-containing NF-κB family members. Therefore, whether the REL family of transcription factors functions as co-activator or co-repressor depend on its subcellular localization, and if they contain a TAD domain.

Gene knockout mouse models for all the five members of NF-κB family of protein have been generated by homologous recombination in mice. These knockout mouse models reveal the different roles of each NF-κB proteins in regulating immune response in mammals (Li and Verma, 2002). p65 knockout mice have massive TNF-dependent liver apoptosis, and are embryonic lethal at E15.5-E16.5, indicating an important role of p65 in development. Mice lacking NF-κB1, NF-κB2 and c-REL have defects in lymphocyte activation, while RELB knockout mice die postnatally from multi-organ inflammation. In addition, RELB is required for dendritic-cell development. Mice

lacking one of the five NF-κB members do not inherit development defects, but all circum to deficiency in the immune system.

Figure 1.2

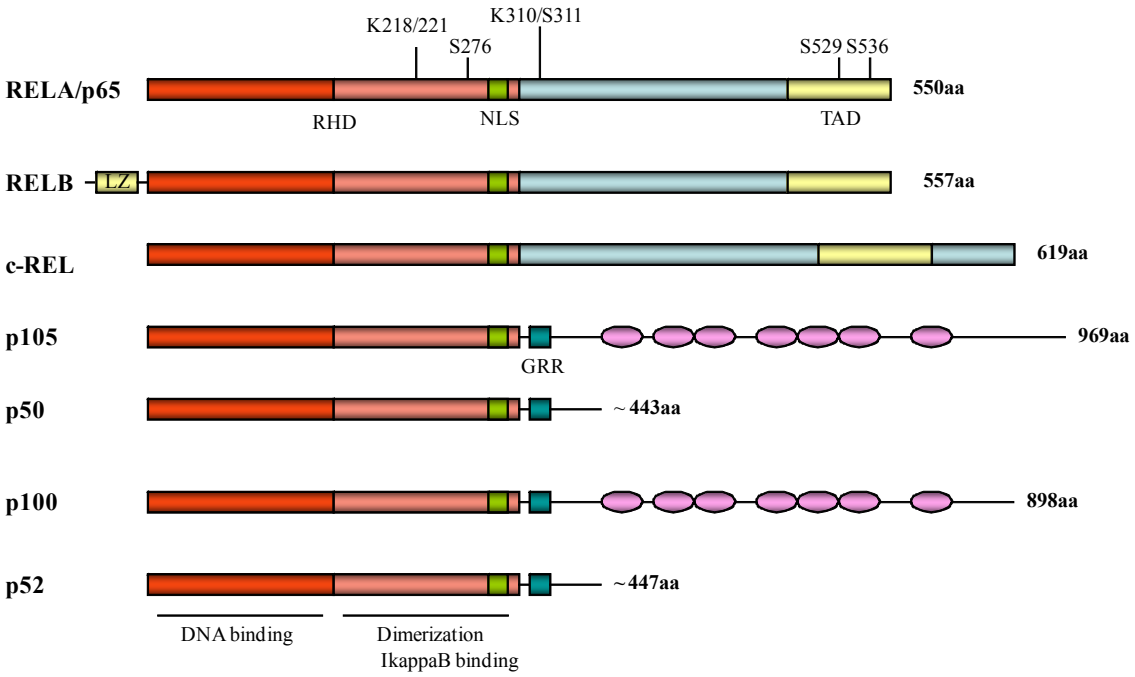

Figure 1.2: The family of mammalian NF-κB/REL proteins

All seven mammalian REL-related proteins- RELA/p65, RELB, c-REL, p105, p100, p52 and p50 contains REL homology domain necessary for DNA binding and IκB association. Only RELA, RELB, c-REL contain carboxy-terminal transactivation domains (TADs) essential for gene expression. The glycine-rich regions (GRR) domains are essential for co-translational processing of p105 to p50 and post-translational processing of p100 to p52. Phosphorylation of RELA at serines (S) 276, 311, 529 and 536 is required for optimal NF-κB transcriptional activity. The 3 main sites of acetylation on RELA at (K) 218, 221, and 310/311 regulate NF-κB transcriptional activity, and IκBα association. The number of amino acids in each human protein is indicated on the right.

1.4 NF-κB in inflammatory diseases and cancer

NF-κB plays a critical role in inflammation and innate immunity through proinflammatory cytokine receptor signaling via the Toll-like receptor (TLR), TNF receptor and IL-1 receptor (Karin, 2006). In inflammatory cells, IKK1-dependent NF-κB pathway promotes tumour cells development through inducing the expression of genes encoding cytokines (IL-1 and TNFα) and growth factors (VEGF and CSF). These secreted cytokines and growth factors bind to the receptors expressed on adjacent tumour cell surface, and further promote clonal expansion of cancerous cells. In the case of the IL-1 and TNF cytokine, interaction of these cytokines to their respective receptors on the cancer cell activates downstream signaling components of the NF-κB pathway, which in turn activate NF-κB to bind to DNA promoter to transcribe antiapoptotic genes, ensuring tumourigenic cell survival and proliferation.

Genetic evidence further support inflammation in tumour promotion, whereby polymorphism in the *TLR* gene cluster and *IL-1β* promoter are associated with high risk of prostate and gastric cancer respectively (Sun *et al*., 2005; El-Omar *et al*., 2000). Although the NF-κB activating cytokine TNF has been named according to its ability to induce tumour cells necrosis and to trigger apoptosis, TNF does not trigger cell death unless it is combined with RNA and protein synthesis inhibitor in cell treatment (Karin, 2006). Enough scientific evidences exist to show that TNFα acts as a tumour promoter in skin and gastric cancer (Lind *et al*., 2004; Oshima *et al*., 2005). Moreover, activation of NF-κB has also been reported to be a tumour promoter in inflammation–associated cancer, namely colitis-associated cancer (CAC) and mucosal-associated lymphoid tissue

(MALT), which further support its role in linking inflammation and immunity to cancer progression (Karin, 2006).

1.5 NF-κB signaling pathway

1.5.1 Signaling to NF-κB through the classical or "canonical" pathway

The first phase of NF-κB activation occurs in the cytoplasm where NF-κB exists in the cytoplasm in an inactive form through its association with the IκB proteins in quiescence cells. IκBs are known to be inhibitors of NF-κB because IκB retains NF-κB in the cytoplasm by masking the nucleus localization sequence (NLS) on NF-κB subunits, thus preventing NF-κB translocation into the nucleus to activate gene transcription. These proteins are identified by the presence of ankyrin repeats which can be proteolytically cleaved and degraded. The IκB family of proteins consist of IκBα, IκBβ, IκBε, IκBζ, IκBγ and B-cell leukemia/lymphoma 3 (BCL3), among the predominant ones are the IκBα, IκBβ and IκBε, while the biological role of IκBγ is not very clear (Figure 1.3). Cells that lack IκBα, IκBβ and IκBε have normal nuclear and cytoplasmic distribution of p65 but significantly increased basal NF-κB dependent gene expression (Tergaonkar *et al*., 2005).

The crystal structure of IκBα and the p65/p50 dimer reveals that IκBα only masks one of the two NLS on the heterodimer, which allows the NF-κB-IκBα complex to shuttle from the cytoplasm to the nucleus (Huxford *et al.*, 1998). The nuclear export signal (NES) located on the N-terminus of IκBα serve to constantly export the NF-κB-IκBα complex out of the nucleus, therefore the NF-κB-IκBα complex shuttle constantly between the cytoplasm and the nucleus, which leads to basal transcriptional activity of NF-κB in non-activated cells (Birbach *et al.,* 2002). Similar to IκBα, IκBε also form a

complex with NF-κB to shuttle between the cytoplasm and nucleus (Lee and Hannink, 2002). On the contrary, IκBβ masks both the NLS of the NF-κB dimer and retain the NF-κB-IκBβ complex in the cytoplasm (Malek *et al.,* 2001).

Traditionally, the role of the IκB proteins functions as inhibitors of NF-κB. New scientific evidence have arised to show that IκBζ and BCL3 may act as co-activators of NF-κB. The IκBζ and p50 complex is found on the promoter of interleukin-6 (IL-6), an NF-κB target gene. The expression of IL-6 has not been found in IκBζ knockout cells, therefore suggesting that IκBζ is indispensable for the expression of IL-6 (Yamamoto *et al.,* 2004). The co-activator function of BCL3 is not completely understood, and BCL3 is found to be associated with p50 and p52-containing homo and heterodimers in the nucleus, and may function to displace the repressive effect of p50 and p52 dimers from the κB sites so that other TAD-containing dimers can bind to the κB sites (Hayden and Ghosh, 2004; Perkins, 2006). Therefore, the repressor function of IκBs has been challenged, as more evidence show that some members of the IκB family of proteins can function as co-activators.

NF-κB signaling is generally considered to occur through either the classical or alternative pathway (Bonizzi and Karin, 2004). It is widely accepted that the classical pathway is essential for innate immunity because it coordinate the expression of a subset of genes (such as IL-6, IL-8, TNFα), involved in inflammation and innate immunity (Bonizzi and Karin, 2004). In the classical pathway, NF-κB is activated through cytokines, such as IL-1, TNFα, and bacteria cell wall lipopolysaccharide (LPS), which bind to their cell surface receptors IL-1 receptor, TNFα receptor and Toll-like receptor 4 (TLR4) respectively. TLRs are evolutionarily conserved pattern recognition receptors

(PRRs) that recognize conserved pathogen-associated microbial patterns (PAMPs) present on various microbes (Kopp and Medzhitov, 2003).

These extracellular cytokines and LPS bind to their respective receptors and employ various different intermediate upstream signaling molecules which converge on the 700-900kDa IKK complex (Chen *et al*., 1996), consisting of IKKα (IKK1), IKKβ (IKK2) and NF-κB essential modifier (NEMO) or IKKγ, to phosphorylate IκBα (Figure 1.4) to release NF-κB from its inhibitor. NEMO has no intrinsic kinase activity but contains a helix-loop-helix and leucine zipper motif known for protein-protein interaction. Upon interaction with upstream signal transduction molecule such as receptor interacting protein kinase 1 (RIPK1), NEMO oligomerizes which in turn activates the IKK1 and IKK2 (Poyet *et al*., 2000), resulting in the auto-phosphorylation of IKK via the T loop serine residues, serine 177 and 181 within the activation loop of the IKK kinase domain (Hacker and Karin, 2006). Activated IKK2 in turn phosphorylates IκBα leading to its ubiquitination by βTrCP proteins and degradation by the 26S proteosome. The importance of the IKK complex in NF-κB activation is shown in murine embryonic fibroblast (MEF) cells lacking both IKK1 and IKK2 or NEMO alone, whereby NF-κB activation is completely blocked in these knockout MEF (Li *et al*., 2000; Rudolph *et al*., 2000).

The classical pathway selectively utilizes IKK2 to phosphorylate IκBα on serine 32 and 36, and IκBβ on serine 19 and serine 23, leading to its ubiquitination by βTrCP proteins and degradation by the 26S proteosome, and the release of NF-κB from the NF-κB-IκB complex (Karin and Ben-Neriah, 2000; Ben-Neriah, 2002), to translocate to the nucleus to activate gene transcription. Upon phosphorylation by IKKs, IκB proteins are

recognized, and ubiquitinated by members of the Skp1-Cullin-Roc1/Rbx1/Hrt-1-F-box (SCF or SCRF) family of ubiquitin ligases. βTrCP, the receptor subunit of the SCF family ubiquitin ligase machinery, binds directly to the phosphorylated E3 recognition sequence (DS*GXXS*) on IκBα (Suzuki *et al*., 1999). Recognition of IκBα leads to polyubiquitination at conserved residues, Lys 21 and Lys 22 on IκBα, by the $SCF^{\beta\text{-}TrCP}$ and the E2 UbcH5 (Scherer *et al*., 1995), leading to its degradation.

Signaling molecules immediately downstream of cell surface receptors are essential intermediate players to relay the message from the cell surface to the internal of the cell to activate the IKK complex. TNF receptors are present on the surface of a wide range of cells, and use a unique set of intermediate signaling protein component different from those that are used by the IL-1 and TLR4 receptors. The ligation of TNFα with its TNF receptor results in receptor trimerization and the recruitment of prosurvial complex consisting of adaptor protein TNF receptor associated via death domain (TRADD), TNF receptor associated protein 2 (TRAF2), RIPK1, cIAP1 and cIAP2 to the cytoplasmic receptor, which then recruits and activate the IKKs to phosphorylate IκBα (Jiang *et al*., 1999; Bradley and Pober, 2001; Hsu *et al*., 1996).

The activation of NF-κB through TNF signaling directly regulates the expression of antiapoptotic genes like Bcl-XL and XIAP. The interesting aspect of TNF signaling is its ability to stimulate death and survival through transcription factor NF-κB and Jun N-terminal protein kinase (JNK), which it activates. The activation of NF-κB leads to survival of cells, while prolonged activation of JNK leads to apoptosis (Guo *et al.,* 1998). It is proposed that XIAP induced by NF-κB blocks JNK activation (Tang *et al.,* 2001), however the effects of JNK and NF-κB are not entirely antagonistic because the

expression of antiapoptotic cIAP protein is co-regulated by both NF-κB and JNK, and TNFα induced apoptosis is increased in JNK1 and JNK2 double-knockout cells (Lamb *et al*., 2003; Ventura *et al*., 2003).

The IL-1 and TLR4 receptor share similar intermediate signaling protein components downstream of its receptors that converge on IKK to activate NF-κB. The IL-1 and TLR4 receptor bear strong homology in the intracellular domain and share a similar Toll-IL-1R (TIR) domain that interacts with downstream adapter, myeloid differentiation primary response gene 88 (MyD88) (Jassens and Beyaert, 2003). MyD88 contains a death domain (DD) that interacts with serine/threonine kinase IRAK1 and IRAK4 (Suzuki *et al*., 2002). IRAK activation and TNF receptor associated protein 6 (TRAF6) recruitment to the signaling complex by IRAK is necessary to activate NF-κB because TRAF6 deficient cells has a complete loss of NF-κB transcriptional activity in IL-1 and TLR4 signaling (Lomaga *et al*., 1999).

The protein that link TRAF6 to IKK activation has remained controversial. Two adaptor proteins have been speculated to link TRAF6 and IKK. The first set of proteins described to be linking TRAF6 and IKK, are transformining growth β activated kinase 1 (TAK1), TAK1-binding protein 1 (TAB1) and TAK1-binding protein 2 (TAB2) (Wang *et al.,* 2001). The TAK1, TAB1 and TAB2 protein complex could be co-purified with TRAF6. RNAi mediated knock down of TAK1 inhibited signaling from the IL-1 receptor (Takaesu *et al*., 2003), and hence demonstrated an essential role of TAK1 in IL-1 signaling. However, the roles of TAB1 and TAB2 are unclear because TAB1 and TAB2 knockout MEF exhibit normal IL-1 signaling (Sanjo *et al*., 2003). The second proposed adapter protein that connects TRAF6 and IKK is the evolutionarily conserved signaling

intermediate in toll pathways (ECSIT) protein. Through yeast two-hybrid screening, ECSIT was identified to be a binding partner of TRAF6, and RNAi-mediated knock down of ECSIT show that ECSIT is required for TLR and IL-1 signaling (Kopp *et al.,* 1999).

Figure 1.3

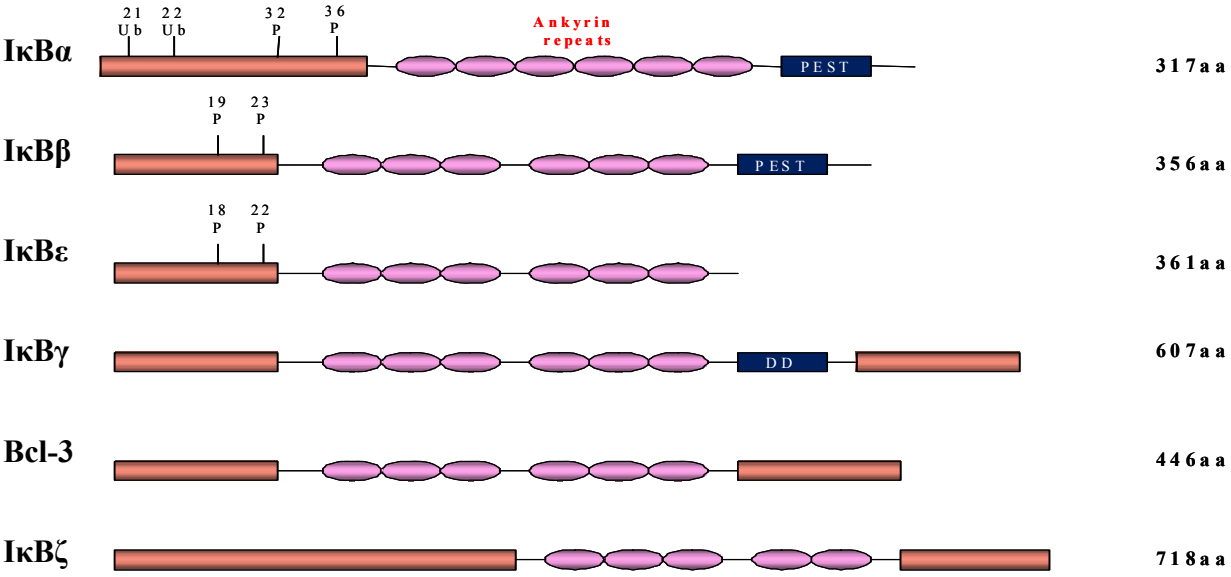

Figure 1.3 The family of mammalian IκB proteins

The family of IκB proteins consists of the IκBα, IκBβ, IκBε, IκBγ, BCL3 and IκBζ. A unique characteristic of these proteins is that they contain ankyrin-repeat domain that mediate interaction with NF-κB and localize NF-κB in the cytoplasm by masking the nuclear localization signal (NLS) of NF-κB. Phosphorylation of IκBα on serine 32 and serine 36 triggers its polyubiquitination and proteosome-mediated degradation, freeing NF-κB into the nucleus to activate gene transcription.

Figure 1.4

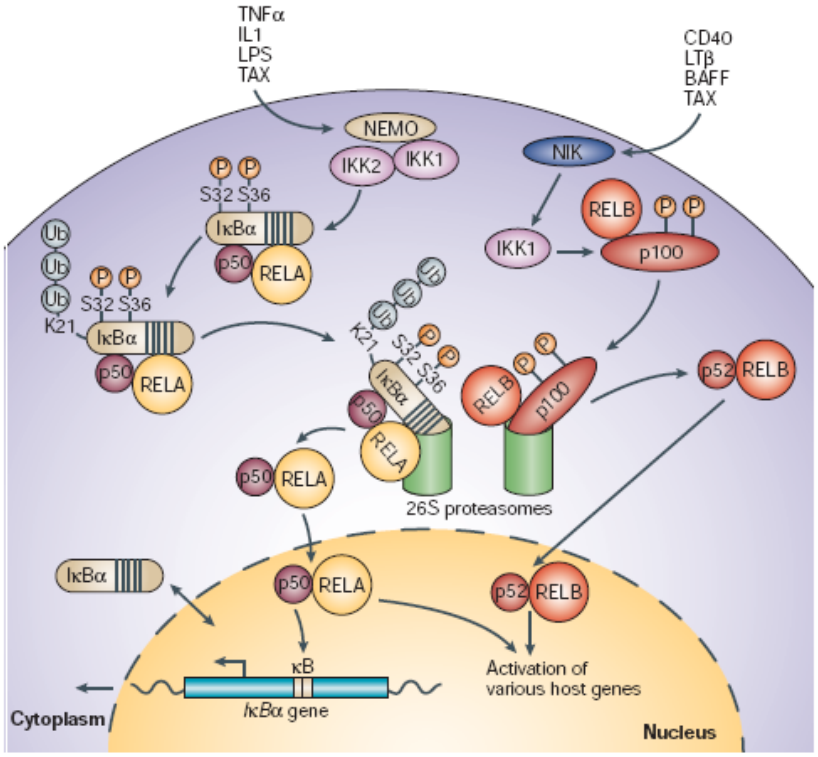

Figure 1.4 Activation of the NF-κB pathway

In the classical NF-κB pathway, NF-κB is activated after cellular activation by TNFα, LPS or IL-1. The IKK complex consist of IKK1 (IKKα), IKK2 (IKKβ) and NEMO (IKKγ). The IKK2 serve as the principal IκBα kinase in the classical pathway. In the alternative pathway, BAFF and CD40 activates NIK and IKK1, IKK1 phosphorylates p100, leading to the processing of p100 by the 26S proteosome to generate the p52-RELB heterodimers to activate transcription. (Reproduced with permission from Nature Reviews Molecular Cell Biology) (Chen and Greene, 2004)

1.5.2 Signaling to NF-κB through the alternative or "non-canonical" pathway

NF-κB can also be activated through the "non-canonical" or alternative pathway through the ligation of CD40L, BAFF and lymphotoxin β (LTβ) to its CD40, BAFF and lymphotoxin β receptor (LTβR) respectively. The alternative pathway is unique in that sense that it does not require IKK2 or NEMO, but requires only IKK1. Upon receptor activation, NF-κB inducing kinase (NIK) phosphorylates IKK1, activated IKK1 in turn directly phosphorylate the heterodimer p100 in association with RELB, leading to processing of p100 by the proteosome to release the transcriptionally active p52:RELB dimer which translocate into the nucleus to activate gene transcription (Xiao *et al*., 2001; Xiao *et al*., 2004). However, the events that occur upstream of NIK is unclear. It is believed that the alternative pathway plays a chief role in the expression of a subset of genes (such as PNAd, GlyCAM-1), involved in the development and maintenance of secondary lymphoid organs (Bonizzi and Karin, 2004).

1.5.3 Signaling to NF-κB through cell stress

NF-κB has been shown to be activated through cell irradiation and DNA damage. The interesting aspect of this signaling is that it does not occur through the conventional initiating receptor ligation. Ionizing irradiation and UV irradiation that causes DNA damage has been shown to activate NF-κB through two distinct mechanisms (Li and Karin, 1998). In the clinical context, patients suffering from ataxia-telangiectasia (AT) have mutations in the ATM gene, whereby these patients are highly sensitive to DNA double strand break (DSB) inducers, such as ionizing irradiation (IR). Exposure of ATM knockout mice to IR resulted in reduced NF-κB DNA binding activity, and IKK kinase

activity when compare to wildtype mice. This data demonstrated *in vivo*, that ATM is required for IR induced IKK-NF-κB pathway (Li *et al*., 2001). NF-κB activation following UV-C radiation is IκB serine 32/36 phosphorylation independent, and take place through the activation of casein kinase II (CKII), instead of IKK, which phosphorylates IκBα in the C-terminal PEST domain, resulting in IκBα degradation (Kato *et al.,* 2003; Lin *et al.*, 1996; Tergaonkar *et al*., 2003). In summary, IR utilize IKK to phosphorylate serine 32 and 36 on IκBα, whereas UV-C utilize CKII instead of IKK, to phosphorylate IκBα in the C-terminal PEST domain, resulting in its degradation and activation of NF-κB. It is generally believed that the activation of NF-κB can lead to antiapoptotic cell signaling, providing an opportunity for cells to repair DNA damage. However, Campbell *et al.*, showed that NF-κB is activated in response to UV-C radiation which led to the repression of antiapoptotic genes (Campbell *et al.,* 2004b). Conflicting experimental data and views exist in the field in the investigation of the biological role of NF-κB activation in response to cell stress, and hence the role of NF-κB is not instantaneously clear.

1.6 Regulation of NF-κB transcriptional activation by post-translation modification

1.6.1 Protein kinases as positive regulators

The first phase of activation of NF-κB sets the stage for the second phase of NF-κB activation. The second phase of NF-κB activation occurs in the nucleus, which involves NF-κB post-translational modification like phosphorylation and acetylation. The initial observation of phosphorylated p65 detected in TNFα-induced cells suggest that phosphorylation might play a role in the biology of NF-κB (Naumann and Scheidereit, 1994). The inducible phosphorylation of NF-κB enhances NF-κB binding to DNA to

activate transcription, and the recruitment of transcriptional co-activator CBP/p300 that aid in transcription. Post-translational modification of NF-κB via phosphorylation therefore enhances the transactivation potential of NF-κB, and may render it constituitively active. Constituitive phosphorylation of NF-κB has been detected in cancer cells and many human disease like inflammation, has deregulated NF-κB activity. Thus, understanding the mechanism of the molecular switch of NF-κB phosphorylation and dephosphorylation will solve the puzzle of deregulated NF-κB in human diseases.

The phosphorylation of NF-κB by various kinases occur in the cytoplasm or nucleus. Several phosphorylation sites on NF-κB have been identified. The phosphorylated residues on NF-κB are serine (S) 276, serine 311, serine 529, and serine 536, whereby the key residues are serine 276 and serine 536 which influence NF-κB transcriptional activity (Figure 1.5). One example of such differential regulation takes place on serine 276, where mitogen and stress-activated protein kinase-1 (MSK1) phosphorylate serine 276 in the nucleus (Vermeulen *et al*., 2003). MSK1 phosphorylates p65 on S276 *in vitro* and *in vivo*. The effects of MSK1 on p65 phosphorylation is seen when L929 mouse fibroblast and human MDA-MB-231 breast cancer cells were treated with MSK1 inhibitor H89. Upon TNFα stimulation, the expression of NF-κB target gene IL-6 mRNA expression in these cells was reduced. Another one of such kinases that has an effect on IL-6 mRNA expression is protein kinase C, zeta (PKC-zeta) that phophosphorylates p65 on serine 311 in response to TNFα (Duran *et al.,* 2003). Mutation of serine 311 to alanine inhibits the prosurvival role of p65, and abrogates the interaction of p65 with its transcriptional co-activator CBP/p300 and RNA polymerase II to the IL-6

promoter. Both MSK1 and PKC kinase exert a positive effect on p65 phosphorylation and the transcription of p65 target gene IL-6.

Protein kinase A (PKA) associates with IκBα and IκBβ in the NF-κB-IκB complexes in the cytoplasm (Zhong *et al.*, 1997). Upon, LPS stimulation in pre-B cells, PKA is activated with correlation to IκB degradation. PKA then phosphorylates p65 on serine 276 in its close proximity, when IκB is degraded. It is believed that phosphorylation of NF-κB in the nucleus aid in the recruitment of transcriptional co-activators for transcriptional activation. The reason to why NF-κB is phosphorylated in the cytoplasm and its significance remains to be unravelled.

Another interesting kinase, CKII regulates NF-κB phosphorylation at two levels; firstly by phosphorylating IκBα to induce its degradation, and releasing NF-κB from its inhibitor, and secondly by phosphorylating p65 on serine 529 directly to increase NF-κB transcriptional activity (Bird *et al*., 1997; Wang *et al*., 2000). CKII kinase has been shown to be necessary for cell cycle progression and proliferation, because its protein levels are often observed to be elevated in proliferating non-neoplastic tissue and solid tumours (Vilk *et al*., 1999; Landesman-Bollag *et al*., 1998). Therefore, CKII may simultaneously co-operate with NF-κB to regulate cancer cell transformation, and cell proliferation.

Another critical residue for phosphorylation on p65 is serine 536 which lies in the TAD domain. IKK kinase has dual function in positively regulating p65, firstly, to phosphorylate IκBα leading to its degradation and disassociation from p65, and secondly, to phosphorylate p65 directly on serine 536 to increase it transactivation potential, upon

TNFα induction of HeLa cells (Sakurai *et al*., 1999). Doxycycline inducible p53 expression in Saos-2-tet-on p53 cells stimulates ribosomal S6 kinase 1 (RSK1), which in turn phosphorylates p65 on serine 536 in the nucleus (Bohuslav *et al*., 2004). The phosphorylation of p65 reduces p65 and newly synthesized IκBα interaction, hence reducing shuttling of p65-IκBα complex out of the nucleus, thus favouring nuclear retention of NF-κB to activate transcription. In addition to CKII kinase, RSK1 negatively regulates IκBα inhibitor function on p65 to elevate p65 transcriptional potential.

Figure 1.5

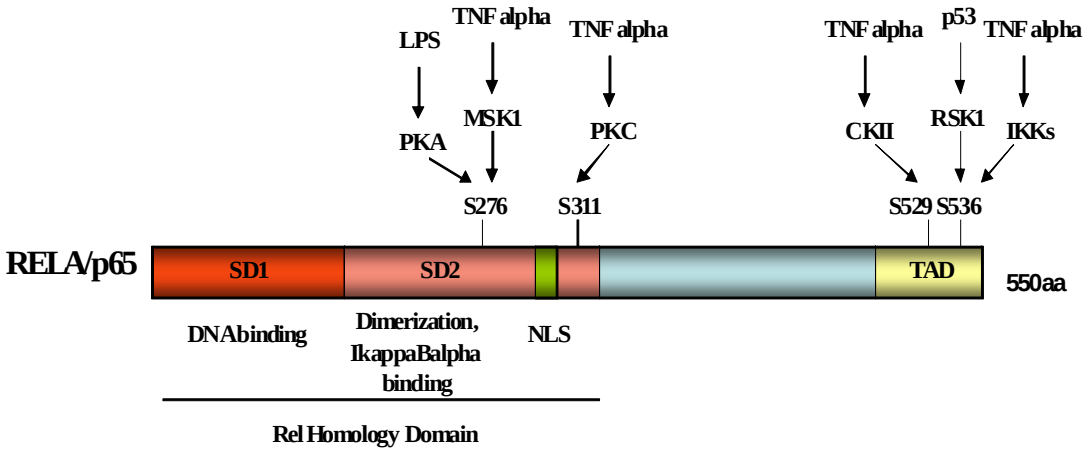

Figure 1.5 Multiple kinases phosphorylate p65 at various sites induced by distinct stimuli

Four different phosphoacceptor sites, serine (S) 276, serine 311, serine 529 and serine 536 have been identified in RELA. Phosphorylation of serine 276 is mediated by PKA and MSK1 which are activated by LPS and TNFα respectively. Serine 311 is phosphorylated by PKC which is activated by TNFα. Phosphorylation of serine 529 is mediated by CKII upon TNFα induction. Serine 536 is targeted for phosphorylation by IKK upon TNFα stimulation or RSK1 which is dependent on p53.

1.6.2 Protein phosphatases as negative regulators

Many kinases have been shown to phosphorylate NF-κB, and the components of the NF-κB signaling pathway. The roles of phosphatases in NF-κB signaling pathway is not as well studied as the kinases. Li *et al.* elucidated the role of phosphatases in NF-κB signaling in a large scale RNAi screening (Li *et al*., 2006). They identified 13 NF-κB suppressing phosphatases out of 250 phosphatases genes, and confirmed the suppression of these phosphatases by RNAi knockdown, and measuring relative NF-κB activity in chemiluminescent transcription factor binding assay (CTFA). Through co-immunoprecipitation (co-IP) experiments, the authors also showed that serine/threonine phosphatase, PP2A physically associates with, and dephosphorylates IKK , p65, and TNF receptor associated protein 2 (TRAF2). TRAF2 is an adaptor protein that lies in the NF-κB signaling pathway, although the significance of TRAF2 phosphorylation is not well-understood.

The serine/threonine phosphatase family of protein comprises of four major phosphatase, PP1, PP2A, PP2B (Calcineurin) and PP2C. These protein phosphatases have been implicated in the negative regulation of the NF-κB signaling pathway. The serine/threonine family of protein phosphastase such as PP1, PP2A and PP2C negatively affect the NF-κB signaling pathway via the IKK complex. Through yeast two-hybrid screening, CUE domain-containing 2 (CUEDC2) protein was identified as an interacting partner of IKK1 and IKK2. CUEDC2 contains CUE domains which recognize mono and polyubiquitin. On top of its function in facilitating intramolecular monoubiquitination, and promote degradation of its interacting partner, CUEDC2 deactivates the IKK kinase,

and repressed the activation of NF-κB through recruiting protein phosphatase PP1 to the IKK complex (Li *et al*., 2008).

The PP2A protein phosphatase has been shown to inhibit and dephosphorylate the IKK complex though its association with IKKγ (Fu *et al*., 2003). PP2A is responsible for the rapid deactivation of IKK, and this effect can be reversed by the interaction of PP2A with the transactivator/oncoprotein Tax of the human T-lymphotrophic virus type 1 (HTLV-1), to result in constituitive IKK activity. In order for Tax to reverse the inhibition of PP2A to rapidly inactivate IKK, IKK-Tax-PP2A has to exist in a stable ternary complex, because PP2A-interaction-defective Tax mutants failed to activate NF-κB.

The PP2Cβ protein phosphatase has been reported to associate with the IKK complex through mass spectrometry studies (Prajapati *et al*., 2004). The association of PP2Cβ with the IKK complex led to the dephosphorylation of IKK2 *in vivo* and *in vitro*, and decreased its kinase activity upon TNFα stimulation. siRNA directed against PP2Cβ increases TNFα-induced IKK activity, and the overexpression of PP2Cβ decreases NF-κB directed gene expression. The overexpression of PP2Cβ reduced the resynthesis of IκBα, a target gene of NF-κB, and affected the phosphorylation of IκBα and its degradation. These lines of evidences suggest that PP2Cβ negatively regulate NF-κB signaling pathway.

The PP2B (Calcineurin) negatively regulate NF-κB signaling through the insulin-like growth factor-1 (IGF-1) in astrocytes (Pons and Torres-Aleman, 2000). IGF-1 protects neurons against a variety of brain pathologies (such as stroke, brain trauma and

multiple sclerosis) associated with glial overproduction of proinflammatory cytokines. The protective function of the IGF-1 signaling pathway is mediated through the induction and activation of PP2B when astrocytes are stimulated with IGF-1. Activation of PP2B by IGF-1 results in PP2B in dephosphorylating IκBα on serine 32, and the dephosphorylation of IκBα protects it from TNFα stimulated degradation, and hence prevented the translocation of p65 to the nucleus to activate transcription of proinflammatory cytokines. Therefore, the therapeutic effect of IGF-1 in the treatment of brain injury is through its inhibitory action on glial inflammatory reaction by negatively regulating NF-κB signaling pathway.

1.7 Involvement of chromatin remodeling in transcriptional control of NF-κB target genes

1.7.1 Chromatin remodeling- histone acetylation and histone deacetylation

The packaging of DNA sequences into nucleosomes and higher-organized chromatin structures has been implicated in the regulation of gene transcription. Tightly packed chromatin block the accessibility of transcription factors, transcriptional co-activators, and the replication machinery to binding DNA promoters, and therefore, inhibit gene transcription. Chromatin remodeling is a process whereby modifications take place on histone tails, resulting in the alteration in nucleosome structure, leading to increased accessibility of transcription factors and the basal transcription apparatus. Modification of histones requires the action of enzymes like ATP-dependent chromatin-remodelling complexes like the SWI/SNF complex to changes the shape or position of specific nucleosomes (Flaus and Owen-Hughes, 2001).

Another group of enzymes histone acetyltransferases (HATs), histone deacetylases (HDACs), kinases and methyl transferases modify amino-terminal tails of histone proteins (H2A, H2B, H3 and H4), therefore influencing chromatin structures and transcriptional activity on DNA (Wu and Grunstein, 2000; Jenuwein and Allis, 2001). The opposing actions of histone acetylases (HATs) and histone deacetylases (HDACs) on the lysine residues of the histone tails influence transcription by modifying chromatin structure. HATs induce an open chromatin structure and transcriptional activation of genes while HDACs induce a closed chromatin structure and transcriptional repression (Figure 1.6).

In order for NF-κB and the transcriptional machinery to gain access to NF-κB target genes promoter, chromatin remodeling is very much required. IKK1 subunit of the IKK kinase phosphorylates histone H3, and modulates chromatin accessibility at NF-κB responsive promoters. In IKK1 knockout MEF cells, decreased levels of phosphorylated H3 on serine^{10} and H3 acetylation has been observed (Anest *et al*., 2003; Yamamoto *et al*., 2003). These observations suggest that the phosphorylation of H3 on serine^{10} trigger the subsequent acetylation of histone H3 on lysine 14. p65 chromatin immunoprecipitation (CHIP) show that IKK1 is crucial for p65 binding to the intracellular adhesion molecule 1 (ICAM1) and monocyte chemotactic protein 1 (MCP1) promoter, but not the IκBα promoter. The mutation of the NLS on IKK1, which prevents its nuclear translocation, results in the complete loss of binding of p65 to the ICAM and MCP1 promoter. Therefore, the effect of IKK1 on κB sites is mostly promoter specific (Gloire e*t al*., 2007).

High basal levels of histone H4 acetylation has been reported surrounding rapidly induced NF-κB target genes, IκBα, manganese superoxide dismutase (MnSOD) and macrophage inflammatory protein 2 (MIP2) (Saccani *et al*., 2001). In response to LPS stimulation, hyperacetylation of histone H3 and H4 within the regulatory regions of interleukin-8 (IL-8), interleukin-12 (IL-12), subunit p40 (IL-12/p40) and macrophage inflammatory protein 1-alpha (MIP1α) genes was also observed (Saccani *et al*., 2001; Zhong *et al*., 2002; Saccani and Natoli, 2002). On the contrary, the opposing action of histone deacetylation can result in decreased NF-κB transcription. Under unstimulated conditions, HDAC1 and p50 form a transcriptionally repressive complex, and the HDAC1-p50 complexes bind to κB sites of NF-κB target genes (Zhong *et al*., 2002). The recruitment of HDAC to NF-κB target gene promoter lead to histone deacetylation in the region, and thus transcriptional repression.

Figure 1.6

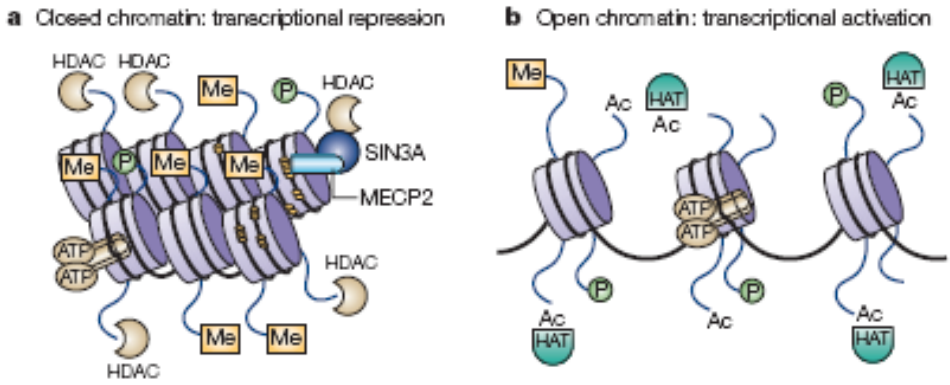

Figure 1.6 Chromatin remodeling regulates transcriptional activity

Post-translational modification on histone tails by methylation (ME), phosphorylation (P) or acetylation (Ac) can alter chromatin structure. Chromatin structure can be regulated by ATP-dependent chromatin remodellers, and the opposing action of histone acetyltransferases (HATs) or histone deacetylases (HDACs). DNA methylation and histone deacetylation induce a closed-chromatin structure and transcriptional repression, while histone acetylation and demethylation of DNA relaxes chromatin, allowing transcriptional activation. (Reproduced with permission from Nature Reviews Drug Discovery) (Johnstone, 2002)

1.7.2 p38 MAPK marks histones of NF-κB target genes

The response of cells to external stress signals and the transmission of the external signals to the inside of the cells are mediated by intracellular kinases. The mitogen activated protein kinase (MAPK), in particular, p38 MAPK, is one such serine/threonine kinase, that acts as a central point for different extracellular stimuli like heat, UV, inflammatory cytokines (IL-1, LPS, and TNF), and osmotic shock (Pearson *et al*., 2001). p38 MAPK function to regulate fundamental cellular processes involved in cell growth, cell cycle and inflammation.

p38α was first isolated as a 38 kDa protein which was rapidly tyrosine phosphorylated in reponse to LPS stimulation (Han *et al*., 1994). Mammalian p38α was originally identified as the molecular target of the pyridinyl imidazole class of compounds, SB203580, known to inhibit the production of proinflammatory cytokines, TNF, IL-1, and LPS-induced human monocyte (Lee *et al*., 1994). There are four p38 isoforms identified p38α, p38β, p38δ and p38γ, where the p38α and p38β are observed to be ubiquitously expressed (Jiang *et al*., 1996; Lechner *et al*., 1996; Jiang *et al*., 1997). p38 are activated by the dual phosphorylation of their Thr-Gly-Tyr motif by upstream mitogen-activated protein kinase kinase (MAPKK), mitogen-activated protein kinase kinase 3 (MKK3) and mitogen-activated protein kinase kinase 6 (MKK6) (Cohen., 1997; Kyriakis and Avruch, 2001), which in turn is phosphorylated by a serine/threonine kinase mitogen-activated protein kinase kinase kinase (MAPKKK) such as apoptosis signal-regulating kinase 1 (ASK1) (Ichijo *et al*., 1997).

p38 MAPK has a substrate preference, for sites containing a serine or threonine followed by a proline residue (Songyang *et al*., 1996). Activated p38 MAPK in turn phosphorylates other physiological substrates like downstream kinases, MAP kinase-activated protein kinase 2 (MAPKAPK2) and MSK1 (Cuenda and Rousseau, 2007). Inflammatory cytokine like TNFα activates p38 MAPK, which in turn phosphorylates and activates MSK1 to phosphorylate p65 on serine 276, and hence increasing p65 transactivation potential. The effect of MSK1 is clearly demonstrated in RAW cells where the phosphorylation of p65 on serine 276 is reduced when MSK protein levels were knocked down (Olson *et al*., 2007). Similarly, the phosphorylation of p65 on serine 529 and 536 occur through IKK and AKT activation in a p38MAPK fashion through inflammatory cytokine IL-1β stimulation (Madrid *et al*., 2001). Several transcription factors such as activating transcription factor-2 (ATF-2), p53 and CHOP, were also shown to be phosphorylated and subsequently activated by p38α (Cuenda and Rousseau, 2007).

p38 MAPK can also influence and coordinate the gene expression of different inflammatory cytokine, for example, interleukin-1, 6, 8 (IL-1, -6 -8), cyclooxygenase-2 (COX2), MCP-1, and TNF (Shapiro and Dinarello, 1995; Beyaert *et al*., 1996; Hwang *et al*., 1997). In addition to phosphorylating downstream kinases and transcription factors, p38 MAPK can also influence chromatin remodeling through the phosphorylation of histones H3 on ser^{10}. Saccani *et. al.* show that inflammatory stimuli like LPS can trigger p38 MAPK indirect phosphorylation of histone H3 on ser^{10}, and by this mechanism, p38 can selectively mark the promoters of various inflammatory genes for example IL-8 and MCP1, for the recruitment of NF-κB to these gene promoter (Saccani *et al*., 2002).

1.7.3 p65 acetylation by p300 and CBP co-activators

Similar to histone proteins that can be acetylated and deacetylated, the p65 protein can undergo reversible acetylation and deacetylation. The significance of p65 phosphorylation on serine 276, 311 and 536 is to recruit transcriptional co-activators CBP/p300 (acetyltransferases), to undergo reversible acetylation when cells are stimulated with TNFα (Zhong *et al*., 2002; Chen *et al*., 2005). The three main sites of acetylation identified on p65 are lysines (K) 218, 221, and 310 (Figure 1.2). p65 acetylation on K221 impairs its interaction with its inhibitor, IκBα, and enhances DNA binding capability of NF-κB, while the acetylation on K310 does not affect its DNA binding capability nor IκBα interaction (Chen *et al*., 2002). Although K310 acetylation does not increase DNA binding nor inhibit IκBα interaction, it is definitely required for the full transcriptional activity of p65.

The activation of NF-κB and its subsequent translocation to the nucleus result in the transcription of its inhibitor and target gene IκBα. *De novo* synthesis of IκBα replenishes intracellular stores of this inhibitor that undergo degradation upon NF-κB activation in the cytoplasm. Newly synthesized IκBα in the nucleus exports NF-κB out of the nucleus into the cytoplasm, stopping NF-κB transcription in the nucleus, owing to the presence of NES on IκBα. The nuclear export of NF-κB is regulated by acetylation of NF-κB on lysine 218 and 221. Acetylation on lysine 218 and 221, renders weak interaction between p65 and IκBα, and hence hamper the nuclear export of p65. However, the deacetylation of lysine 218 and 221 by HDAC3 highly enhances p65 interaction with IκBα, and thus favour nuclear export of p65 into the cytoplasm to terminate p65 transcription (Chen *et al*., 2001). Therefore, the dynamics of post-

translational modification like acetylation, deacetylation and phosphorylation on p65 influence the transcriptional activity of p65.

1.8 Objectives of study

Given the importance of how post-translation modification on NF-κB, and histone modifications such as histone deacetylation can affect the recruitment of NF-κB, and the transcriptional apparatus to gene promoters, in the first part of the thesis (chapter 3), I investigated the possibility of WIP1 in regulating the phosphorylation status and transcriptional activation of the p65 subunit of NF-κB, and in the second part of my thesis (chapter 4), I undertake the genome wide screening (microarray analysis) of genes that are associated to the NF-κB signaling pathway, genes that are activated or repressed by the HDAC inhibitor, TSA, in the event of chromatin remodeling.

Chapter 2
Materials and methods

2.1 Table 1: List of antibodies

Antibody	**Company**	**Catalogue number**	**Working Dilution**	**Source (Clone)**
Actin	Santa Cruz	sc-1616	1:1000	Goat polyclonal IgG
FLAG M2	Sigma-Aldrich	F3165	1:1000	Mouse monoclonal IgG1
FLAG M2	Sigma-Aldrich	F7425	1:1000	Rabbit polyclonal IgG
IκBα (C21)	Santa Cruz	sc-203	1:1000	Rabbit polyclonal IgG
Phospho IκBα (ser32)	Cell signaling technology	9241L	1:1000	Rabbit polyclonal
NF-κB p65 (C20)	Santa Cruz	sc-372	1:1000	Rabbit polyclonal IgG
NF-κB p65 (F6)	Santa Cruz	sc-8008	1:1000	Mouse monoclonal IgG1

Phospho p65 (ser536)	Cell signaling technology	3031L	1:1000	Rabbit polyclonal
Phospho p65 (ser468)	Cell signaling technology	3039S	1:1000	Rabbit polyclonal
p38 MAPK	Santa Cruz	Sc-535	1:1000	Rabbit polyclonal
Phospho p38 (Thr180/Tyr182)	Cell signaling technology	9211	1:1000	Rabbit polyclonal
WIP1 (H-300)	Santa Cruz	Sc-20712	1:1000	Rabbit polyclonal IgG
WIP1	BD lab		1:500	Mouse monoclonal
Clusterin	Upstate	05-354	1:500	Mouse monoclonal IgG1κ
STAT3	BD Biosciences	610190	1:2500	Mouse monoclonal

				IgG1
RAD9	BD Biosciences	611324	1:250	Mouse monoclonal IgG1
Bid	Santa Cruz	Sc-6538	1:1000	Goat polyclonal
RAD21	Oncogene Research Products	NA80	1:250	Mouse monoclonal IgG1
β-tubulin	BD Biosciences	556321	1:1000	Mouse monoclonal IgM
Lamin B	Oncogene Research Products	NA12	1:1000	Mouse monoclonal IgG1κ
Rabbit IgG-H&L (HRP)	Abcam	AB6721	1:5000	Goat polyclonal
Mouse IgG-HRP	Santa Cruz	Sc-2031	1:2000	Goat polyclonal
Goat IgG-HRP	Santa Cruz	Sc-2033	1:2000	Donkey

				polyclonal
p53 (DO-1)	Santa Cruz	Sc-126	1:2000	Mouse monoclonal IgG_{2a}
p21 (C19)	Santa Cruz	Sc-397	1:2000	Rabbit IgG

2.2 List of primers

Gene (Human)	Sequence	Tm (°C)
1. β-actin (1) forward	5'- CATGTACGTTGCTATCCAGGC -3'	55
2. β-actin (1) reverse	5'- AGGTCCAGACGCAGGATGG-3'	55
3. β-actin (2) forward	5'- GCCAACCGCGAGAAGATGA-3'	55
4. β-actin (2) reverse	5'- CCA TCA CGA TGC CAG TGG TA-3'	55
5. Bid forward	5'- TGAACCAGGAGTGAGTCGGA-3'	55
6. Bid reverse	5'- AGCTCTCTGCGGAAGCTGTT-3'	55
7. BNIP3L forward	5'- GTGGAGCTACCCATGAACAG-3'	55
8. BNIP3L reverse	5'- TGCCCATCTTCTTGTGGCGA-3'	55
9. Clusterin forward	5'- TCTCAGACAATGAGCTCCAG-3'	55
10. Clusterin reverse	5'- CTTCTAGGTTGCTGAGCAGT-3'	55
11. IκBα forward	5' - CGCACCTCCACTCCATCC -3'	55
12. IκBα reverse	5'- AGCCATGGATAGAGGCTAAGTGTAG-3'	55
13. IRAK1 forward	5'- TTCTCGGAGGAGCTCAAGATC- 3'	55
14. IRAK1 reverse	5' - GTAGCCAGCAAAGTCCACAAT-3'	55
15. IL-2Rγ forward	5'- TTGAAGCCATCATTACCATTC -3'	55

16. IL-2Rγ reverse	5’- ATAGTGGTCAGGAAGAAATCA-3’	55
17. IL-6 forward	5’- TACATCCTCGACGGCATCTCA-3’	55
18. IL-6 reverse	5’- CAGTGATGATTTTCACCAGGC-3’	55
19. IL-8 forward	5 - GCCAACACAGAAATTATTGTAAAGCTT-3’	55
20. IL-8 reverse	5’- CCT CTGCACCCAGTTTTCCTT -3’	55
21. LTβR forward	5’- CTATGTCTCAGCTAAATGTAG-3’	55
22. LTβR reverse	5’- GGTCTTCCGTTTGCTTGTGCA-3’	55
23. NF-κB1 forward	5’- TTATGTATGTGAAGGCCCATC -3’	55
24. NF-κB1 reverse	5’- AGATCCCATCCTCACAGTGTT -3’	55
25. Perp forward	5’- ATTGGAGGTCTCCTTGCCTT -3’	55
26. Perp reverse	5’- GTAGTTGAGGAGGCAGCAGA -3’	55
27. RAD9 forward	5’- ACGAGCTCTACCTGGAAC-3’	55
28. RAD9 reverse	5’- CTTCATCAGGATCTTACAGCG-3’	55
29. RAD21 forward	5’- TGCCTGAGGAAAATCGGGAA-3’	55
30. RAD21 reverse	5’- GATGTTCCCAACTTCTTCTCTC-3’	55
31. STAT3 forward	5’- TCCAACATCTGTCAGATGCC -3’	55
32. STAT3 reverse	5’- TTCTCTGCCAGTGTAGTCAG -3’	55

33. TNFα forward	5’- TGGTATGAGCCCATCTATCTG-3’	55
34. TNFα reverse	5’- AGACTCGGCAAAGTCGAGATA-3’	55
35. WIP1 forward	5’- GGCTGTACTCGCTGGGAGTGAGCG-3’	55
36. WIP1 reverse	5’- AGGCAACGGCTGAGACAGCGACCG -3’	55

Gene (Mouse)	Sequence	Tm (°C)
1. β-actin forward	5’- TTCGTTGCCGGTCCACA-3’	55
2. β-actin reverse	5’- ACCAGCGCAGCGATATCG-3’	55
3. ICAM forward	5’- GTGAACTGTTCTTCCTCATGC-3’	55
4. ICAM reverse	5’- CACTCTCCGGAAACGAATACA-3’	55
5. IκBα forward	5’ - ACTTGGCAATCATCCACGAAG-3’	55
6. IκBα reverse	5’- TCACAGCCAGCTTTCAGAAGT-3’	55
7. IL-6 forward	5’- AAGAGACTTCCATCCAGTTGC-3’	55
8. IL-6 reverse	5’- CTCCGACTTGTGAAGTGGTAT-3’	55
9. IRF forward	5’- CTGGCTAGAGATGCAGATTAA-3’	55
10. IRF reverse	5’- GACAGGCATCCTTGTTGATGT-3’	55
11. MCP1 forward	5’- CCACTCACCTGCTGCTACTCA-3’	55
12. MCP1 reverse	5’- TGGTGATCCTCTTGTAGCTCT-3’	55

13. MIP1α forward	5'- CGTTCCTCAACCCCCATC-3'	55
14. MIP1α reverse	5'- TGTCAGTTCATGACTTTGTCA-3'	55
15. TNFα forward	5'- ACAGAAAGCATGATCCGCG-3'	55
16. TNFα reverse	5'- CTGGGCCATAGAACTGATG-3'	55

2.3 DNA/RNA methodology

2.3.1 RNA isolation

5 X 10^6 cells were treated with 10 ng/ml TNFα or 2 ng/ml IL-1 and cell culture medium was removed after treatment. **Homogenisation:** The cells were scraped off tissue culture plates using a cell scraper and resuspended in 1 ml TRIzol (Invitrogen, #15596-026). The homogenized sample was allowed to stand for 5 min at room temperature, to ensure disassociation of nucleoprotein complexes. **Phase separation:** 200 µl of chloroform was added and the tubes were mixed vigorously for 15 sec and incubated at room temperature for 3 min. The tubes were centrifuged at 13, 000 rpm for 15 min at 4°C. **RNA Precipitation:** The clear upper phase was collected and equal volume of 70% ethanol was added (to give a final ethanol concentration of 35%) to the collected sample drop by drop to avoid local precipitation. **RNA wash:** The sample was applied to RNAeasy column (Qiagen RNAeasy kit, #74106) and placed in a 2 ml collection tube. The tube was centrifuged 15 sec at 13, 000 rpm and the flow through was discarded. 700 µl of buffer RW1 was added, and the tube was centrifuged 15 sec at 13, 000 rpm. The flow through and collection tube was discarded. Transfer column to a clean 2 ml collection tube, add 500 µl buffer RPE, centrifuge 15 sec at 13, 000 rpm. Discard flow through. Add another 500 µl of buffer RPE, centrifuge 2 min at 13, 000 rpm and discard flow through.

Repeat centrifugation step at 13, 000 rpm for 1 min to completely dry column. Elute RNA by adding 30 µl of RNase/nuclease-free water directly to column membrane, centrifuge 1 min at 13, 000 rpm.

2.3.2 First strand cDNA synthesis

First strand cDNA synthesis was performed using Superscript™ First-Strand Synthesis System for RT-PCR (Invitrogen, #11904-018) according to manufacturers' recommendations. The following components were prepared in RNase/nuclease-free eppendorf tubes for each reaction:

Components	Volume
1. Random hexamers	1 µl
2. 10 mM dNTP mix	1 µl
3. 1 ug total RNA	Variable
4. RNase/nuclease-free water	Top up to a total volume of 11 µl

The above mixture was heated to 65°C for 5 min and quickly chilled on ice for 1 min. The following was then added to each tube: 4 µl 5 X First-strand buffer, 1 µl 0.1M DTT, 1 µl RNaseOUT™ recombinant ribonuclease inhibitor (40 units/µl) and 1 µl of Superscript™ II RT enzyme. The tubes were mixed and incubated at 25°C for 5 min followed by 50°C for 60 min. The reaction was terminated by heating at 70°C for 15 min.

2.3.3 Mini-preparation of plasmid DNA

Small scale plasmid DNA preparation was carried out using QIAprep Miniprep Kit (Qiagen, #27104) according to manufacturer's instructions. Briefly, a single colony from a freshly streaked selective plate was inoculated into 3-5 ml of LB containing ampicillin (100 μg/ml) in a 15 ml falcon tube. The bacterial culture was incubated for 12-16 hr at 37°C with vigorous shaking (~300 rpm). Cells were harvested by centrifugation at 4, 000 rpm in 4°C for 15 min. The pelleted cells were resuspended in 250 μl P1 buffer containing RNase A solution (final concentration of 0.1 mg/ml), followed by mixing gently in 250 μl of P2 lysis Buffer. The mixture was neutralized in 350 μl of N3 buffer and centrifuged at 13, 000 rpm for 10 min. The supernatant containing plasmid DNA was passed through the QIAprep spin column to allow DNA binding to the column and centrifuged at 13, 000 rpm for 60 sec. The flow through was discarded. The bound plasmid DNA was washed with 0.75 ml of PE buffer and centrifuged for 60 sec. The flow through was discarded and the QIAprep column was centrifuged for an additional 1 min to remove residual wash buffer. The QIAprep column was placed in a clean 1.5 ml microcentrifuge tube. The plasmid DNA was eluted with 50μl of EB buffer by centrifugation at 13, 000 rpm for 1 min.

2.3.4 Maxi-preparation of plasmid DNA

Large scale plasmid DNA preparation was carried out using QIAprep Maxiprep kit (Qiagen, #12163) according to manufacturer's instructions. Briefly, the starter culture was inoculated in 250 ml ampicillin (100 μg/ml) containing LB at a dilution of 1/1000. The bacterial culture was incubated at 37°C for 12-16 hr with vigorous shaking (~300

rpm). Cells were harvested by centrifugation at 6, 000 rpm in 4°C for 15 min. The pelleted cells were resuspended in 10 ml P1 buffer containing RNase A solution (final concentration of 0.1 mg/ml), followed by mixing gently in 10 ml of P2 lysis buffer and allowed to stand at room temperature for 5 min. The cell lysate was neutralized with 10 ml of chilled P3 buffer and mixed gently by inverting 4-6 times. The lysate was poured into the barrel of the QIAfilter maxi catridge and incubated at room temperature for 10 min. Meanwhile, the QIAGEN-tip 500 was equilibrated by applying 10 ml QBT buffer and the tip was allowed to empty by gravity flow. The cap from the QIAfilter maxi catridge outlet nozzle was removed and the plunger was inserted into the catridge, and the lysate was filtered into the equilibrated QIAGEN-tip 500. After the lysate pass through completely, the tip containing bound DNA was washed twice with 30 ml of QC buffer. Plasmid DNA was eluted into polycarbonate centrifuge tubes with 15 ml of QF buffer. The eluted DNA was precipitated by adding 10.5 ml of room temperature isopropanol and centrifuged immediately at 15, 000 rpm in 4°C for 30 min. After the centrifugation step, the supernatant was carefully poured out and the DNA pellet was washed with 70% ethanol and centrifuged for a further 10 min at 15, 000 rpm. The supernatant was carefully poured out without disturbing the pellet. The pellet was allowed to air-dry at room temperature for 5-10 min and redissolved in 200-300 μl of water.

2.3.5 Sybr green real-time PCR

Sybr green real-time PCR was carried out using BIORAD iQ™ SYBR green supermix (BIORAD, #170-8882), according to manufacturer's instructions. The real-time PCR reaction was set-up as follow:

Components	Volume
1. iQ SYBR green supermix	12.5 µl
2. Forward primer (2.5 µM)	2.5 µl
3. Reverse primer (2.5 µM)	2.5 µl
4. Water	5.0 µl
5. cDNA (5-25X diluted)	2.5 µl

The PCR reaction was set up as follow:

Step	Temperature	Time
PCR cycling and detection (40 cycles):		
1.	95°C	30 sec
2.	95°C	15 sec
3.	55°C	45 sec

Melt curve analysis:

4.	95°C	1 min
5.	55°C[+]	1 min
6.	55°C[*]	10 sec

[+] Approximately 5°C below the Tm (melting temperature) of primers

[*] The reaction is repeated at step 6 for 81 cycles, increasing each by 0.5°C each cycle

2.3.6 Quantitect sybr green real-time PCR

Sybr green real-time PCR was carried out using QuantiTect[R] SYBR[R] Green PCR (QIAGEN, #204143), according to manufacturer's instructions. The real-time PCR reaction was set up as follow:

Components	Volume
1. Sybr Green	12.5 µl
2. Forward primer	0.3 µM
3. Reverse primer	0.3 µM
4. cDNA	1 µl
5. DEPC water	Top up to a total volume of 25 µl

The PCR reaction was set up as follow:

Step	Temperature	Time
PCR detection and cycling step (35 cycles):		
1. PCR initial activation step	95°C	15 min
2. Denaturation	94°C	15 sec
3. Annealing	50-60°C	30 sec
4. Extension	72°C	30 sec

2.3.7 Agarose gel electrophoresis

6 X DNA loading dye (0.1% bromophenol blue, 40% sucrose, 240 mM Tris-HCL pH7.4, 60 mM EDTA-Na pH8.0) was added to plasmid DNA/PCR products to a final concentration of 1 X. 1-2% (W/V) agarose gel (Invitrogen, 15510-027) was prepared by dissolving agarose gel in 1X TAE buffer (0.04 M Tris-acetate, 0.001 M EDTA) through heating in a microwave oven. 0.5 μg/ml ethidium bromide was added to the agarose gel cooled down to room temperature and the gel was poured into a gel cast mould and allowed to solidify. The solidified agarose gel was ran in a electrophoresis tank with 1X TAE buffer. DNA samples and 1 μg of 2 log DNA ladder (New England Biolabs, N3200S) were loaded into the gel wells and the gel was ran at 100 volts. The separated DNA bands were visualized using UV trans-illuminator (Syngene Bio Imaging).

2.3.8 DNA sequencing

The sequencing of DNA was performed by PCR. 500 ng of plasmid and 3.2 ρmol of primer and 8 µl of big dye mix (obtained from core sequencing facility) were mixed to a total volume 20 µl. The cycling conditions for the PCR sequencing is as follow:

Step	Temperature	Time
1. Initial denaturation	96°C	2 min
2. Denaturation	96°C	30 sec
3. Annealing	50°C	30 sec
4. Extension	60°C	4 min

The reaction was repeated from step 1 to 4 for 25 cycles. After the PCR reaction is completed, the DNA was precipitated with 80 µl of 100% ethanol and allowed to stand at room temperature for 15 min and then centrifuged at 13, 000 rpm for 20 min. The supernatant was discarded and the DNA pellet was washed with 150 µl of 70% ethanol and centrifuged at 13, 000 rpm for 5 min. The ethanol was discarded and the DNA pellet was left to air dry. The DNA was resolved and read using Perkin-Elmer ABI prism 377 sequencer (performed by Dr. Alice Tay's laboratory).

2.3.9 One-step RT-PCR

One-step RT-PCR was carried out using one-step RT-PCR kit (QIAGEN, #210212), according to manufacturer's instructions. The one-step RT-PCR reaction was set up as follow:

Components	1X
1. One step RT-PCR buffer (5 X)	10 µl
2. dNTP	2 µl
3. Forward primer (25 ρmol/µl)	2 µl
4. Reverse primer (25 ρmol/µl)	2 µl
5. One step PCR enzyme mix	2 µl
6. Template RNA (2 ug)	Variable
7. DEPC water	Top up to total volume of 50 µl

The PCR reaction was set up as follow:

Step:	Temperature	Time
1. Reverse transcription	50°C	35 min
2. Initial PCR activation step	95°C	15 min

Three step cycling

3. Denaturation	94°C	15 sec
4. Annealing[+]	50°C-68°C	30 sec
5. Extension[*]	72°C	1 min
6. Final Extension	72°C	10 min

+ Approximately 5°C below the Tm (melting temperature) of primers

* The reaction is repeated from step 2 to 4 for 25-40 cycles

2.4 Protein methodology

2.4.1 Protein concentration determination by Bradford assay

Protein standards of 5 mg/ml, 2.5 mg/ml, 1.25 mg/ml, 0.625 mg/ml, 0.3125 mg/ml and 0 mg/ml were prepared from 10 mg/ml BSA (New England Biolabs, B9001S). 5µl of the protein standards were added to 995 µl of 20% (V/V) Bio-rad protein assay reagent (Bio-rad laboratories, #500-0006), and allowed to stand at room temperature for 5 min. The protein standards were transferred to plastic cuvettes and absorbance was read at 595 nM in a photospectrometer (GeneQuant, Amersham Biosciences). A standard curve was generated with the absorbance reading against protein concentration. Protein samples absorbances were compared against the standard curve and the protein concentration was determined.

2.4.2 Protein isolation from mouse tissue

5-10 mg of mouse tissue were cut into small pieces and resuspended in PBS containing protease inhibitors (Roche, #11697498001), 200 mM sodium vanadate and 10 mM sodium fluoride. The sample was subjected to sonication (Sonics Vibracell) for 15 sec (repeated 3 X) at 30% amplitude, with 10 sec to cool in between. The sample was centrifuged at 13, 000 rpm for 20 min, and the supernatant containing the protein was transferred to a clean eppendorf tube.

2.4.3 Western blotting

Cells were lyzed on ice in RIPA lysis buffer (150 mM NaCl, 1% NP40, 0.5% Sodium deoxycholate, 0.1% SDS, 50 mM Tris pH 8.0) containing protease inhibitor (Roche, #11697498001). The cell pellet was centrifuged at 13, 000 rpm for 10 min at 4°C, the supernatant containing protein was transferred to a clean eppendorf tube and the protein concentration was determined (see 2.4.1). 2 X Protein loading buffer (100 mM Tris-HCl pH 6.8, 4% (W/V) SDS, 0.2% (W/V) bromophenol blue, 20% (V/V) glycerol and 200 mM DTT) was added to the protein sample to a concentration of 1 X, followed by protein denaturation by boiling at 95°C for 5 min before subjecting to SDS-PAGE gels electrophoresis at 150 volts. After protein separation, the protein was transferred onto immunoblot PVDF membrane (Bio-rad laboratories, #162-0177) for 1 hr at 100 volts. Membranes were blocked with 5% (W/V) non-fat milk or 3% (W/V) bovine serum albumin in PBST or TBST for 1 hr at room temperature on a shaker. After the blocking step, primary antibody was added to the blocking solution at working concentration and left to incubate overnight at 4°C. Membranes were washed in PBST (1.5 mM Potassium

phosphate monobasic, 2.68 mM potassium chloride, 8 mM sodium phosphate dibasic, and 0.1% tween-20) or TBST (20 mM Tris base, 138 mM NaCl and 0.1% tween-20), and the appropriate species of horseradish peroxidase (HRP)-linked secondary antibody was added to the membrane in the appropriate blocking agent and incubated for 1 hr at room temperature. The membranes were washed in PBST or TBST followed by detection by ECL western blotting detection reagent (Amersham Biosciences, #RPN2106) and X-ray film (Amersham Biosciences, #28906844).

2.4.4 Immunoprecipitation

Adherent cells were washed with ice cold PBS and the cells were lyzed in IP lysis buffer (0.5% NP40 alternative, 170 mM NaCl, 50 mM Tris pH 8.0, 50 mM NaF), and harvested by scraping off the cells. The cell lysates were kept on ice for 20 min followed by centrifugation at 13, 000 rpm for 10 min at 4°C. The supernatant were transferred to a clean tube and the protein concentration was determined (see 2.4.1). 1 mg of protein cell lysates were pre-cleared with 200 µl of pre-washed 10% (W/V) protein G agarose beads slurry (Amersham Biosciences, #17-0618-02) and incubated at 4°C for 1 hr. The beads were removed by centrifugation at 13, 000 rpm in 4°C for 30 sec. 1 µg of antibody and 200 µl of beads slurry was added to the pre-cleared lysate and the sample was tumbled overnight at 4°C on a tube rotator (Barnstead thermolyne). The beads were collected by centrifugation at 13, 000 rpm in 4°C and washed 4 X with 1 ml IP wash buffer (100 mM NaCl, 200 mM Tris pH 8.0, 0.5% NP40). After the final wash, the beads were resuspended in 2 X loading buffer (see 2.4.3) and the protein was denatured by boiling at 95°C for 5 min before loading and resolving on a SDS-PAGE gel.

2.4.5 Transient transfection methods

2.4.5.1 Lipofectamine 2000 transfection for plasmid DNA

HeLa cells with a 70% confluency were transiently transfected with lipofectamine™ 2000 (Invitrogen, #11668-019), according to manufacturer's instructions. Briefly, adherent cells were washed with PBS and the media was replaced with DMEM containing 1% FCS without antibiotics before transfection. The complexes are prepared as follow:

Components	6 well	10cm dish
Lipofectamine 2000	2 µl	12 µl
OptiMEM	150 µl	900 µl
Plasmid	1 µg	6 µg
OptiMEM	150 µl	900 µl
Plating media	700 µl	4200 µl

(1% FCS, no antibiotics)

Diluted lipofectamine and diluted DNA were mixed together and incubated at room temperature for 20 min. After 20 min incubation, the complexes were added to the cells and mixed gently. 4-6 hr later, replace media with DMEM containing 10% FCS and antibiotics. Incubate the cells at 37°C in a CO_2 incubator for 18-48 hr prior to testing of transgene expression.

2.4.5.2 Lipofectamine 2000 transfection for siRNA oligonucleotides

The procedure for the transfection is the same as mentioned in 2.4.5.1 except the complexes were prepared as follow:

Components	6-well (1X)
Lipofectamine 2000	5 µl
OptiMem	245 µl

Components	6-well (1X)
siRNA oligonucleotide (10 µM)	20 µl
OptiMem	230 µl

The target sequences of the pre-designed siRNA oligos from Ambion are shown below:

Oligo ID no.	Sense sequence
1. 2566	5'-GGAAAUGUCCAAUCAGGGAtt-3'
2. 2658	5' -GGAAAUUCAAAAUGCUGUCtt-3'
3. 2745	5' -GGAAGAACCCUAAAUUUAUtt-3'

Oligo ID no.	Antisense sequence
1. 2566	5’ -UCCCUGAUUGGACAUUUCCtg-3’
2. 2658	5’ -GACAGCAUUUUGAAUUUCCtt-3’
3. 2745	5’-AUAAAUUUAGGGUUCUUCCtg-3’

The negative control 4611, 4613 and 4615 comprised of a 19 bp scrambled sequence with 3’ dT overhangs and no significant homology to any known gene sequences from mouse, rat, or human.

2.4.6 Nuclear extraction

Nuclear extraction of cells was performed using a nuclear extraction kit (Panomics, #AY2002). Briefly, the cells are grown to near confluency ($1X10^7$ cells per 10 cm tissue culture plate) before harvesting. The plate was washed with 10 ml of ice cold PBS twice. 1 ml of Buffer A mix was added to each plate, and the plates were left on ice in an ice bucket, and the ice bucket was left to shake at 150 rpm on a shaking platform for 10 min. After shaking, the cells were scraped off the plate with a plastic cell scraper and mixed by pipetting up and down several times to disrupt cell clumps in an eppendorf tube. The tubes were centrifuged at 13, 000 rpm for 5 min at 4°C. The supernant (cytosolic fraction) was transferred into a clean eppendorf tube. The cell pellet was resuspended in 150 µl Buffer B mix and vortexed for 10 sec. The tubes were left to lay flat in an ice bucket and left to shake on a shaking platform at 200 rpm for 2 hr. After shaking, the tubes were centrifuged at 13, 000 rpm for 5 min at 4°C. The supernatant (nuclear extract) was transferred to a clean eppendorf tube. The protein concentration of the cytosolic and

nuclear extract was determined (see 2.4.1) before subjecting to analysis on a SDS-PAGE gel.

Buffer A mix	Volume
1) 1 X Buffer A*	1 ml
2) 100 mM DTT	10 µl
3) Protease inhibitor cocktail	10 µl
4) 10% IGEPAL	40 µl

* Prepare a 1 X diluted working solution from a 10 X Buffer A Stock (100 mM HEPES pH 7.9, 100 mM KCl, 100 mM EDTA).

Buffer B mix	Volume
1) 1 X Buffer B+	147 µl
2) Protease inhibitor cocktail	1.5 µl
3) 100 mM DTT	1.5 µl

+ Prepare a 1 X diluted working solution from a 5 X Buffer B Stock (100 mM HEPES pH 7.9, 2 M NaCl, 5 mM EDTA, 50% glycerol).

2.5 Mammalian cell culture and assays

2.5.1 Cell culture and drug treatments

Mammalian cell lines, Saos-2 cells expressing a tet-on inducible WIP1 phosphatase, HeLa control, HeLa WIP1siRNA, transformed WT and transformed WIP1 knockout MEF (All the above cell lines were kind gifts from BD lab). HeLa, HCT116, Saos-2 and MEF cells were cultured in DMEM, and U937 and Jurkat cells were cultured in RPMI 1640 supplemented with 10% heat inactivated FCS, 100 units/ml penicillin, 100 μg/ml streptomycin in a humidified atmosphere at 37°C and 5% CO_2 incubator. TNFα and IL-1 was purchased from Calbiochem (catalogue no. 654205 and 407611) and reconstituted in PBS containing BSA to a stock concentration of 10 μg/ml and 2 μg/ml respectively. Trichostatin A (TSA) was purchased from Sigma-Alrich (catalogue no. T8552) and reconstituted in DMSO to a stock concentration of 1 mM. p38 MAPK inhibitor SB202190 was purchased from Sigma-Aldrich (catalogue no. S7067) and reconstituted to a stock concentration of 15 mM. Okadaic acid was purchased from Millipore (catalogue no. 19-130) and reconstituted to a stock concentration of 100 μM. Doxycycline hydrochloride was purchased from Sigma-Aldrich (catalogue no. 44577) and reconstituted to a stock concentration of 5 mg/ml.

2.5.2 Apoptosis assay- PI staining

Apoptosis was measured using fluorescence-activated cell sorting (FACS) analysis of cells in sub-G_1 phase. Cells were harvested and fixed in 70% ethanol. The fixed cells were then stained with 50 μg/ml propidium iodide (BD Pharmingen, #556463) after treatment with RNase (100 μg/ml). The stained cells were analyzed for DNA content by

FACS Calibur (BD Biosciences) and the cell cycle fractions were quantified with Cellquest software (BD Biosciences).

2.5.3 Cell proliferation assay-Wst-1

To measure cell survival by Wst-1 (Roche, # 11644807001), cells were plated at 1-2X10^6 cells per well in a 96 well plate and treated with 1 μM TSA. Wst-1 was added to the cell culture medium at a 1:10 dilution and incubated at 37°C for 1 hr or until the colour of the medium turned red (incubation time can vary according to the cell number in the culture). The absorbance was measured at a wavelength of 420 nM.

2.5.4 Sytox-hoechst cell staining

To determine the apoptosis of cells, cells were plated at 1-2X10^6 cells per well in a 96 well plate and treated with 1 μM TSA. The cell cultures were stained with a mixture of the membrane permeable DNA dye Hoechst-33342 (Invitrogen, #H3570) at a final concentration of 500 ng/ml and the membrane impermeable DNA dye SYTOX (Invitrogen, #S7020) at a final concentration of 500 nM. Apoptotic cells were photographed using a Zeiss epifluorescence microscope with an attached Nikon Coolpix digital camera.

2.5.5 Luciferase reporter gene assay

HeLa cells were transfected with lipofectamine 2000 (see 2.4.5.1). 0.5 μg of NF-κB luciferase reporter plasmid, 0.2 μg *Renilla* plasmid and 0-2 μg of WIP1 plasmid was transfected into each well in a 6 well plate. The total amount of transfected DNA in each well was kept constant by adding empty vector pGL3 basic vector. To correct for

variation in transfection efficiency, reporter firefly luciferase activity was normalized to *Renilla* luciferase activity which was measured using the dual luciferase reporter assay system kit (Promega, #E1980), according to manufacturer's instructions. Briefly, the cells were lysed in passive lysis buffer (PLB) with gently shaking on a rocking platform for 15 min at room temperature. Cell lysates were centrifuged at 13, 000 rpm for 30 sec to clear the cell debris. The supernatant was transferred to a clean eppendorf tube. 20 µl of each cell lysate sample (in triplicate) was dispense into each well of a 96 well plate. 100 µl of luciferase assay reagent (LARII) was added to each sample and the activity of firefly luciferase was quantified using a luminometer (Berthold technologies). Subsequently, 100 µl of Stop and Glo reagent which simultaneously quenches firefly luciferase activity and activates *Renilla* luciferase was added to the sample. Similarly, the activity of *Renilla* was quantified in a luminometer.

2.5.6 *In vitro* phosphatase assay

Activated, phosphorylated p65 and p65 S536A mutant protein was immunoprecipitated from whole cell lysates as described in 2.4.4. After the last wash, the beads were centrifuged at 13, 000 rpm for 30 sec. The beads from each sample were resuspended in 160 µl of phosphatase buffer (50 mM Tris-HCl pH7.5, 0.1 mM EGTA, 0.02% 2-mercaptoethanol, 40 mM NaCl, 30 mM $MgCl_2$). 160 µl of beads from each sample were split into two separate tubes (80 µl each) with one tube containing 1 µg of recombinant WIP1 phosphatase protein (a kind gift from BD lab), while the other tube contain mock buffer (50 µl 2 X phosphatase buffer + 50 µl 100% glycerol). The tubes were incubated in a 30°C heat block for 1 hr and the phosphatase reaction was terminated by addition of 2

X SDS loading buffer. Samples were resolved on a SDS-PAGE gel and subjected to immunoblot analysis using anti-phospho p65 antibody.

2.6 Microarray hybridization and data analysis

2.6.1 Sample (probe) labeling by reverse transcription

Step1: Total RNA isolated from TSA-treated cells was prepared as a RNA mix as follow:

Components	Volume
1. Sample RNA (Cy5)	40 μg
2. Oligo dT (0.5 mg/ml)	2 μl
3. RNase-free water	variable
Total volume	19 μl

Components	Volume
1. UHR RNA (reference, Cy3) [+]	40 μg
2. Oligo dT (0.5 mg/ml)	2 μl
3. RNase-free water	variable
Total volume	19 μl

[+] Universal human reference RNA (UHR) was obtained from Stratagene, #740000

Step 2: Heat to 65°C for 10 min and cool on ice for 2 min.

Step 3: Prepare RT reaction mix as follow:

Components	Volume
1. 5 X 1st strand buffer	8 µl
2. 20 X low T dNTP mix	2 µl
(10 mM A, C & GTP, 4 mM dTTP)	
3. Cy5 or Cy3 dUTP (1 mM)	4 µl
4. 0.1 M DTT	4 µl
5. RNasin (30 U/µl)	1 µl
6. Superscript II (200 U/µl)	2 µl
Total volume	21 µl

Step 4: Add RNA mix to RT reaction mix to pre-mix to heat block pre-set to 42°C for 1.5 hr.

Step 5: After heating, put reactions on ice.

Step 6: Add 5 µl of 0.5 M EDTA and mix well.

Step 7: Add 10 µl of 1 M NaOH (fresh), mix well and centrifuge at 13, 000 rpm for 10 sec.

Step 8: Put on heat block pre-set to 65°C for 30 min, after heating, cool to room temperature for 5 min.

Step 9: Add 25 µl of 1 M Tris-HCl (pH 7.5).

2.6.2 Probe purification

Step1: Label on white area of column, push column into the collection tube.

Step 2: Wash Microcon YM-30 centrifugal filter unit (Millipore, #42410) with 500 µl of water, spin 13, 000 rpm for 10 min, leave approximately 30 µl of water in the column.

Step 3: Add 400 µl of water to RT reaction tube (Cy3 labeled) and load onto pre-washed column, spin 13, 000 rpm for 7 min.

Step 4: Add 450 µl of water and centrifuge again (repeat wash until the eluate colour is not so intense.

Step 5: Change a clean tube, invert Cy3 to a clean tube and spin at 13, 000 rpm for 1 min.

Step 6: Combine Cy3 to Cy5 column (pre-washed), mix well and carefully not to break membrane. Load 400 µl of water and spin 13, 000 rpm for 10 min. After centrifugation, make sure volume left in the column is approximately 10 µl.

Step 7: To elute sample, invert column into a clean tube, centrifuge 13, 000 rpm for 1 min.

Step 8: Check the volume of eluate, bring the volume to 18 µl using water. Add 4 µl of herring sperm DNA (Sigma-Aldrich, #D3159), heat 100°C for 2 min, add 22 µl of DIG Easy Hyb hybridization buffer (Roche, #1603558), centrifuge at 13, 000 rpm for 10 min.

2.6.3 Microarray hybridization

2.6.3.1 Pre-hybridization

Step 1: Add 44 µl of DIG Easy Hyb hybridization buffer (Roche, #1603558) to printed oligonucleotide microarray slide (Genome Institute of Singapore) and cover with slip. Place the slide in the hybridization chamber. Add approximately 30 µl of water to the sides of the hybridization chamber to keep chamber hydrated. Tighten chamber (diagonally) before immersing into a 42°C water bath for at least 1 hr.

Step 2: After incubation, place slides into distilled water gently for 2 min, allowing slip to come off naturally to avoid scratching the surface of the printed oligonucleotide slide.

Step 3: Dunk the slides into water for 2 min.

Step 4: Dunk the slides into isopropanol for 2 min.

Step 5: Spin the slides at 100 g for 4 min to dry slide.

2.6.3.2 Hybridization

Step 1: Add 44 µl of labeled cDNA to the printed slide and cover with a cover slip. Place the slide in the hybridization chamber. Add approximately 30 µl of water to the sides of the hybridization chamber to keep the chamber hydrated. Tighten the chamber diagonally before immersing into a 42°C water bath overnight.

Step 2: After hybridization overnight, place the slides into distilled water for 2 min to remove cover slip gently.

Step 3: Dunk the slides into washing buffer (SSC) sequentially from a higher concentration to a lower concentration- 2 X SSC, 1 X SSC, 0.2 X SSC, 0.05 X SSC for 2 min at each concentration.

Step 4: Spin the oligonucleotide slides at 100 g for 4 min to dry slide and scan for image analysis using Genepix 3.0 software (Axon Instruments, Inc., Foster City, CA).

2.6.4 Data analysis

The microarray image processing, analysis and normalization was performed using Genepix 3.0 software. Briefly, a normalization factor was calculated to rescale each gene in the array so that the median fluorescence ratio of all spots was 1.0. The data were then filtered so that only spots with intensities two times greater than the background were used in the analysis. The log ratio for each time point was then normalized for each gene to that of the untreated cells (time 0) to obtain the relative expression pattern. The genes that showed substantial differences after TSA treatment were selected based on 2-fold change of expression value for at least two time points across all experiment conditions. A total of 723 of 19, 000 genes met the criteria and were further analyzed using clustering and display program (rana.stanford.edu/software) developed by Eisen *et al.* (Eisen *et al*., 1998).

Chapter 3
WIP1 phosphatase negatively regulates p65 transcriptional activity

3.1 Introduction

p38 MAPK can influence the expression of proinflammatory cytokines through chromatin remodeling and positively affecting the transactivation potential of NF-κB indirectly through phosphorylating its downstream substrate kinase such as MSK1 (Olson *et al*., 2007). Inhibiting p38 MAPK activity by mutation or addition of p38 MAPK inhibitor in LPS stimulated macrophages decreased TNFα cytokine mRNA expression, and thus has a negative effect in inflammation (Campbell *et al*., 2004a). The Wildtype p53 induced phosphatase 1 (WIP1) is a negative regulator of p38 MAPK and function to inactivate p38 MAPK through the dephosphorylation of threonine 180 and tyrosine 182 on active p38 MAPK (Takekawa *et al*., 2000). Since inactivating p38 MAPK can negatively affect inflammation, it is possible that WIP1 phosphatase may exert a negative effect on inflammation through p38 MAPK.

The WIP1 phosphatase is initially discovered in WMN burkitt's lymphoma cells, and is induced by ionizing radiation (IR) and UV in a p53 dependent manner (Fiscella *et al*., 1997). WIP1 belongs to the serine/threonine PP2C family of phosphatases, and like many PP2C phosphatases, is magnesium dependent for its activation, and insensitive to inhibition by okadaic acid. WIP1 phosphatase recognizes and dephosphorylates phosphoserine and phosphothreonine in the p (S/T) Q motif, and in addition, acidic, hydrophobic, or aromatic amino acids surrounding the p (S/T) Q sequence have a positive influence, while basic amino acids have a negative influence on substrate dephosphorylation (Yamaguchi *et al*., 2007). The protein targets of WIP1 phosphatase include tumour suppressor p53 which mediates apoptosis, and cell cycle regulation checkpoint proteins like ATM (Sheeram *et al*., 2006), CHK1(Lu *et al*., 2005) and CHK2

(Fujimoto *et al*., 2006), which are activated upon DNA damage (Figure 3.1). It was proposed that WIP1 functions to reverse DNA damage response by dephosphorylating the above proteins, restoring the cells to its homeostatic state, after cells have adequately repair its DNA.

The role of WIP1 is controversial, and has also been proposed to be an oncogene. WIP1 is often observed to be amplified and overexpressed in human tumours. WIP1 dephosphorylate p53 on serine 15, although there is no physical interaction observed by co-immunoprecipitation (Lu *et al*., 2005). WIP1 may therefore inactivate p53 whereby p53 is still intact in these tumour cells. WIP1 is proposed to create a negative loop for p53 by dephosphorylating p38 MAPK (Takekawa *et al*., 2000), an upstream kinase of p53, and its interacting partner MDM2 which promotes its degradation (Lu *et al*., 2007). The p38 MAPK physically associate with p53 and phosphorylate p53 on serine 33 and serine 46 in response to UV radiation to stimulate p53 mediated transcription, cell cycle and apoptosis. WIP1 by inactivating p38 MAPK disrupt p53 mediated apoptosis. In addition, WIP1 also dephosphorylates MDM2, and inhibits its autoubiquitination, thus stabilizing MDM2 protein levels. Stabilized MDM2 protein has increased affinity for p53, bind p53 and promote its ubiquitination and degradation, thus disrupting the proapoptotic function of p53. The WIP1 phosphatase thus acts as a gatekeeper in the p53-MDM2 autoregulatory loop.

Increased inflammation has been observed in the organs of WIP1 deficient mice as compared to their wildtype counterparts (Choi *et al*., 2002). It remains unclear if WIP1 phosphatase can regulate the activity of NF-κB through direct dephosphorylation of NF-κB, or any of the signaling component of the NF-κB pathway, or indirectly through

dephosphorylation of p38 MAPK, therefore resulting in the increased inflammation of organs observed in the WIP1 deficient mice. In this section, we investigate if WIP1 phosphatase can affect the phosphorylation status as well as the transcriptional activation of NF-κB.

Figure 3.1

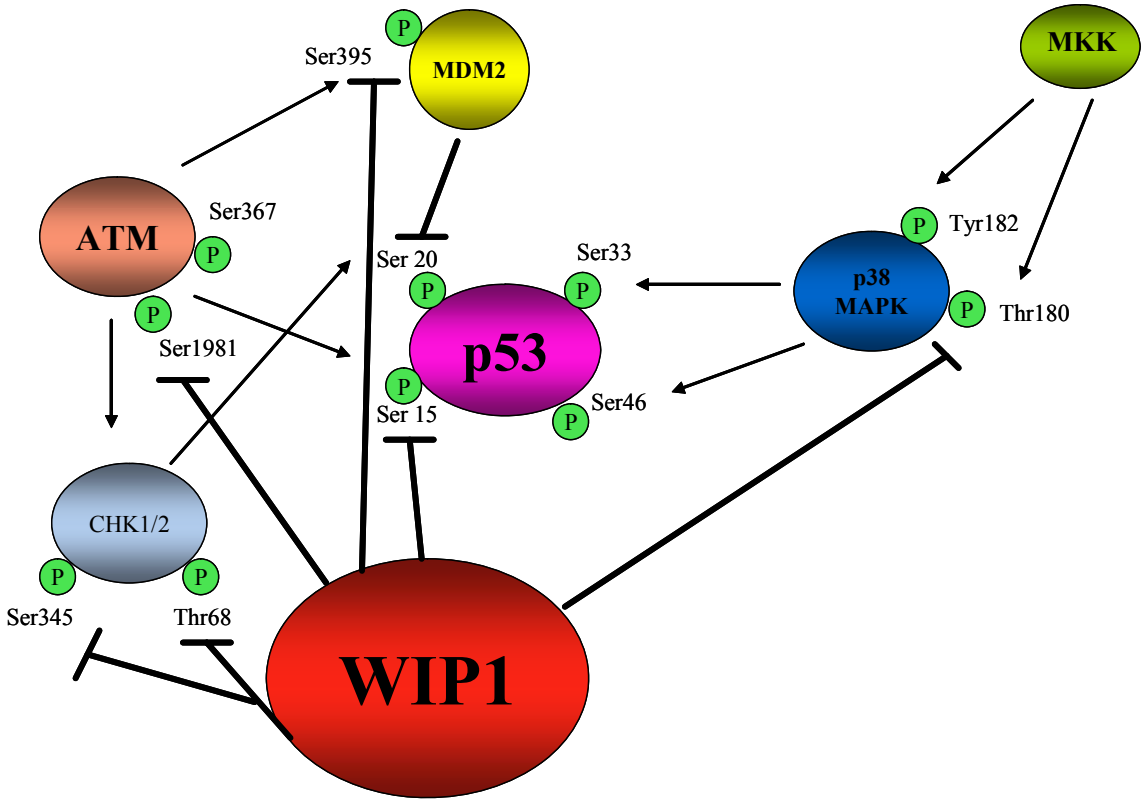

Figure 3.1 WIP1 in cell cycle regulation and apoptosis

WIP1 plays a role in apoptosis by dephosphorylating p53 on serine 15, p38MAPK on threonine 180 and tyrosine 182, and MDM2 on serine 395. WIP1 also return cells to its homeostatic state by dephosphorylating cell cycle regulation checkpoint proteins ATM on serine 1981, CHK1 on serine 345, and CHK2 on serine 68.

3.2 Mice lacking WIP1 show increased activation of NF-κB and phosphorylation of p65 on serine 536

NF-κB is a transcription factor and is directly involved in the transcription of inflammatory cytokines such as TNFα and MIP1α. The role of WIP1 in regulating NF-κB transcriptional activation was investigated via measuring mRNA transcript of its target genes IκBα, TNFα and MIP1α by real-time PCR. Because MEF from WIP1 knockout mice do not survive long in culture, they were transformed with two oncogenes, E1A and Ras to immortalize the MEF so as to prolong their life span in culture. As shown in Figure 3.2, the basal mRNA level of MIP1α, TNFα and IκBα was approximately 10-fold, 35-fold, and 2-fold higher respectively in unstimulated WIP1 deficient transformed MEF as compared to wildtype transformed MEF (Figure 3.2A).

As increased inflammation was observed in the organs of WIP1 deficient mice (Choi *et al*., 2002), we investigated the activation of NF-κB through its phosphorylation status because NF-κB phosphorylation has been correlated with its enhanced transcriptional activity. We analyzed a panel of mouse organs, the brains, heart, spleen, thymus (data not shown), kidneys, and lungs of wildtype and WIP1 deficient mice and found that the phosphorylation of p65 on serine 536 was higher in the kidneys of WIP1 deficient mice (Figure 3.2B) and approximately 2-fold higher as shown by densitometric quantification of the western blot results (Figure 3.2C). Although the levels of phosphorylated p65 is increased in the kidney of WIP1 deficient mice, the levels of total p65 is shown to be consistent and not affected by the phosphorylation levels of p65 on serine 536 (Chew *et al.*, 2009).

Figure 3.2

A

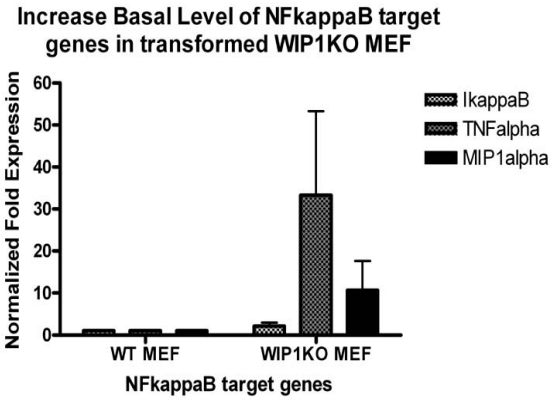

B

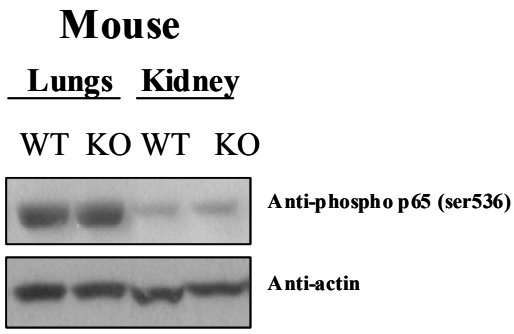

C

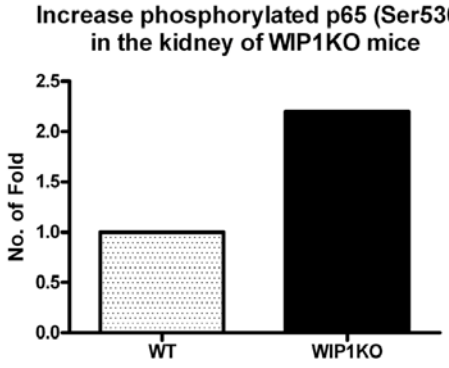

Figure 3.2 Mice lacking WIP1 show increased activation of NF-κB and phosphorylation of p65 on serine 536.

A) Sybr green real-time PCR of NF-κB target genes IκBα, MIP1α and TNFα in unstimulated wildtype and WIP1 deficient MEF using gene-specific primers. Data is the mean standard deviation (S.D.) of two samples in one experiment representative of three independent experiments. B) Western blot detection of phosphorylated p65 on serine 536 using a specific phosphos-antibody in WIP1 wildtype and WIP1 deficient mouse tissues. C) Phosphorylated p65 in the kidney of WIP1 deficient mice was quantitated using a densitometer (Bio-rad laboratories).

3.3 Overexpression of WIP1 reduces p65 transcriptional activity

WIP1 is encoded by the protein phosphatase magnesium-dependent 1 delta (PPM1D) gene, which was mapped to 17q22/q24, a hotspot that is observed to be amplified in breast, lung, pancreas, bladder, liver cancer and neuroblastoma (Li *et al*., 2002; Bulavin *et al*., 2002; Saito-Ohara *et al*., 2003; Hirasawa *et al*., 2003). Since p65 has an antiapoptotic role and mostly deregulated in cancer, we investigated if WIP1 overexpression affects the p65 transactivation potential in human HeLa cells. We co-transfected increasing concentration (0-2 μg) of WIP1 plasmid DNA with pGL3 vector control into HeLa cells, and constant levels of NF-κB luciferase reporter construct, and treat the cells with IL-1. Using dual luciferase reporter assay, we measured the transactivation of p65 with a κB site linked to the luciferase reporter gene. Transfecting 1 μg of WIP1 expression plasmid DNA in HeLa cells is sufficient to increase the mRNA levels of WIP1 4-fold as shown in Figure 3.4.1A and hence its protein expression. Overexpression of WIP1 in HeLa cells resulted in a decrease in the transactivation potential of p65 on its target gene promoter in a WIP1 dosage-dependent manner (Figure 3.3A). Overexpressing 1 μg of WIP1 reduced the transactivation potential of p65 by almost 2.5-fold whereas doubling the amount of WIP1 overexpression to 2 μg further decrease the transactivation potential of p65 by another 2-fold.

A parallel experiment was done to investigate the expression of the endogenous NF-κB target genes such as IL-8 and TNFα in HeLa cells. Overexpressing WIP1 in HeLa cells has a negative effect on the endogenous IL-8 and TNFα mRNA expression in a WIP1 dosage-dependent manner. The effect of overexpressing 1 μg of WIP1 in HeLa cells is not as dramatic as doubling the amount of WIP1 overexpression to 2 μg whereby

the expression of TNFα mRNA was reduced to an impressive 6-fold (Figure 3.3B), while the expression of IL-8 mRNA was reduced to 2-fold (Figure 3.3C).

Figure 3.3

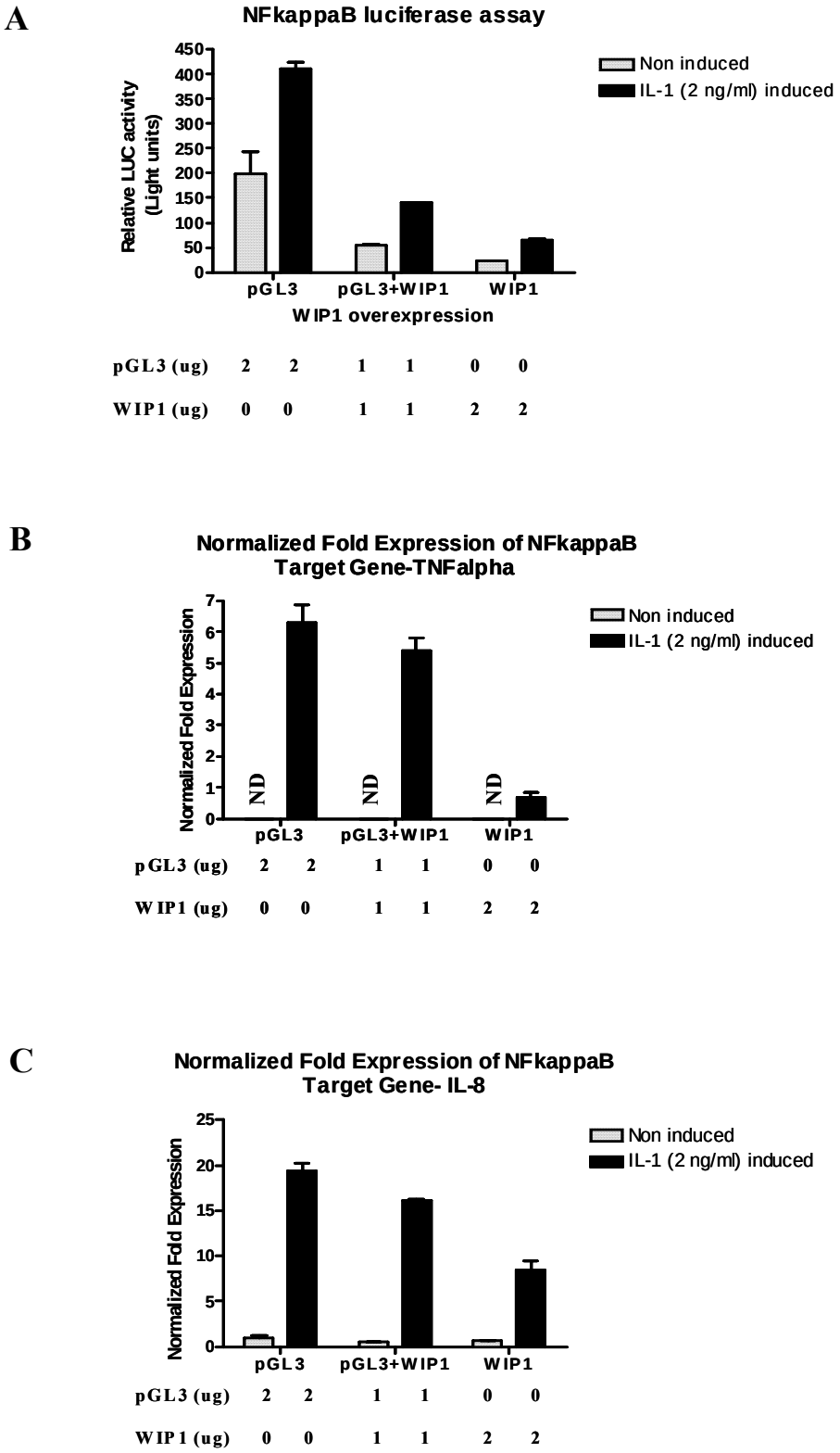
A
NFkappaB luciferase assay
Relative LUC activity (Light units)
450
400
350
300
250
200
150
100
50
0
Non induced
IL-1 (2 ng/ml) induced
pGL3
pGL3+WIP1
WIP1
WIP1 overexpression
pGL3 (ug) 2 2 1 1 0 0
WIP1 (ug) 0 0 1 1 2 2
B
Normalized Fold Expression of NFkappaB Target Gene-TNFalpha
Normalized Fold Expression
7
6
5
4
3
2
1
0
ND
ND
ND
Non induced
IL-1 (2 ng/ml) induced
pGL3
pGL3+WIP1
WIP1
pGL3 (ug) 2 2 1 1 0 0
WIP1 (ug) 0 0 1 1 2 2
C
Normalized Fold Expression of NFkappaB Target Gene- IL-8
Normalized Fold Expression
25
20
15
10
5
0
Non induced
IL-1 (2 ng/ml) induced
pGL3
pGL3+WIP1
WIP1
pGL3 (ug) 2 2 1 1 0 0
WIP1 (ug) 0 0 1 1 2 2

Figure 3.3 Overexpression of WIP1 reduces p65 transcriptional activity.

HeLa cells were co-transfected with expression plasmid encoding WIP1, vector control pGL3 basic vector plasmid, 0.5 μg NF-κB luciferase reporter plasmid and 0.2 μg *renilla* plasmid according to material and methods. 48 hours after transfection, the cells were stimulated with 2 ng/ml of IL-1 for 12-16 hours. A) Luciferase activity of NF-κB activation was measured according to manufacturer's instructions. Endogenous mRNA expression of TNFα (B) and IL-8 (C) was measured in real-time PCR using gene-specific primers. Data is the mean S.D. of two samples in one experiment representative of two independent experiments.

3.4 WIP1 regulates NF-κB activation and phosphorylation of p65 on serine 536

Consistent with the results in the WIP1 knockout MEF and WIP1 deficient mice, reducing endogenous WIP1 protein levels using lentivirus in HeLa cells by 30% (as measured by densitometric quantification of the western blot autorad X-ray film shown in Figure 3.4.2A) resulted in the activation of p65 as shown by the time kinetics of IκBα phosphorylation (and subsequent degradation) in response to TNFα induction and an increase in phosphorylated p65 (Figure 3.4.2B), and the expression of the transcript of its target genes IL-8 and TNFα (Figure 3.4.2 C & D). This result suggested that a small amount of WIP1 protein knockdown by 30% is sufficient to increase p65 phosphorylation on serine 536 (Chew *et al*., 2009).

Since the reduction of WIP1 in HeLa cells enhances p65 phosphorylation and transcription of its target genes, we investigated if overexpression of WIP1 would bring about an opposite effect. As shown in Figure 3.4.1A, the overexpression of WIP1 by 4-fold and the induction of WIP1 mRNA by TNFα resulted in the reduction of p65 phosphorylation when HeLa cells were treated with TNFα (Figure 3.4.1D). The reduction of p65 phosphorylation occurred upon 30 min of TNFα treatment and diminished greatly by 60-90 min. The measurement of WIP1 mRNA in HeLa cells in Figure 3.4.1A was done as an indication of transient overexpression of WIP1 protein because the antibody for WIP1 do not work well in HeLa cells. Next, we extended our investigation to other human cancer cell lines. In a human WIP1 inducible Saos-2 cells (Figure 3.4.1 E & F), we observed a reduction in the phosphorylation of p65 upon 30 min of TNFα treatment, and the kinetics of diminishing p65 phosphorylation happen in a similar fashion in both

the HeLa and Saos-2 cells (45-90 min TNFα treatment). Since the phosphorylation of p65 can lead to the recruitment of transcriptional co-activators to enhance transcription of NF-κB target genes, we investigated if the transcription of NF-κB genes were abated in WIP1 overexpressing cells. As seen in Figure 3.4.1 B and C, overexpressing WIP1 result in the dimunition of its target genes, IκBα and TNFα.

Figure 3.4.1

A

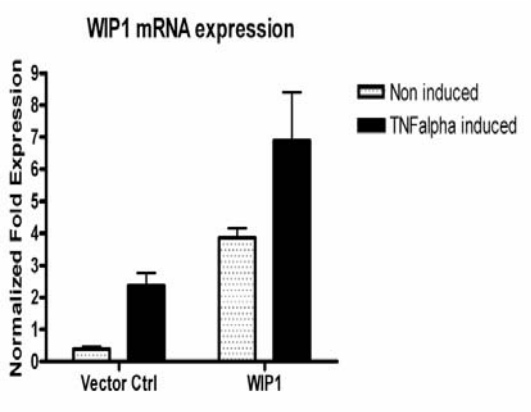

B

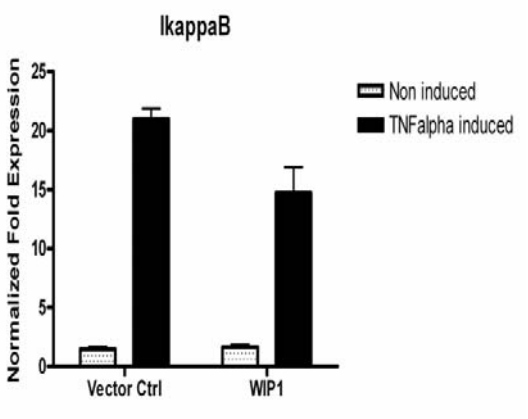

C

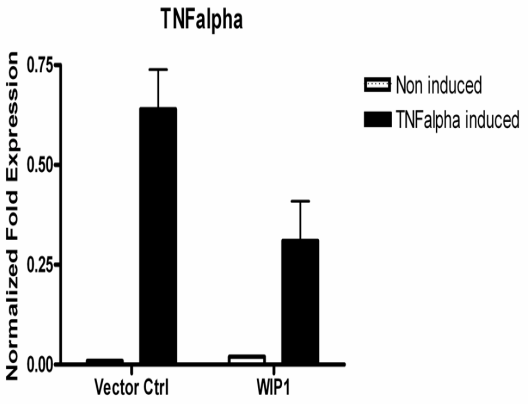

Figure 3.4.1

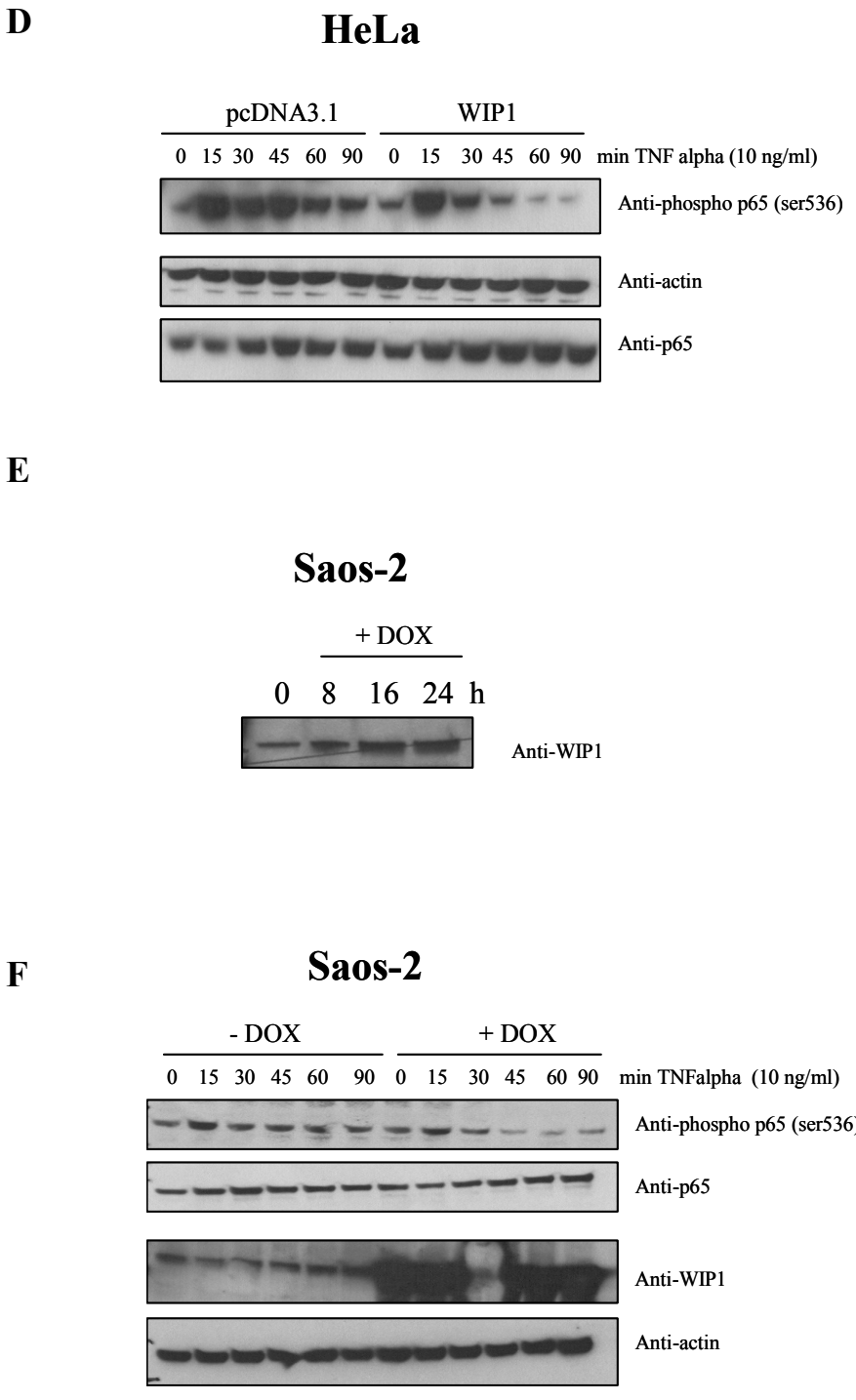
D
HeLa
pcDNA3.1
WIP1
0 15 30 45 60 90 0 15 30 45 60 90 min TNF alpha (10 ng/ml)
Anti-phospho p65 (ser536)
Anti-actin
Anti-p65
E
Saos-2
+ DOX
0 8 16 24 h
Anti-WIP1
F
Saos-2
- DOX
+ DOX
0 15 30 45 60 90 0 15 30 45 60 90 min TNFalpha (10 ng/ml)
Anti-phospho p65 (ser536)
Anti-p65
Anti-WIP1
Anti-actin

Figure 3.4.1 WIP1 regulates NF-κB activation and phosphorylation of p65 on serine 536.

1 μg of either WIP1 expression plasmid or vector control (pcDNA3.1) plamid was transfected into HeLa cells per well (6 well plate). A) WIP1 overexpression in HeLa cells was quantified by measuring WIP1 mRNA transcript in real-time PCR using gene-specific primers. B & C) NF-κB activation was ascertained through the measurement of the transcription of its target gene, IκBα and TNFα in control and WIP1 overexpressing HeLa cells treated with 10 ng/ml of TNFα for 90 min. Data is the mean S.D. of two samples in one experiment representative of two independent experiments. E) Saos-2 cells expressing doxycycline-inducible WIP1 was treated with 5 μg/ml doxycycline for 0, 8, 16 and 24 hours to induce overexpression of WIP1. Detection of phosphorylated p65 on serine 536 in (D) WIP1 overexpressing HeLa cells and (F) Saos-2 expressing doxycycline-inducible WIP1 cells. Cells were pre-treated with 5 μg/ml doxycycline overnight, followed by 10 ng/ml of TNFα for 15, 30, 45, 60 and 90 min. Cellular protein was extracted using RIPA lysis buffer. Phosphorylated p65 and total p65 was analyzed using whole cell lysates in western blot. Anti-actin was used as a loading control.

Figure 3.4.2

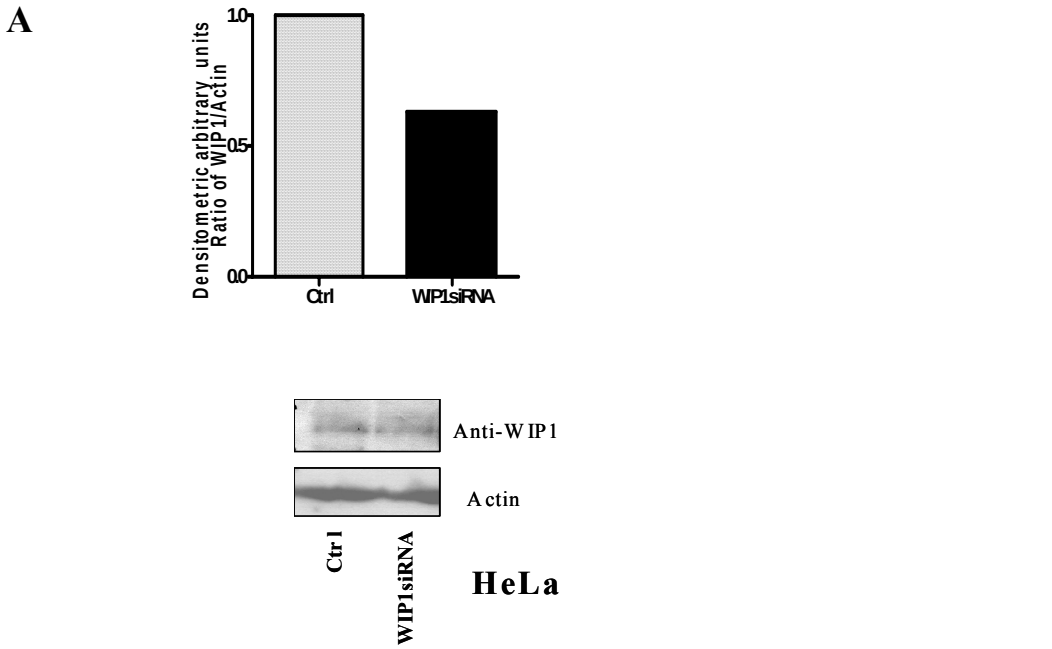
A
Densitometric arbitrary units
Ratio of WIP1/Actin
1.0
0.5
0.0
Ctrl
WIP1siRNA
Anti-WIP1
Actin
Ctrl
WIP1siRNA
HeLa
B
HeLa
CTRL
WIP1siRNA
0 15 30 45 60 90 0 15 30 45 60 90 min TNFalpha (10 ng/ml)
Anti-phospho p65 (ser536)
Anti-p65
Anti-IkappaBalpha
Anti-actin

Figure 3.4.2

C

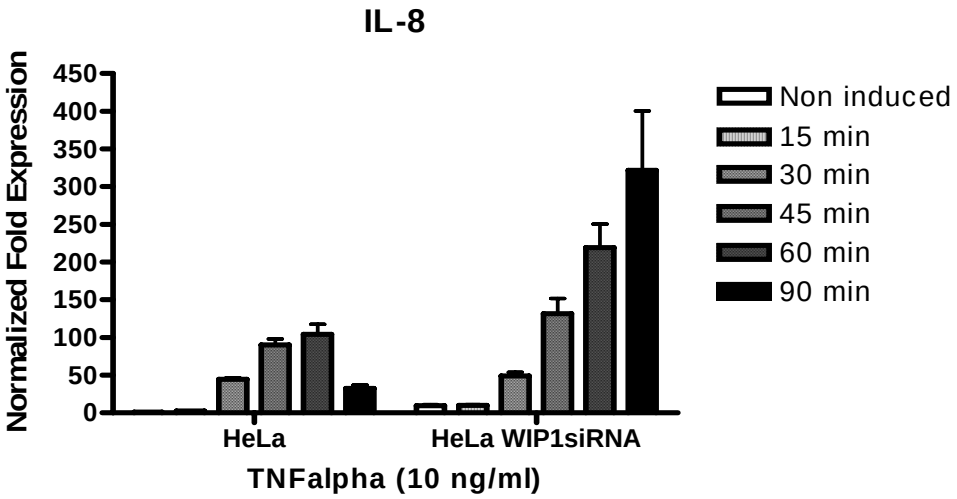

D

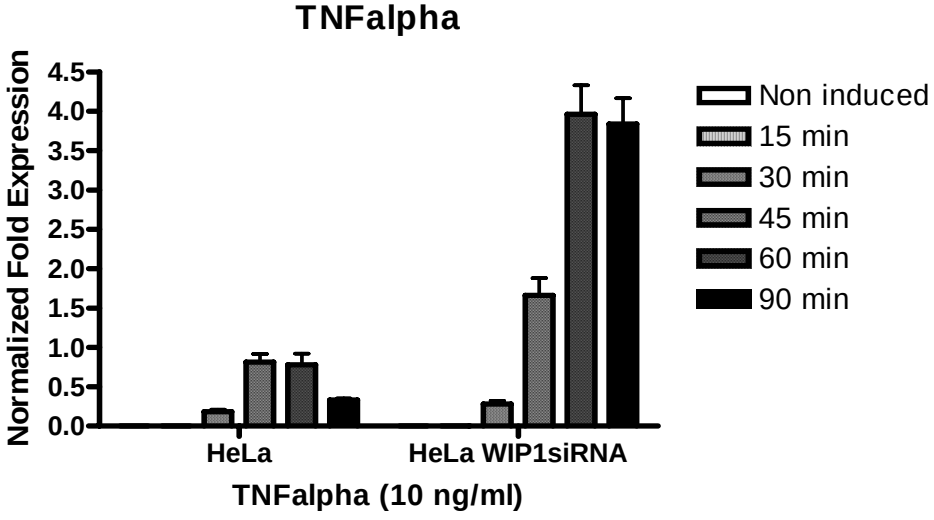

Figure 3.4.2 Knock down of WIP1 increases activation and phosphorylation on serine 536 of p65.

A) Endogenous WIP1 protein levels were knocked down using lentivirus in HeLa cells and quantitated using a densitometer (Bio-rad laboratories). B) Control and WIP1 knockdown HeLa cells were treated with 10 ng/ml of TNFα for 15, 30, 45, 60 and 90 min. Treated cells were harvested and lyzed in RIPA lysis buffer. Phosphorylated p65, total p65 and total IκBα proteins were analyzed using whole cell lysates in western blot. Anti-actin was used as a loading control. C & D) NF-κB activation was ascertained through the measurement of the transcription of its target genes, IL-8 and TNFα in real-time PCR using gene-specific primers. Data is the mean S.D. of two samples in one experiment representative of three independent experiments.

3.5 NF-κB target genes are regulated in a p38 MAPK dependent and independent manner

p38 MAPK is responsible for the indirect phosphorylation of histone H3 surrounding the promoters of NF-κB target genes, therefore promoting the transcription of these genes in inflammation. p38 MAPK can also positively affect the transactivation potential of NF-κB indirectly via the phosphorylation of MSK1 and IKK. Thus, we investigated if p38 MAPK affect NF-κB phosphorylation and its target genes in wildtype and p38 MAPK knockout MEF. As shown in Figure 3.5.1A, TNFα treatment did not lead to activation of p38 (as measured by by threonine 180/tyrosine 182 phosphorylation) in the p38 MAPK knockout MEF. The phosphorylation status of p65 on serine 536 was unaffected by the absence of p38 MAPK as seen in the p38 MAPK knockout MEF, and the kinetics of p65 phosphorylation was comparable to that of the wildtype MEF. We screened a panel of NF-κB target genes (Figure 3.5.1 B & C) in the p38 MAPK knockout MEF and found that genes like IL-6, IRF1 and ICAM were expressed normally in WT MEF but completely abolished in p38MAPK knockout MEF . On the contrary, the mRNA levels of TNFα, IκBα and MCP1 were expressed in the p38 MAPK knockout MEF like as in wildtype MEF.

In view that the WIP1 phosphatase can dephosphorylate p38 MAPK and inactivate p38 MAPK, we check if the effect of WIP1 on the phosphorylation of p65 and the transcription of p65 target genes was due to its direct effect via p38 MAPK. If WIP1 is acting on p65 through p38 MAPK, phosphorylation of p65 should decrease when WIP1 siRNA HeLa cells are treated with p38 MAPK inhibitor SB202190. SB202190 inhibits p38 MAPK activity without affecting its phosphorylation, consistent with the

inhibitor's known mechanism of action, mainly inhibiting p38 MAPK by binding to the ATP site in p38 MAPK (Dmitrieva *et al*., 2002). The phosphorylation of p65 in the WIP1 siRNA HeLa cells treated with p38 MAPK inhibitor remain the same as in wildtype HeLa cells (Figure 3.5.2 A & B). The mRNA levels of IL-6 and IL-8 were elevated in WIP1 siRNA HeLa cells but the addition of a p38 MAPK inhibitor diminished IL-6 and IL-8 mRNA expression level (Figure 3.5.2C), whereas the gene expression of TNFα was unaffected in the presence or absence of p38 MAPK inhibitor (Figure 3.5.2D).

Figure 3.5.1

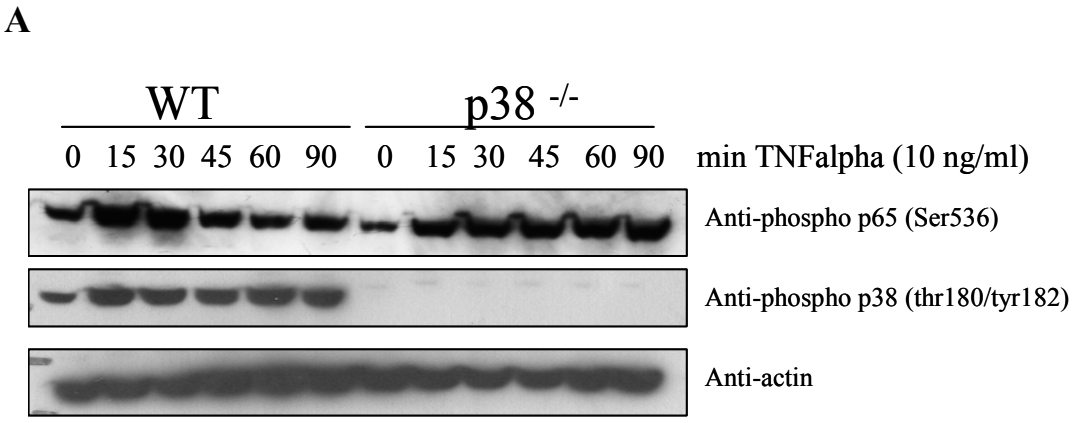
A
WT
p38 -/-
0 15 30 45 60 90 0 15 30 45 60 90 min TNFalpha (10 ng/ml)
Anti-phospho p65 (Ser536)
Anti-phospho p38 (thr180/tyr182)
Anti-actin

Figure 3.5.1

B **p38 MAPK dependent genes**

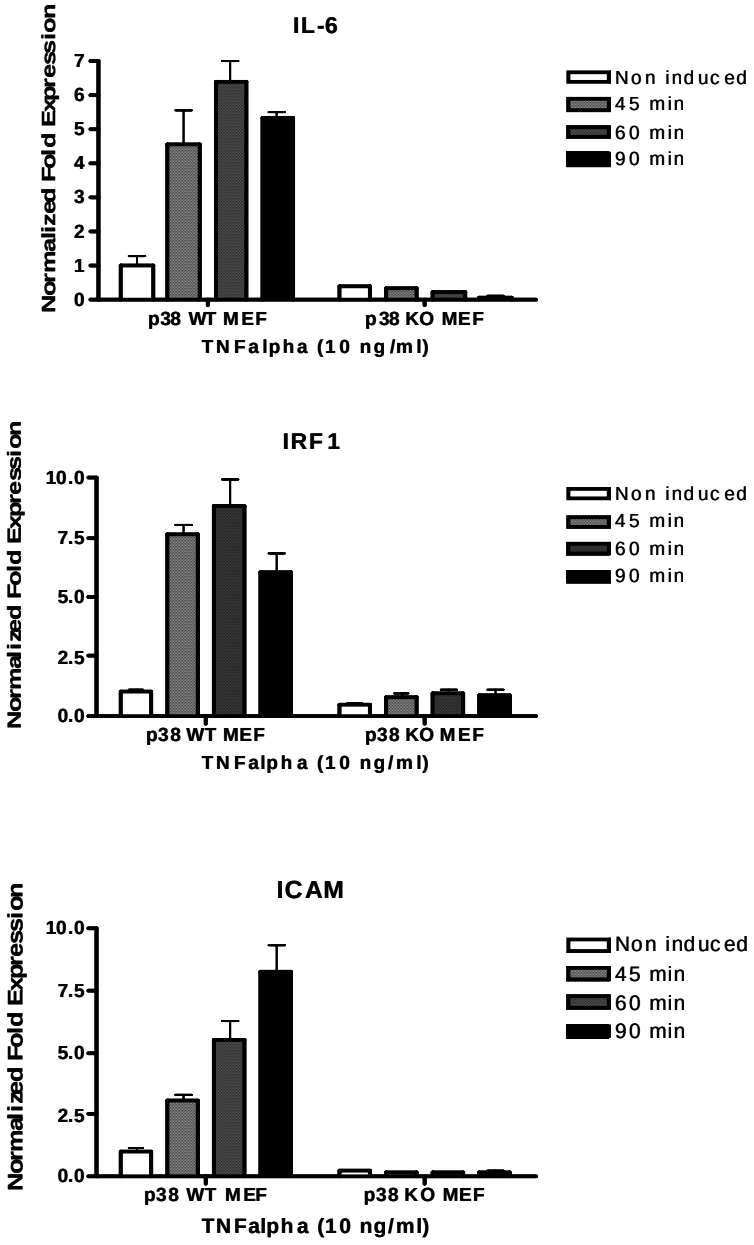

Figure 3.5.1

C **p38 MAPK independent genes**

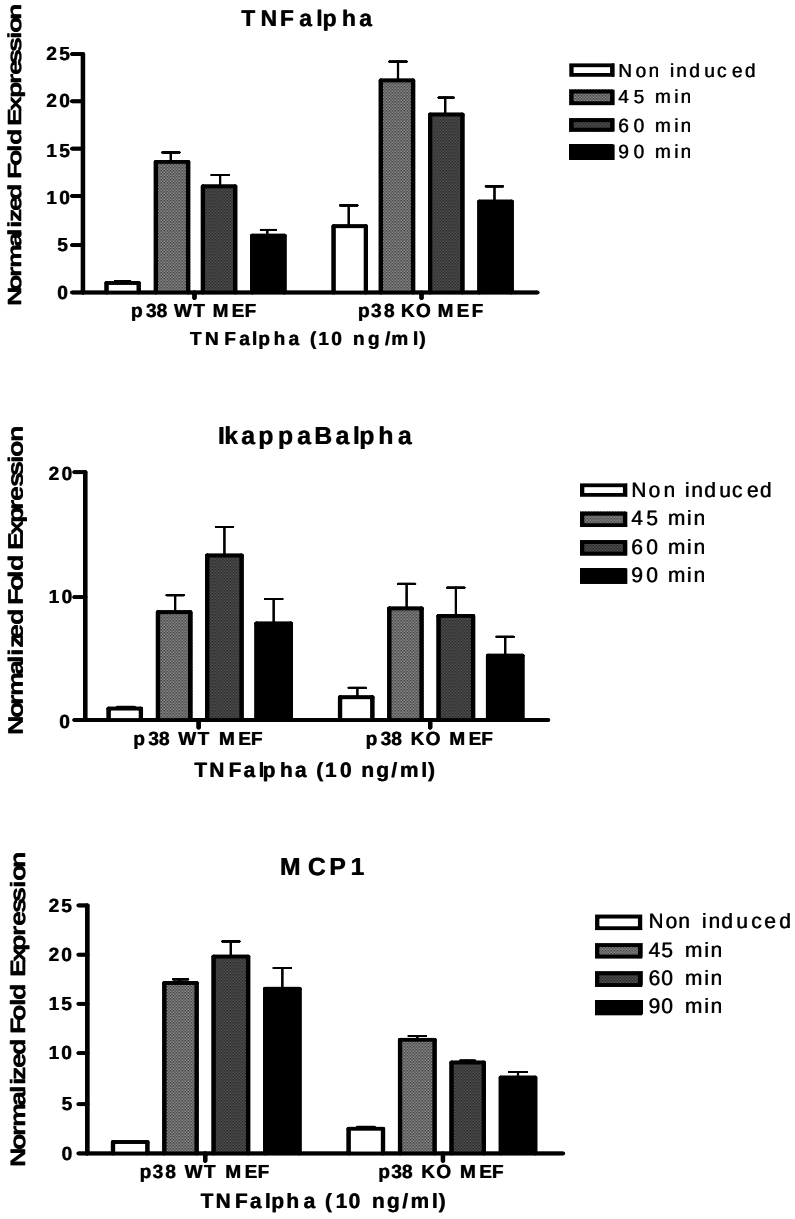

Figure 3.5.1 NF-κB target genes are regulated in a p38 MAPK dependent and p38 MAPK independent manner.

A) WT and p38 MAPK knockout MEF were treated with 10 ng/ml of TNFα for 15, 30, 45, 60 and 90 min. Treated cells were harvested and lyzed in RIPA lysis buffer. Phosphorylated p65 and total p38 MAPK were analyzed using whole cell lysates in western blot. Anti-actin was used as a loading control. B & C) NF-κB activation was ascertained through the measurement of the transcription of its target genes, IL-6, IRF1, ICAM, TNFα, IκBα and MCP1 in real-time PCR using gene specific primers. Data is the mean S.D. of two samples in one experiment representative of two independent experiments. WT and p38 MAPK knockout MEF were treated with 10 ng/ml of TNFα for 45, 60 and 90 min. These target genes are further classified into p38 MAPK dependent or independent genes.

Figure 3.5.2

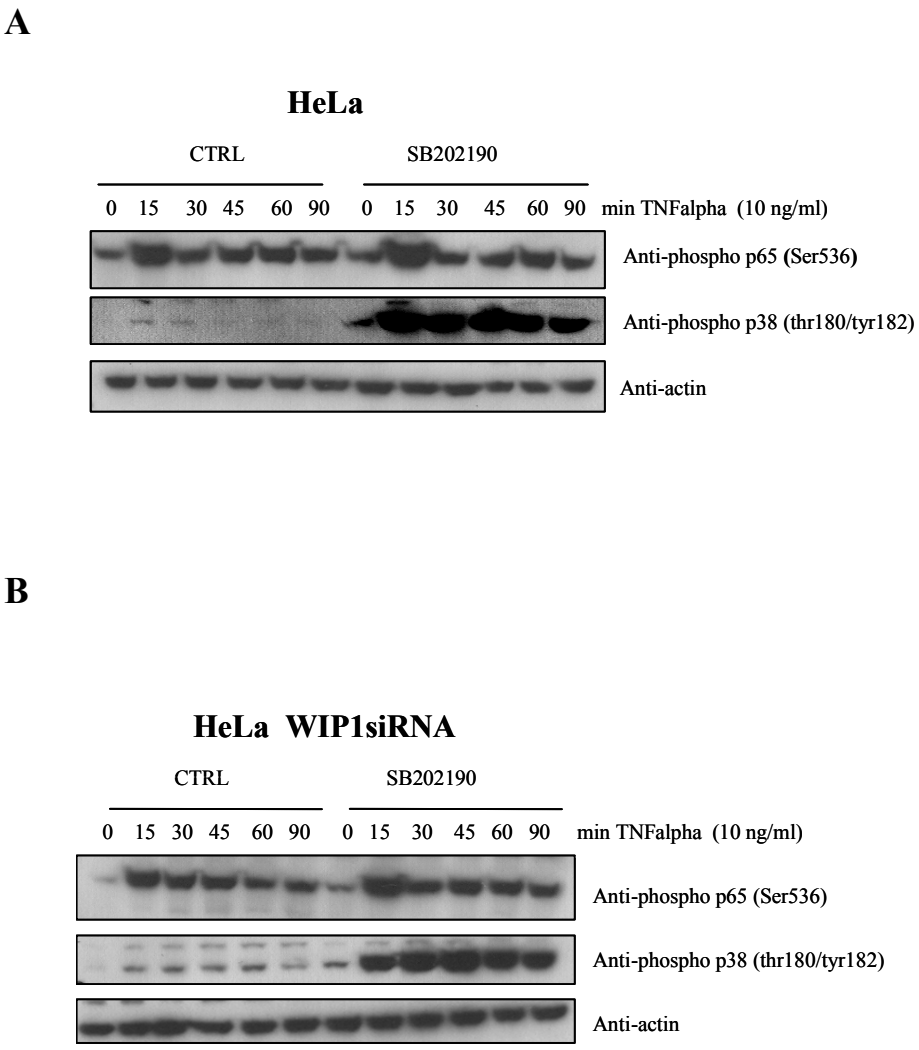
A
HeLa
CTRL
SB202190
0 15 30 45 60 90 0 15 30 45 60 90 min TNFalpha (10 ng/ml)
Anti-phospho p65 (Ser536)
Anti-phospho p38 (thr180/tyr182)
Anti-actin
B
HeLa WIP1siRNA
CTRL
SB202190
0 15 30 45 60 90 0 15 30 45 60 90 min TNFalpha (10 ng/ml)
Anti-phospho p65 (Ser536)
Anti-phospho p38 (thr180/tyr182)
Anti-actin

Figure 3.5.2

C **p38 MAPK dependent genes**

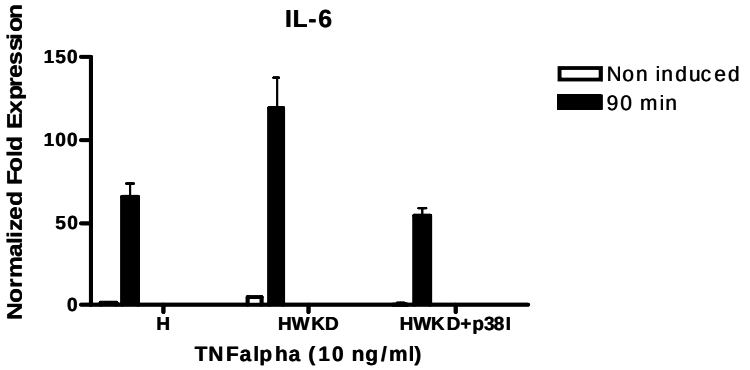

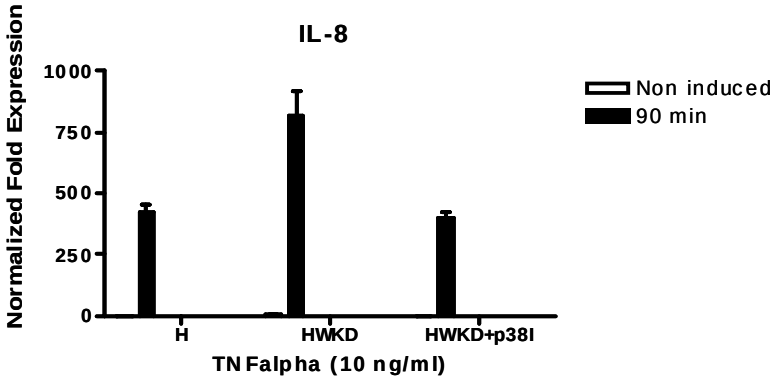

D **p38 MAPK independent genes**

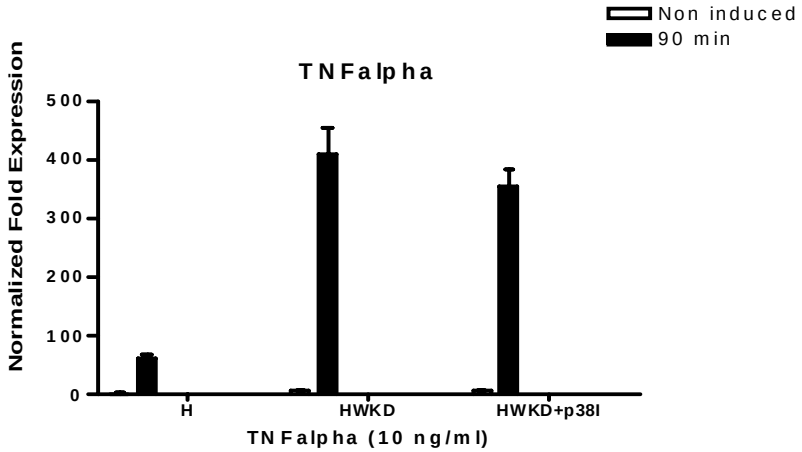

Figure 3.5.2 NF-κB target gene independent of p38 MAPK regulation.

A & B) Control and WIP1 siRNA HeLa cells were treated overnight with 10 μM p38 MAPK inhibitor SB202190 (p38I), and subsequently with 10 ng/ml TNFα for 15, 30, 45, 60 and 90 min. Phosphorylated p65 on serine 536 and p38 MAPK threonine 180 and tyrosine 182 were analyzed in western blot using specific phospho-antibody. C & D) NF-κB activation is ascertained in WIP1siRNA HeLa (HWKD) cells by measuring NF-κB target genes IL-6, IL-8 and TNFα in real-time PCR using gene-specific primers. Data is the mean S.D. of two samples in one experiment representative of two independent experiments. These target genes are further classified into p38 MAPK dependent or independent genes.

3.6 PP2A phosphatase does not synergize with WIP1 in regulating NF-κB dependent transcription

The PP2A phosphatase has been the most well-documented phosphatase that dephosphorylates p65, and its signaling component in the NF-κB signaling pathway by far. We investigated the possibility of a co-operation of PP2A and WIP1 phosphatase in dephosphorylating p65, and "switching off" p65 activation. Okadaic acid is a toxic polyether fatty acid produced by dinoflagellates, and is a potent inhibitor of PP2A. Ozaki *et al.* demonstrated that 100 nM of okadaic acid enhances phosphorylation of p65 on serine 536, the consequential translocation of NF-κB from the cytosol to the nucleus, and the stimulation of NF-κB transcriptional activity in luciferase assay in osteoblastic MG63 cells (Ozaki *et al*., 2006). Although treating HeLa cells with 25 nM of okadaic acid is a concentration that is lower than what is published in the literature, it is still effective in stimulating the phosphorylation of p65 on serine 536. We observed an increment in p65 phosphorylation in okadaic acid treated cells as compared to control cells (Figure 3.6A). Next, we treated WIP1 siRNA HeLa cells with 25 nM okadaic acid to see if inhibiting PP2A would bring about an increment of p65 phosphorylation. As shown in Figure 3.6B, adding okadaic acid to WIP1 siRNA cells do not enhance p65 phosphorylation, therefore there may not be a synergistic effect of PP2A and WIP1. Next, we investigated if the inhibition of PP2A in WIP1 siRNA HeLa cells has any effect on p65 transcription. Inhibiting PP2A in HeLa cells brought an increase in the mRNA transcript of IL-6, IL-8 and TNFα as compared to untreated cells. However, inhibiting PP2A in WIP1 siRNA HeLa cells did not result in a further increase in the transcription of these NF-κB target

genes when compared to wildtype HeLa cells treated with okadaic acid or WIP1siRNA HeLa cells (Figure 3.6 C).

Figure 3.6

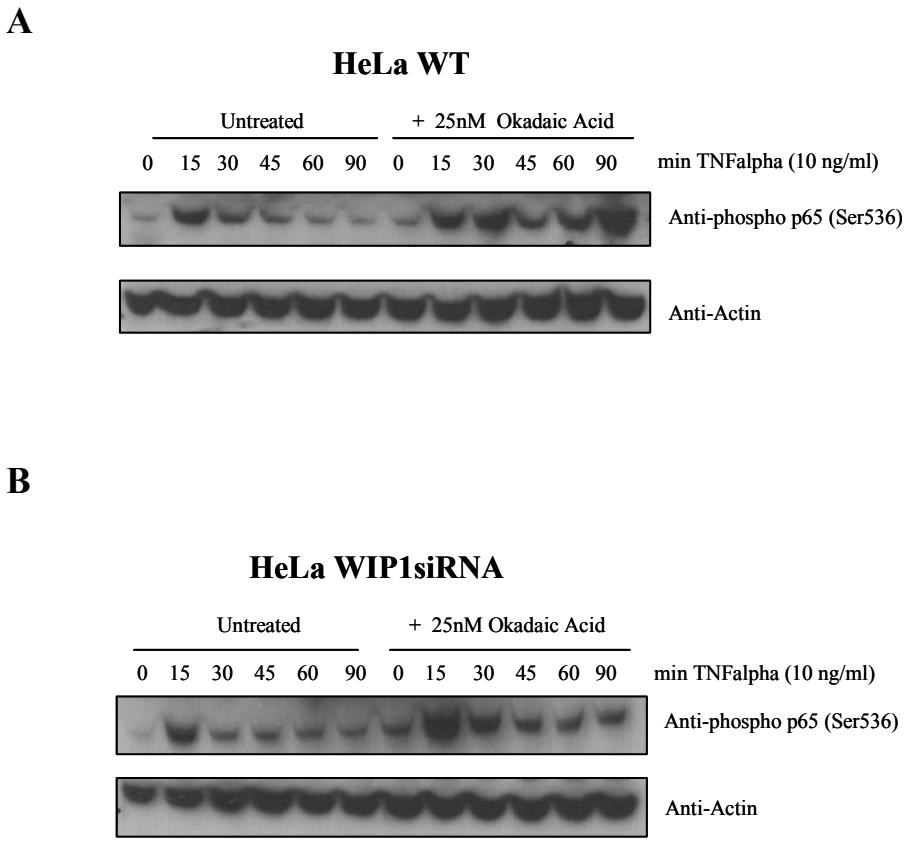
A
HeLa WT
Untreated
+ 25nM Okadaic Acid
0 15 30 45 60 90 0 15 30 45 60 90
min TNFalpha (10 ng/ml)
Anti-phospho p65 (Ser536)
Anti-Actin
B
HeLa WIP1siRNA
Untreated
+ 25nM Okadaic Acid
0 15 30 45 60 90 0 15 30 45 60 90
min TNFalpha (10 ng/ml)
Anti-phospho p65 (Ser536)
Anti-Actin

Figure 3.6 PP2A does not synergize with WIP1 to regulate NF-κB dependent transcription.

WIP1 siRNA (B) and wildtype HeLa (A) cells were pre-treated with 25 nM of okadaic acid for 12-16 hours before stimulating the cells with 10 ng/ml TNFα. Treated cells were lyzed in RIPA lysis buffer and whole cell lysates were analyzed with p65 serine 536 phospho-antibody in western blot. Anti-actin antibody was used as a loading control.

Figure 3.6

C

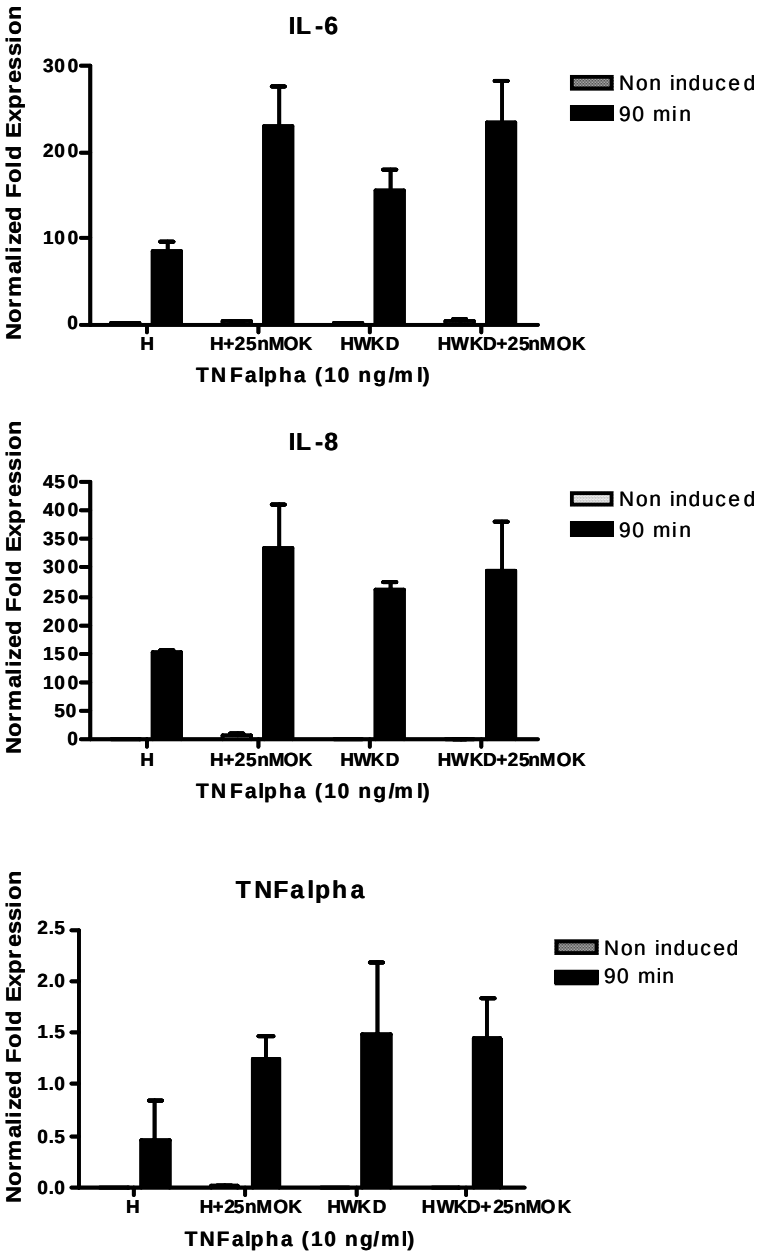
IL-6
Normalized Fold Expression
300
200
100
0
H
H+25nMOK
HWKD
HWKD+25nMOK
TNFalpha (10 ng/ml)
Non induced
90 min
IL-8
Normalized Fold Expression
450
400
350
300
250
200
150
100
50
0
H
H+25nMOK
HWKD
HWKD+25nMOK
TNFalpha (10 ng/ml)
Non induced
90 min
TNFalpha
Normalized Fold Expression
2.5
2.0
1.5
1.0
0.5
0.0
H
H+25nMOK
HWKD
HWKD+25nMOK
TNFalpha (10 ng/ml)
Non induced
90 min

Figure 3.6 PP2A does not synergize with WIP1 to regulate NF-κB dependent transcription.

(C) Sybr green real-time PCR of NF-κB target genes in wildtype (H) and WIP1siRNA HeLa (HWKD) cells pre-treated with okadaic acid (OK), and subsequently treated with TNFα for 90 min using gene-specific primers. Data is the mean S.D. of two samples in one experiment representative of three independent experiments.

3.7 WIP1 dephosphorylates p65 directly on serine 536

So far, we have shown that WIP1 has an effect on p65 phosphorylation on serine 536 *in vivo*. We investigated if WIP1 can directly dephosphorylate p65 on serine 536 *in vitro,* in phosphatase assay. We overexpressed FLAG-tag wildtype p65, and p65 serine 536 to alanine mutant (S536A) in HeLa cells. We stimulated the activation and phosphorylation of p65 with TNFα, and immunoprecipated activated p65. The protein G agarose beads containing bound, activated p65 was incubated with purified WIP1 recombinant protein in phosphatase buffer. As shown in Figure 3.7A lane 2 and 4, WIP1 efficiently dephosphorylates endogenous and activated p65 on serine 536. The p65 S536A mutant do not get phosphorylated at serine 536 and therefore dephosphorylation by WIP1 do not occur (lanes 5-8). Levels of phosphorylated p65 on serine 468 were shown as controls.

Figure 3.7

A

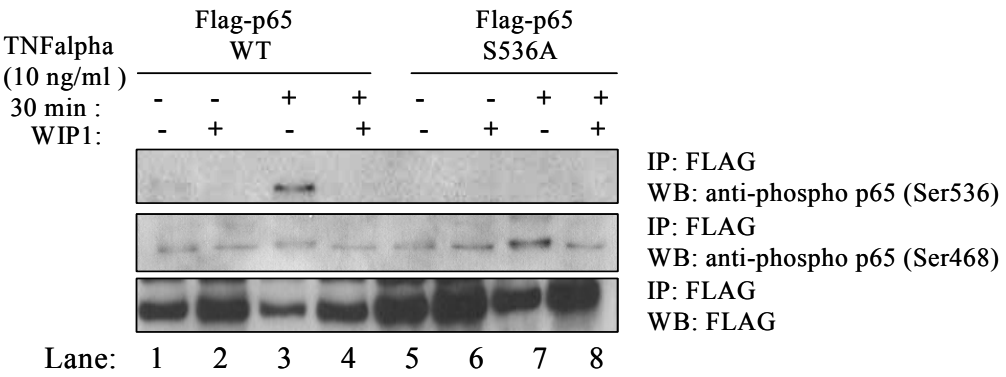
Flag-p65
WT
Flag-p65
S536A
TNFalpha
(10 ng/ml)
30 min :
WIP1:
- - + + - - + +
- + - + - + - +
IP: FLAG
WB: anti-phospho p65 (Ser536)
IP: FLAG
WB: anti-phospho p65 (Ser468)
IP: FLAG
WB: FLAG
Lane: 1 2 3 4 5 6 7 8

B

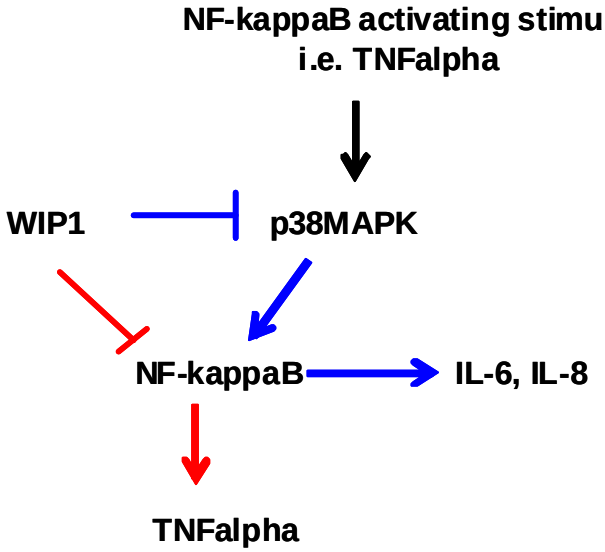
NF-kappaB activating stimuli
i.e. TNFalpha
WIP1
p38MAPK
NF-kappaB
IL-6, IL-8
TNFalpha

Figure 3.7 WIP1 dephosphorylates p65 directly on serine 536.

A) p65 wildtype and S536A mutant expression plasmid were transfected into HeLa cells at 10 μg per 10 cm plate. 48 hours after transfection, the cells were treated with 10 ng/ml of TNFα for 30 min. After treatment, the cells were harvested and lyzed in IP lysis buffer. 1 mg of whole cell lysates was immunoprecipitated with rabbit anti-FLAG antibody. The protein G agarose beads containing immunoprecipitated mutant and activated FLAG-tag wildtype p65 were incubated with recombinant WIP1 protein in phosphatase buffer containing $MgCl_2$ for 60 min. The *in vitro* phosphatase reaction was terminated with SDS loading buffer. Phosphorylated p65 on serine 536 and serine 468 were analyzed in western blot using specific phospho-antibody. The immunoprecipitation of p65 was verified with mouse anti-FLAG antibody. B) A model based on our studies demonstrate that NF-κB activating stimuli induces p38 MAPK pathway activation. WIP1 negatively regulates NF-κB in two ways. Firstly, WIP1 regulates NF-κB by negatively regulating p38 MAPK which has a positive effect on NF-κB target genes IL-6 and IL-8. Secondly, WIP1 negatively regulates NF-κB directly by dephosphorylating NF-κB and affecting its target gene TNFα.

3.8 Discussion

Constituitively activated, phosphorylated p65 has been observed in many cancer cells. Since p65 is a transcription factor for many antiapoptotic genes, it is possible that constituitive action of p65 render cancer cells resistant to apoptotic stimuli. p65 undergo a cycle of phosphorylation and dephosphorylation event regulated by kinases like MSK1, PKA, PKC, RSK1, CKII and IKK and phosphatase PP2A in human cancer cells. The role of phosphatases is to dephosphorylate active p65, to switch off constituitive p65 in cancer cells so that cancer cells can respond to apoptotic stimuli. One possibility of constituitive p65 activation may be due to disruption of phosphatase activity, and hence basal transcriptional activation of p65, which is often observed in cancer.

The WIP1 phosphatase is often overamplified in cancer, and thus its role as an oncogene has been implicated in cancer. It has been postulated that when WIP1 is highly expressed in cancer, dephosphorylates the tumour suppressor p53, whereby p53 is still intact in this cancer cells. WIP1 therefore disrupt p53 proapoptotic function in cancer cells. We have investigated if WIP1 can affect p65 function in apoptosis in cancer cells through p65 target gene regulation, in particular antiapoptotic genes. To our surprise, there is no difference in the mRNA expression of antiapoptotic genes such as Bcl-XL and XIAP, between control cells and WIP1 overexpressing or deficient cells (data not shown). Instead, we found differences in the mRNA expression of inflammatory cytokines, which are NF-κB target genes. Therefore, other than its oncogenic role in cancer, we propose that WIP1 has a role in negatively regulating inflammation by affecting NF-κB phosphorylation and hence the transcription of inflammatory cytokines. Deficiency of WIP1 leads to the increase of phosphorylation of p65 on serine 536 in the

kidneys of WIP1 deficient mice probably suggesting p65 role in inflammation is more apparent in the kidneys (see Figure 3.2B).

By far, the serine/threonine family of protein phosphatase PP1, PP2A and PP2B (calcineurin), and PP2C has been implicated in negatively regulating the NF-κB signaling pathway by dephosphorylating IKK and IκBα. Only PP2A has been shown to physically associate with, and dephosphorylate p65 (refer to section 1.6.2). Here, we showed that the deficiency of endogenous WIP1 phosphatase, which belongs to the PP2C family of serine/threonine protein phosphatases, resulted in the activation and phosphorylation of the p65 subunit of the NF-κB transcription factor, while its overexpression is sufficient to reduce the activation of p65. However, unlike PP2A, the physical interaction between WIP1 and p65 is probably transient, similar to the transient interaction of WIP1 with p53 (Lu *et al.*, 2005), because we did not pull down p65 when we overexpressed WIP1 or when we do the reverse in co-immunoprecipitation experiment (data not shown). It is interesting to note that treatment of HeLa control cells with TNFα for 15 min showed an induction and up-regulation of phosphorylated p65 but this up-regulation was not observed at later time points e.g. 30-90 min when compared to the sustained phosphorylation of p65 in WIP1siRNA cells at these time points (Figure 3.4.2B). It is highly possible that the treatment of the control cells with TNFα may result in the induction and up-regulation of WIP1 which in turn dephosphorylates p65 in the later time

points, whereby TNFα induction and up-regulation on WIP1 occurs at the transcriptional level in the control cells as shown in Figure 3.4.1A, although we have not shown experimentally that TNFα up-regulates WIP1 at the protein level.

p38 MAPK co-ordinates and influence the expression of many proinflammatory cytokines such as IL-6, IL-8 and TNFα through indirect histone phosphorylation in a promoter-specific manner. We show that p38 MAPK do not affect phosphorylation of p65 and the lack of p38 MAPK causes an abolishment of IL-6 mRNA expression in MEF, whereas in the p38 MAPK WT MEF, the expression of IL-6 occurs as usual (Figure 3.5.1B). A marked increase in IL-6 and IL-8 mRNA expression was observed in WIP1siRNA HeLa cells when compared to control HeLa cells. The addition of p38 MAPK inhibitor in WIP1siRNA HeLa cells caused a 2-fold decrease on IL-6 and IL-8 mRNA expression when compared to untreated WIP1siRNA HeLa cells (Figure 3.5.2C). This result suggest that the expression of these cytokines is dependent on p38 MAPK, and that the presence of WIP1 inactivates p38 MAPK, possibly through dephosphorylation of p38 MAPK in these HeLa cells, resulting in the decrease of IL-6 and IL-8 mRNA expression. Interestingly, the expression of TNFα mRNA is the same with or without the addition of p38 MAPK inhibitor (Figure 3.5.2D) in the WIP1siRNA HeLa cells, suggesting the expression of TNFα mRNA, unlike IL-6 and IL-8, is not dependent on p38MAPK. Therefore, WIP1 negative regulation on TNFα mRNA expression is not going through the p38 MAPK signaling pathway, but is definitely a direct effect of WIP1 on p65. The significance of this result is that WIP1 negatively regulates p65 in two ways. Firstly, WIP1 negatively regulates p38 MAPK which has a positive effect on NF-κB target genes IL-6 and IL-8 and secondly, WIP1 negatively

regulates NF-κB directly by dephosphorylating NF-κB and thus affecting its target gene TNFα. (see Figure 3.7B).

Since PP2A may compensate for the lack of endogenous WIP1 phosphatase activity in HeLa cells, we inhibited PP2A activity in the WIP1 siRNA HeLa cells using okadaic acid. We showed that inhibiting PP2A did not lead to a further increase in the expression of TNFα mRNA (Figure 3.6C), and therefore, we investigated if the regulation of the expression of TNFα mRNA is solely dependent on WIP1. True enough, we show that WIP1 can dephosphorylate p65 on serine 536 through *in vitro* phosphatase assay (Figure 3.7A). The phosphorylation of p65 on serine 536, a critical residue that lies in the transcriptional activation domain (TAD), is necessary for p65 transcriptional activation. Hence WIP1 dephosphorylation of p65 on serine 536 thus resulted in the reduced transcription of p65 target gene TNFα. WIP1 by dephosphorylating serine 536 on p65, may disrupt the recruitment of transcriptional co-activator such as p300, necessary for p65 acetylation, and its full transcriptional activation, and the assembly of the transcriptional machinery on κB sites on the TNFα promoter.

The deregulation and overproduction of TNFα has been implicated in human diseases such as autoimmue disorders like rheumatoid arthritis, systemic lupus erythematosus, multiple sclerosis, sepsis and cancer. Therefore, TNF production has to be tightly regulated in order to prevent the onset of such human diseases. TNF can be regulated transcriptionally and post transcriptionally. Transcriptional activation of TNFα occurs through the binding of NF-κB to the TNFα promoter, while post-transcriptional regulation of TNFα occurs by modulation of its mRNA stability (Sun *et al.*, 2007). Therefore consistent with its nuclear localization, WIP1 can negatively modulate NF-κB

transcriptional activity through post-translational modification on p65 to affect TNFα at the transcriptional level, in response to TNF receptor stimulation. WIP1 thus provide a negative feedback signal to control the overproduction of TNFα, in situation where the TNF receptor is over stimulated in an autocrine fashion. Here, we reported a novel finding, and we propose a model whereby WIP1 negatively regulates the classical NF-κB signaling pathway, and may thus serve as a potential useful therapeutic target in the treatment of chronic inflammatory diseases, whereby the overproduction of TNFα is due to the constituitive action of NF-κB (Figure 3.8).

Figure 3.8

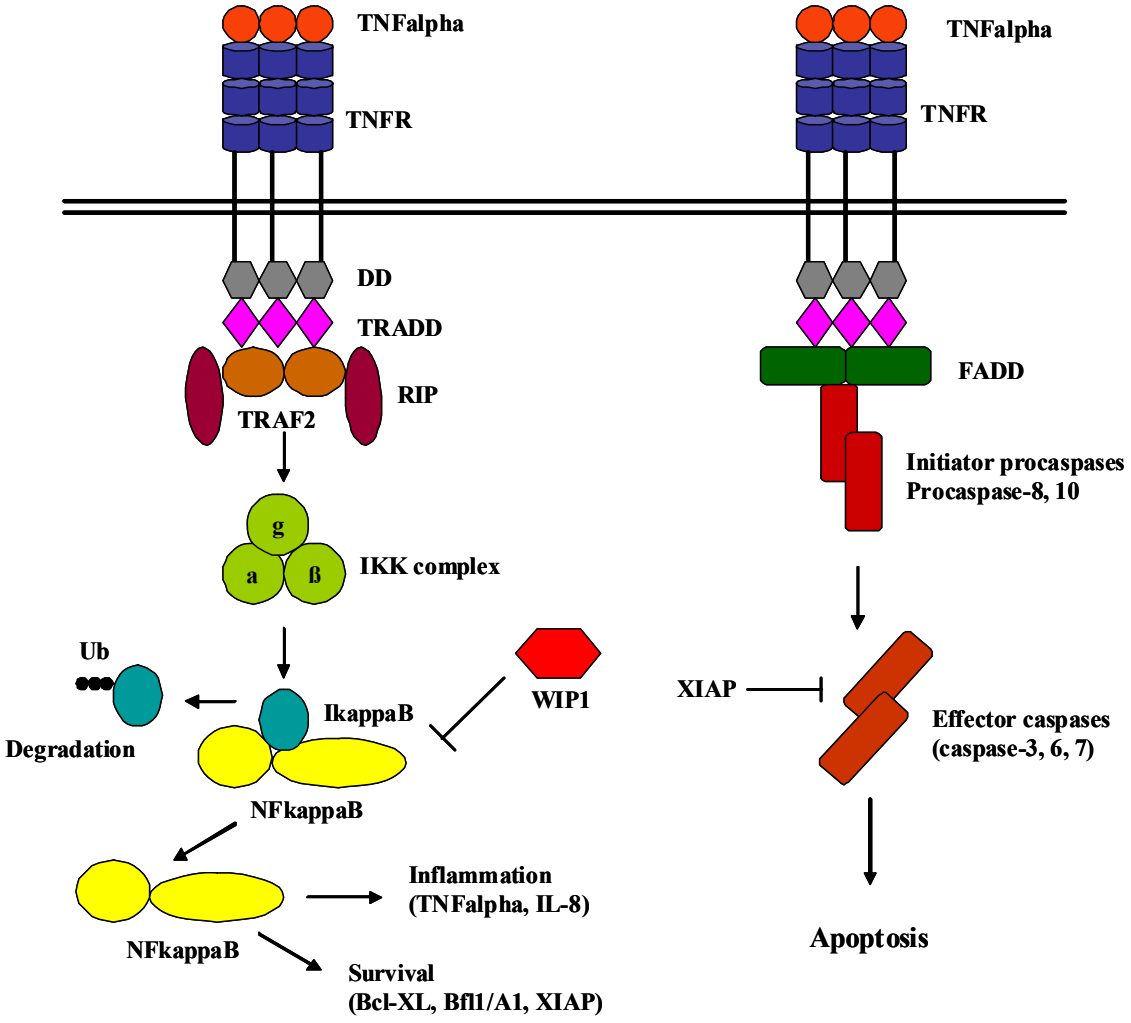

Figure 3.8 Model of WIP1 phosphatase modulating the NF-κB signaling pathway

WIP1 can negatively modulate NF-κB transcriptional activity on the TNFα promoter in the nucleus in response to TNF receptor stimulation, and hence generate a negative feedback loop in the overproduction of TNFα.

3.9 Conclusion and future directions

The investigation of WIP1 phosphatase in regulating the p65 subunit of NF-κB is a fruitful and rewarding venture. *In vivo,* the lack of WIP1 phosphatase in MEF result in the increase basal level of NF-κB target genes IκBα, MIP1α and TNFα, and p65 is also observed to be constituitive phosphorylated on serine 536, particularly in the kidneys of WIP1 deficient mice. We also showed that deficiency of WIP1 phosphatase resulted in the activation of NF-κB in HeLa cells, and its overexpression is sufficient to reduce the transcriptional activity of NF-κB on its target genes in HeLa cells. We also showed that the serine/threonine protein phosphatase PP2A does not synergize with WIP1 to negatively regulate p65. *In vitro*, we showed that WIP1 phosphatase negatively regulated TNFα transcriptionally, independently of p38 MAPK, through the direct dephosphorylation of p65 on serine 536.

Stress responses such as IR and UV-C activate NF-κB. Since WIP1 phosphatase is initially discovered in WMN burkitt's lymphoma cells, and is induced by IR and UV (Fiscella *et al*., 1997), there exist a possibility of WIP1 negatively regulating p65 in respect to DNA damage responses. We have not explored this possibility, although this avenue of future research work is of great significance especially when the ATM kinase (a downstream target of WIP1) is often activated via the stress induced pathway and ATM is required for IR induced IKK-NF-κB pathway (Li *et al*., 2001). WIP1 may indirectly negatively regulate NF-κB via ATM or by directly dephosphorylating p65 in respect to DNA damage responses. Right now, we have only shown WIP1 effects on p65 via the classical NF-κB signaling pathway, future work could be carried out to investigate if WIP1 can affect p65 via the stress induced pathway.

Multiple kinases like MSK1, PKA, PKC, GSK-3β, RSK1, CKII and IKK phosphorylate p65 at various sites such as serine 276, 311, 529 and 536 (Figure 3.9). The closer residue to serine 536 on p65 is serine 529, and the postulated serine 535 on p65. The phospho-antibody used to detect the phosphorylation of p65 on serine 536 may also recognize these sites. We are synthesizing phosphopeptides containing phosphorylated serine 529 (PNGLL**pS**GDEDF), serine 536 (GDEDFS**pS**IADMD), serine 311 (YETFK**pS**IMKKS) and positive control p38 MAPK (TDDEM**pT**G**pY**VAT) for *in vitro* phosphatase assay (phosphatase kinetic studies), to corroborate that WIP1 indeed dephosphorylates p65 on serine 536 only.

Since IKK is known to phosphorylate p65 on serine 536, upon TNFα induction, this may placed IKK in close proximity to WIP1. Hence *in vitro* phosphatase assay of WIP1 using activated IKK as a substrate can be carried out to investigate if WIP1 dephosphorylate IKK, and hence result in the reduction of phosphorylation of p65 on serine 536. This experiment is designed to investigate and confirm WIP1's direct effect on serine 536 of p65 and serves to confirm the reduction of phosphorylated p65 is not due to the consequence of WIP1 dephosphorylating IKK in close proximity.

We have also successfully identified NF-κB target genes that are independent of p38 MAPK regulation in p38 MAPK knockout MEF such as TNFα, IκBα and MCP1, in particular TNFα, which WIP1 phosphatase directly regulates. It would be worthwhile to engage in the search for more NF-κB target genes whose mRNA expression is directly regulated by WIP1 phosphatase, to show that WIP1 phosphatase can regulate other cytokine gene expression in addition to TNFα in the immune system at the transcriptional

level. Microarray studies could be performed to do a genome wide screening of NF-κB target genes that is regulated directly by WIP1 phosphatase.

The phosphorylation on p65 leads to the recruitment of transcriptional co-activator like p300 and the transcriptional machinery to NF-κB target gene promoters. Since WIP1 dephosphorylate p65, it would be ideal to perform co-IP experiments of p65 and p300 in WIP1 overexpressing HeLa cells, to show that WIP1 overexpression may lead to reduction in p65 phosphorylation and p300 interaction and recruitment to NF-κB target gene promoters, chromatin remodeling, and hence the reduction in the mRNA expression of NF-κB target genes. To gather more supporting evidence, experiments such as chromatin immunoprecipitation assay (CHIP) could be performed to show less binding of p65 to its target gene promoters in WIP1 overexpressing HeLa cells.

NF-κB is a transcription factor crucial for the production of proinflammatory cytokines in innate immunity. Macrophages are immune cells that form the first line of defence in the innate immune response, and they are the main source of TNFα when the body experience an infection. Since we show that WIP1 negatively regulates p65 target gene TNFα upon TNF receptor stimulation, we would also like to investigate the physiological relevance of WIP1 phosphatase regulation on TNFα, or other yet unknown inflammatory cytokine production in peritoneal macrophages isolated from wildtype and WIP1 deficient mice.

Figure 3.9

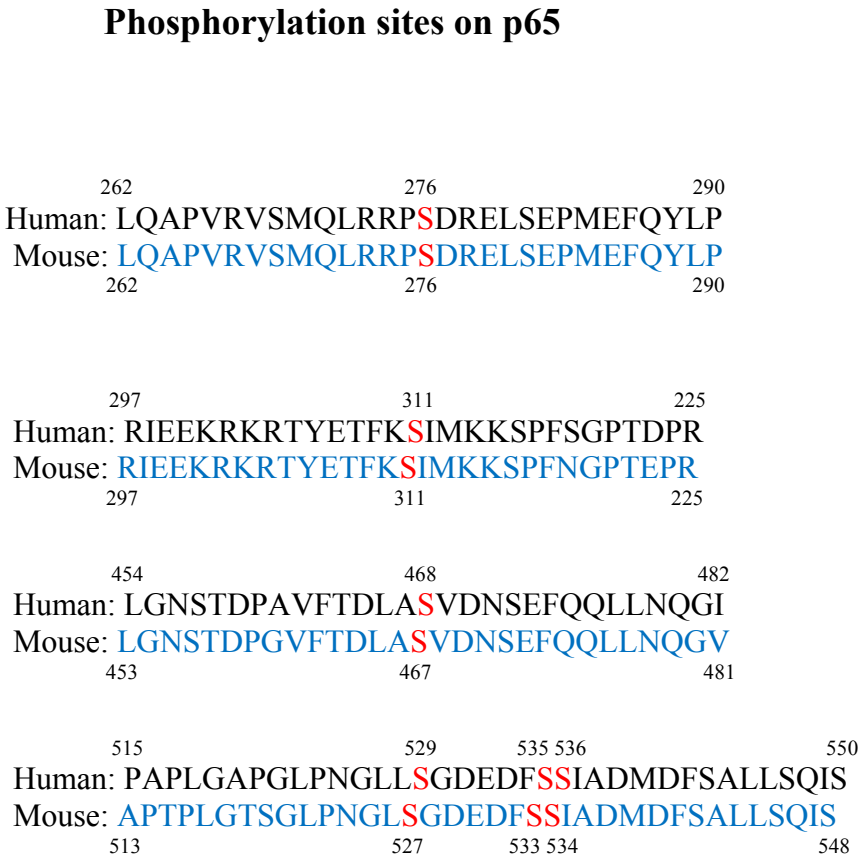

Figure 3.9 Phosphorylation sites on p65

The amino acid sequence of full-length mouse (in blue print) and human (in black print) p65. The phosphorylation sites of p65 are depicted in red.

3.10 Perspective

The fundamental processes in terminating NF-κB activation is not entirely understood, and is an area of intense research. Most efforts in abrogating NF-κB activation has focussed on targeting IKK by using IKK inhibitors or IκB super repressors which are resistant to degradation, and thus forestall NF-κB disassociation from IκBα. In mammalian cells, a natural form of terminating NF-κB activation exist via a negative feedback loop, through the synthesis of IκB mRNA upon NF-κB translocation to the nucleus to bind DNA and activate transcription of its inhibitor, the IκB gene.

Kinjyo *et al* and Nakagawa *et al* showed that Suppresor of signaling-1 (SOCS-1) is a negative regulator of NF-κB, and decreases NF-κB transcriptional activity in LPS signaling (Kinjyo *et al*., 2002; Nakagawa *et al*., 2002). Multiple inflammatory organ diseases, hallmarks of LPS-associated disease, have been observed in SOCS-1 knockout (KO) mice. LPS forms an integral part of gram negative bacteria and can provoke a life-threatening condition called toxic shock. Chronic repeated exposure to LPS cause a transient increase in the threshold of endotoxin tolerance as a way of protection from endotoxic shock syndrome by down-regulating TLR4 and decreased NF-κB activation. The authors simultaneously reported reduced tolerance for LPS in SOCS-1 knockout cells, and the overexpression of SOCS-1 in cells exhibited a dose-dependent attenuation of NF-κB action in reporter gene assay. The phosphorylation of IκBα which leads to its degradation and an indicator for the activation of NF-κB was also observed to be enhanced in SOCS-1 deficient murine peritoneal macrophages. These experimental evidences further support that SOCS-1 protein is a negative regulator of NF-κB.

IKK1 is an essential kinase in the NF-κB alternative pathway that regulates the development and maintenance of secondary lymphoid organs. Macrophages that lack IKK1 have higher efficiency in the phagocytic clearance of *E.coli* K-12 as compared to wild type macrophages. LPS-induced IKK1 mutant macrophages have low levels of IκB proteins, elevated gene expression and production of proinflammatory cytokines and chemokines like TNFα, MIP1α, MCP1 and COX2. Moreover, IKK1 mutant macrophages have accelerated IκBα degradation upon LPS stimulation and most probably is due to the kinase hyperactivity in the IKK complex lacking IKK1 (Li *et al*., 2005; Lawrence *et al*., 2005). Experimental data has therefore shown IKK1 as a negative regulator in the NF-κB classical pathway.

In this section, we report the identification of a novel and direct negative regulator of the p65 subunit of NF-κB which is WIP1 phosphatase, thus adding it to a list of negative regulators of NF-κB signaling, which include the above mentioned SOCS-1 and IKK1. The importance of such a negative regulation by WIP1, is that WIP1 action on NF-κB is direct, in modulating NF-κB signaling, to regulate the expression of the proinflammtory cytokine, TNFα. Steed *et al*., had used structure-based design therapeutics to engineer variant TNF protein that form heterodimers with native TNF that do not bind TNF receptors, and hence unable to activate the TNF receptor pathway by means of sequestration as a possible means of anti-inflammatory biotherapeutics (Steed *et al*., 2003). The significance of our studies provided another avenue of an anti-inflammatory biotherapeutics, other than preventing the live firing of TNF receptor through sequestration, is to target NF-κB post-translation modification through WIP1 phosphatase.

Chapter 4

Microarray studies and functional analysis of genes regulated by the HDAC inhibitor-TSA

4.1 Introduction

The structure of the chromatin is influenced by acetylation which is dependent on the activities of HATs and HDACs. HDACs are chiefly involved in the repression of gene transcription by removing charge-neutralizing acetyl groups from the histone lysine tails resulting in the compaction of the chromatin structure. The "closed" structure of the chromatin prohibits the accessibility of transcription factors, transcriptional co-activators, and the replication machinery from binding to the DNA promoters, and therefore, inhibits gene transcription. Four classes of mammalian HDAC have been identified and they are involved in modeling the structure of chromatin. Class I HDACs consist of HDAC 1, 2, 3, and 8, and class II HDACs consist of HDAC 4, 5, 6, 7 and 9. The third class of HDACs consist of SIRT1-7 which is homologues of yeast and mouse Sir2 and is insensitive to the HDAC inhibitor trichostatin A (TSA) and vorinostat/suberoylanilide hydroxamic acid (SAHA). All class I and II HDACs are zinc-dependent enzymes and class III HDACs require NAD^+ for their enzymatic activity (Blander and Guarante, 2004). Class I HDACs are primarily localized in the nucleus and ubiquitously expressed, while class II HDACs can be primarily cytoplasmic but able to migrate between cytoplasm and nucleus, and are tissue-restricted in expression (Xu *et al*., 2007). Class IV HDACs are represented by HDAC11, which like yeast Hda1 similar 3, has conserved residues in the catalytic core region shared by both class I and II enzymes (Gao *et al*., 2002).

In non-hodgkin's lymphoma, the LAZ3/BCL6 is overexpressed and functions as a transcriptional repressor through the recruitment of HDACs, leading to lymphoid oncogenic transformation (Dhordain *et al*., 1998). Given this example of the

physiological importance of inhibiting HDACs, the rationale of utilizing HDAC inhibitors in the treatment of leukaemias is relevant. Although the mechanism of HDAC inhibitors are not completely understood, inhibiting HDACs bring about at the cellular and molecular level, the accumulation of acetylated histones and transcription factors (which can also be acetylated by HATs), reactivation of epigenetically silenced tumour suppressor genes, cell cycle arrest and apoptosis in cancer. HDAC inhibitor induced cell death include apoptosis by the extrinsic pathway through the up-regulation of death receptors Fas and FasL, Trail and its receptor DR-5 in a mouse model of acute promyelocytic leukemia (APL) induced by valproic acid (Insinga *et al*., 2005); apoptosis by the intrinsic pathway via the release of cytochrome c (Bolden *et al.*, 2006), AIF and Smac/DIABLO from the mitochondrial intermembrane space (Rosato *et al*., 2006; Ruefli *et al*., 2001), and activation of caspase-9 (Bolden *et al.*, 2006) and via reactive oxygen species (ROS)-facilitated cell death (Ungerstedt *et al*., 2005).

The classes of compounds discovered as HDAC inhibitors include: short chain fatty acids/aliphatic acids (for example, 4-phenylbutyrate and valproic acid), hydroxamic acid (Oxamflatin, SAHA and TSA), bezamides (MS-275), and cyclic tetrapeptides (depsipeptide, trapoxin, and apicidin) (Marks *et al*., 2001). In general, HDAC inhibitors have been employed in the treatment of cancer due to their anti-tumourigenic activity on cancer cells but not on normal cells, unlike chemotherapy which kill both cancer and normal healthy cells. Hydroxamic acid such as TSA was initially developed as an antifungal agent, has a potent inhibitory action on class I and class II HDACs, inhibiting HDACs at micromolar or nanomolar concentration compared to other HDAC inhibitors where their effective concentration is at the millimolar range. In addition, TSA also has a

longer half life *in vivo* and bioavailabilities when compared to other HDAC inhibitors (Johnstone, 2002). In this section, we investigated the global expression of genes in human cancer cells treated with TSA using DNA microarray to look for interesting genes and to study their functions and signaling pathways.

4.2 Concentration and time course studies of TSA treatment on HCT116, Jurkat and U937 human cancer cells

It was reported that TSA can inhibit histone deacetylases at nanomolar concentration (Johnstone, 2002). We did a titration studies on a range of human cancer cell lines such as colorectal cancer cells (HCT116), leukemia T-cell (Jurkat) and monocytic (U937) cells to test the toxicity of TSA. As seen in Figure 4.2.1A-D, the lethal concentration (LC50) is 100 nM for HCT116 and Jurkat cells at 24 hours, and the LC50 remains at 100 nM in both cell lines after treatment for 48 hours while the LC50 for U937 is at 1 μM for 24 hours (Figure 4.2.1 E & F). Next, we investigated the effect of 1 μM TSA on all three cell lines at various treatment times. Using sytox-hoechst staining, it was observed that the treatment of these cell lines with 1 μM TSA for 24 hours resulted in apoptosis (Figure 4.2.2). The treatment of these cells with 1 μM TSA for even bigger times of 36 hours and 48 hours is highly toxic leading to apoptosis of all cells (Figure 4.2.3 A, C & E). Therefore, we then treated with 1 μM TSA at time points shorter than 24 hours to determine the optimal time kinetics of the treatment. Figure 4.2.3 B, D and F showed the percentage of surviving cells upon treatment of cells with 1 μM of TSA for 4, 8, 10, 12, 14, 16 and 24 hours. After these time course studies, we selected the TSA concentration at 1 μM and the treatment time of 0, 4, 8, 12 hours as the optimal conditions and time-point for isolation of RNA and microarray hybridization studies.

Figure 4.2.1

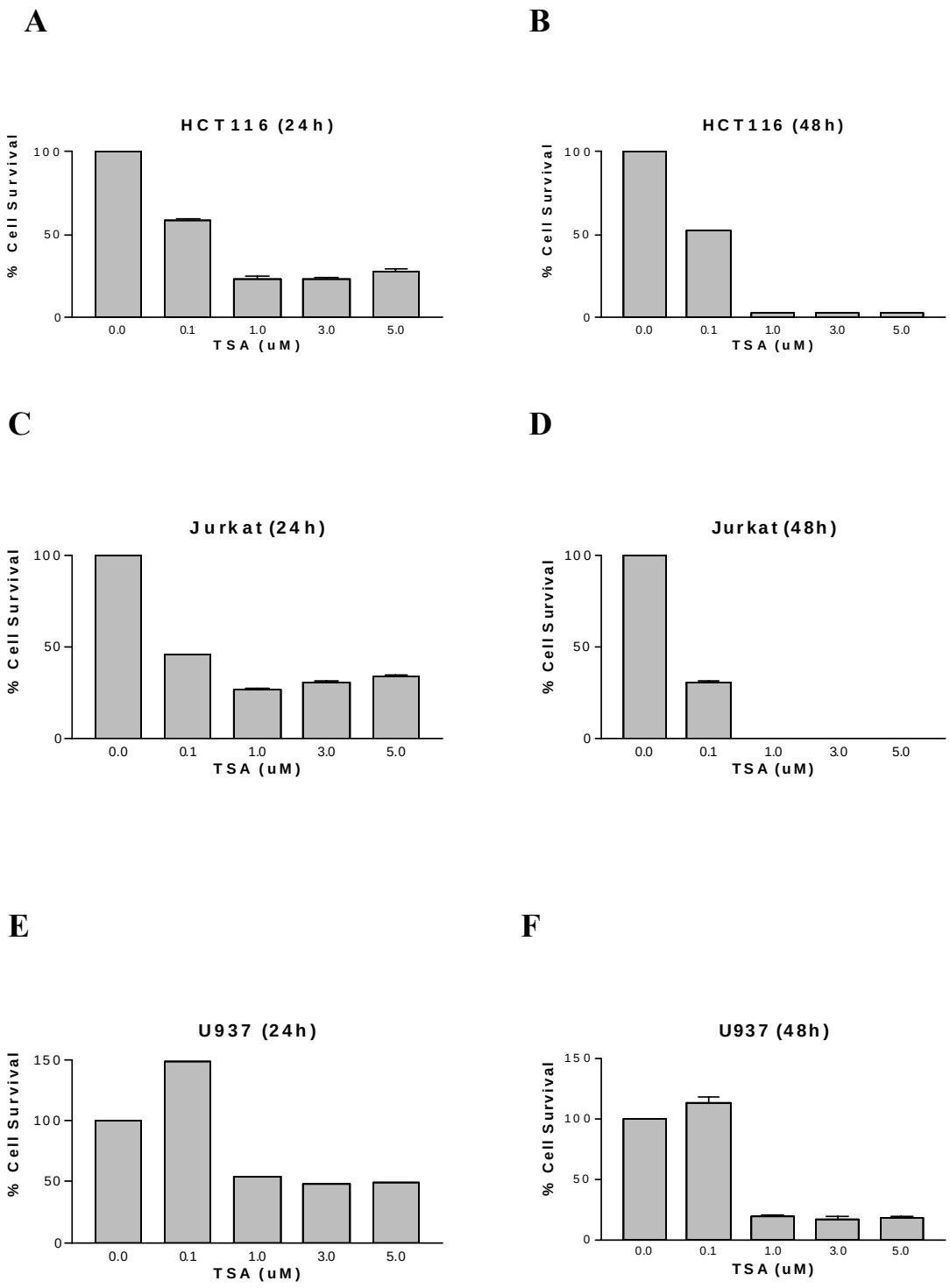
A
HCT116 (24h)
% Cell Survival
100
50
0
0.0
0.1
1.0
3.0
5.0
TSA (uM)
B
HCT116 (48h)
% Cell Survival
100
50
0
0.0
0.1
1.0
3.0
5.0
TSA (uM)
C
Jurkat (24h)
% Cell Survival
100
50
0
0.0
0.1
1.0
3.0
5.0
TSA (uM)
D
Jurkat (48h)
% Cell Survival
100
50
0
0.0
0.1
1.0
3.0
5.0
TSA (uM)
E
U937 (24h)
% Cell Survival
150
100
50
0
0.0
0.1
1.0
3.0
5.0
TSA (uM)
F
U937 (48h)
% Cell Survival
150
100
50
0
0.0
0.1
1.0
3.0
5.0
TSA (uM)

Figure 4.2.1 Concentration studies of TSA treatment on HCT116, Jurkat and U937 cells.

HCT116 (A & B), Jurkat (C & D) and U937 (E & F) cells were treated with 0.1, 1, 3, and 5 μM TSA for 24 and 48 hours and cell survival for each concentration was measured using Wst-1. Data is the mean S.D. of three samples in one experiment representative of two independent experiments.

Figure 4.2.2

A

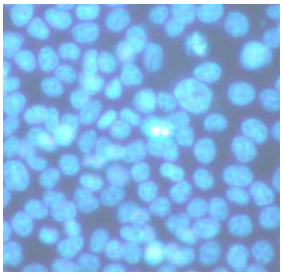

HCT116 Control

B

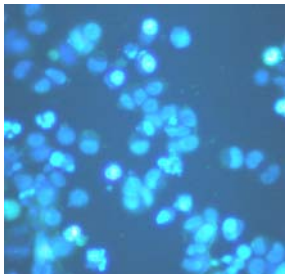

HCT116
(1 uM TSA, 24h)

C

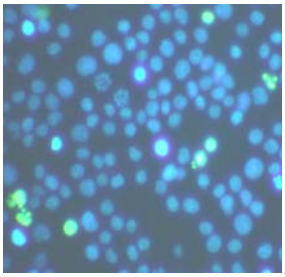

Jurkat Control

D

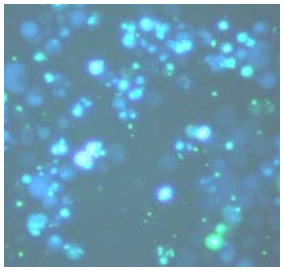

Jurkat
(1 uM TSA, 24h)

E

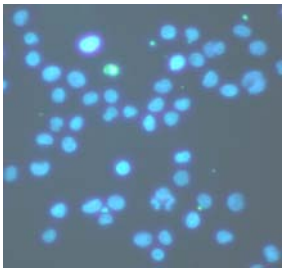

U937 Control

F

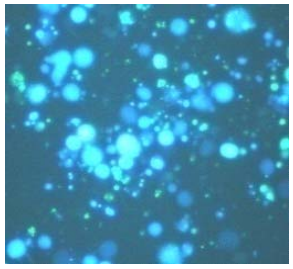

U937
(1 uMTSA, 24h)

Figure 4.2.2 Sytox-hoechst staining of HCT116, Jurkat and U937 cells treated with 1 μM TSA for 24 hours.

Control HCT116, Jurkat, and U937 and TSA-treated cells were stained with sytox-hoechst stain to visualize apoptotic cells. Necrotic cells (damaged and sytox-permeable) were stained green and apoptotic cells (hoechst-stained, condensed and fragmented nuclei) were stained blue.

Figure 4.2.3

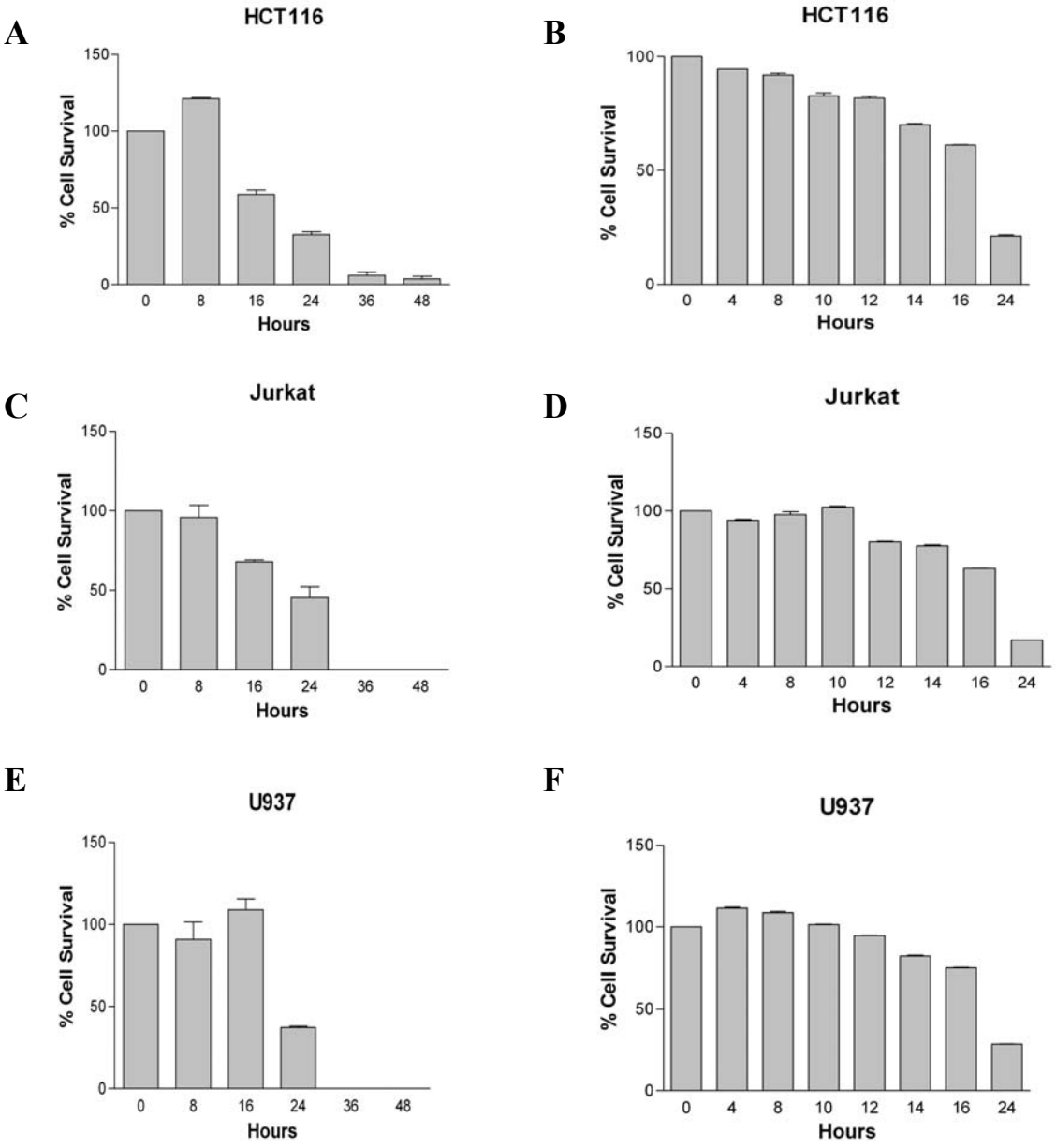
A
HCT116
% Cell Survival
150
100
50
0
0 8 16 24 36 48
Hours
B
HCT116
% Cell Survival
100
50
0
0 4 8 10 12 14 16 24
Hours
C
Jurkat
% Cell Survival
150
100
50
0
0 8 16 24 36 48
Hours
D
Jurkat
% Cell Survival
150
100
50
0
0 4 8 10 12 14 16 24
Hours
E
U937
% Cell Survival
150
100
50
0
0 8 16 24 36 48
Hours
F
U937
% Cell Survival
150
100
50
0
0 4 8 10 12 14 16 24
Hours

Figure 4.2.3 Time course studies of TSA treatment on HCT116, Jurkat and U937 cells.

HCT116, Jurkat and U937 cells were treated with 1 μM TSA for 0, 8, 16, 24, 36 and 48 hours (A, C & E) and for 0, 4, 8, 10, 12, 14, 16 and 24 hours (B, D & F). Cell survival for each time point was measured using Wst-1. Data is the mean S.D. of three samples in one experiment representative of two independent experiments.

4.3 Microarray analysis of genome wide effects in gene expression in response to TSA treatment

To study the effect of inhibiting HDAC on the regulation of gene expression, we used spotted oligonucleotide arrays representing 19, 000 gene set (Genome Institute of Singapore). HCT116, Jurkat, and U937 cells were treated with 1 μM of TSA for 0, 4, 8 and 12 hours. The expression of 723 genes changed significantly when using the criteria of 2-fold cut off after TSA treatment. 111 out of the 723 genes displayed progressive changes in gene expression across the four time points, out of which 36 genes are up-regulated and 75 genes are down-regulated. Among the 111 genes, we selected a few interesting genes for further verification by real-time PCR (Figure 4.3). These genes were genes involved in the NF-κB pathway like lymphotoxin β receptor (LTβR), interleukin 2 receptor (IL-2R), IRAK1 and NF-κB1 (precursor of IκB). Interestingly, we also noticed apoptotic genes to be regulated in all 3 cells lines. They were clusterin, RAD9, BNIP3L, STAT3, PDCD2, Bid, RAD21 and PIGPC1 (Perp). We also verified the expression of these genes by RT-PCR, real-time PCR and western blot.

Figure 4.3

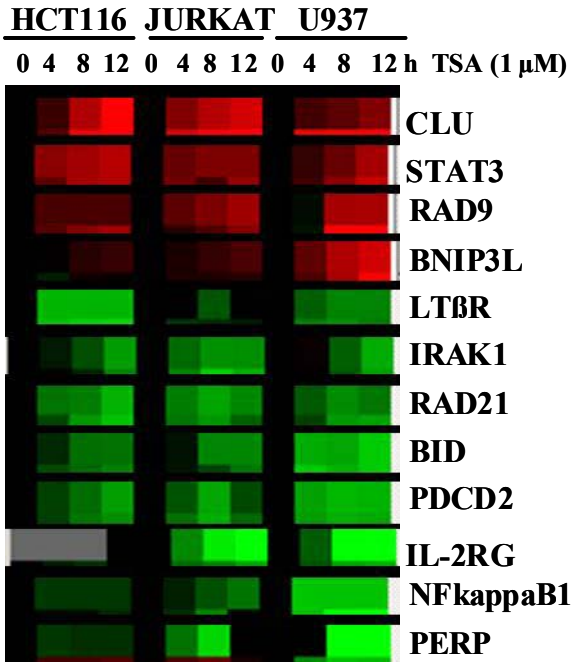

Figure 4.3 Microarray analysis of genome wide effects in gene expression in response to TSA treatment.

Clustering analysis depicting genes that are regulated by TSA. Cluster and treeview were used to cluster genes showing progressive changes (2-fold in 4 time points) in gene expression. Red and green represent up-regulation and down-regulation, respectively, relative to the untreated control (black). The intensity of colour correlates to the magnitude of change. Only selected genes are shown.

4.4 TSA inducible genes

We classified the genes that have expression that exhibited progressive changes across the four time points into TSA inducible and TSA repressed genes. These TSA inducible genes were observed in all three cell lines in the microarray analysis and they are clusterin, STAT3, RAD9 and BNIP3L. However, upon validation by real-time PCR, the transcript of these genes was not regulated across the three cell lines similar to that in the microarray. We found that clusterin was up-regulated in HCT116, Jurkat and U937 cells, STAT3 was up-regulated in HCT116 and U937 cells and not in Jurkat, Bnip3L and RAD9 were up-regulated only in U937 cells. On the contrary, Perp which was shown to be repressed in the microarray was up-regulated in Jurkat cells in the RT-PCR (Figure 4.4A). We confirmed by real-time PCR that the fold change was indeed more than 2-fold, as reflected in the microarray data (Figure 4.4 B & C). Furthermore, we also examined these genes at the protein levels. As seen in Figure 4.4D, the levels of clusterin protein were increased in HCT116, Jurkat and U937, the levels of STAT3 were increased in HCT116 and U937 cells, and RAD9 protein level was increased in U937.

Figure 4.4

A

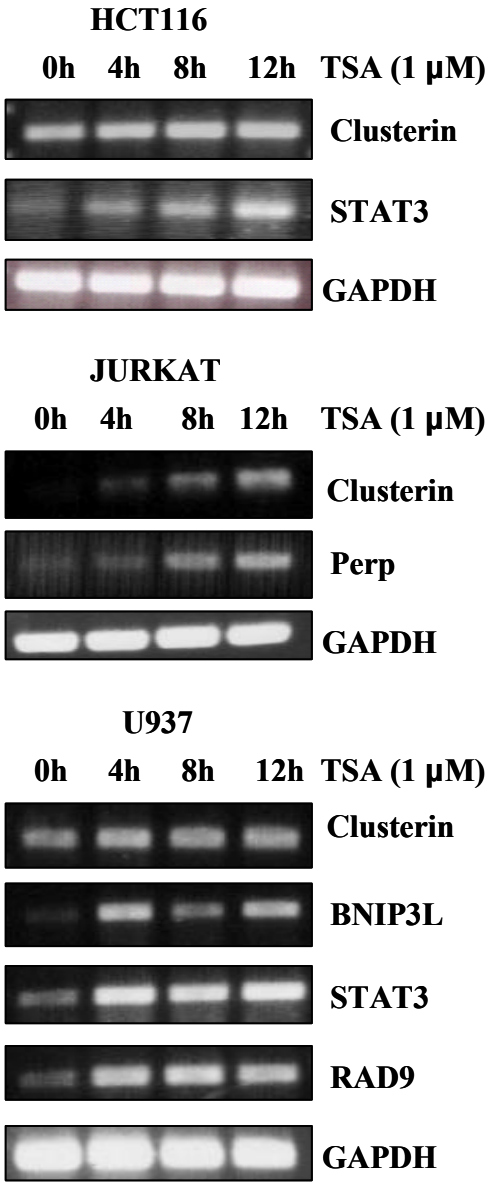
HCT116
0h 4h 8h 12h TSA (1 μM)
Clusterin
STAT3
GAPDH
JURKAT
0h 4h 8h 12h TSA (1 μM)
Clusterin
Perp
GAPDH
U937
0h 4h 8h 12h TSA (1 μM)
Clusterin
BNIP3L
STAT3
RAD9
GAPDH

Figure 4.4

B

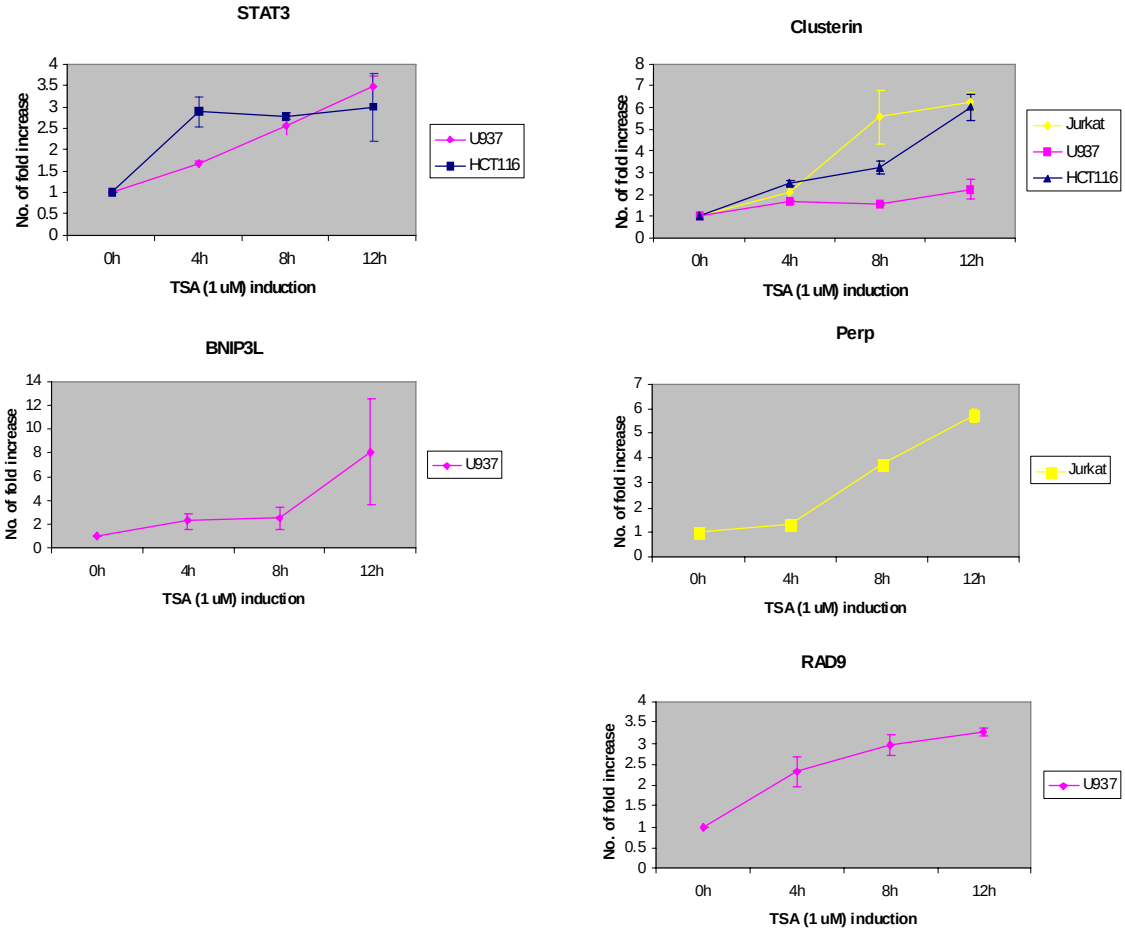

C

Gene	Cell Line	Fold Increase
Clusterin	Jurkat	6.0
	U937	2.0
	HCT116	6.0
STAT3	U937	3.5
	HCT116	3.0
RAD9	U937	3.5
BNIP3L	U937	8.0
PERP	Jurkat	6.0

Figure 4.4

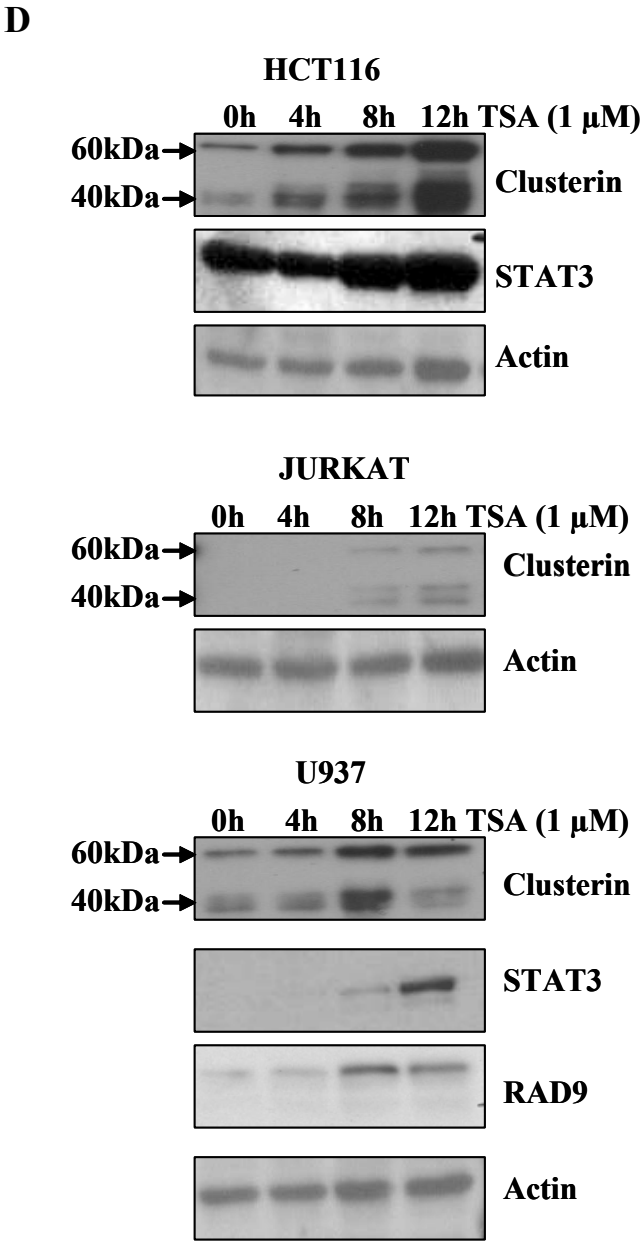
D
HCT116
0h 4h 8h 12h TSA (1 μM)
60kDa
40kDa
Clusterin
STAT3
Actin
JURKAT
0h 4h 8h 12h TSA (1 μM)
60kDa
40kDa
Clusterin
Actin
U937
0h 4h 8h 12h TSA (1 μM)
60kDa
40kDa
Clusterin
STAT3
RAD9
Actin

Figure 4.4 TSA inducible genes.

RT-PCR (A), real-time PCR (B) and western blot (D) of TSA induced genes in the microarray. Actin was used as a loading control in the western blot. RT-PCR and real-time PCR were performed using gene-specific primers and the fold of inducibility by 12 hours TSA treatment for the real-time results was tabulated (C). In (B), data is the mean S.D. of three samples in one experiment representative of three independent experiments.

4.5 TSA repressed genes

The TSA repressed genes that exhibited progressive changes across the four time points in all three cell lines on the microarray are LTβR, IRAK1, RAD21, Bid, PDCD2, IL-2R, and NF-κB1. Interestingly, a number of these genes such as LTβR, IL-2R, IRAK1 and NF-κB1 are associated with the NF-κB signaling pathway. Although the above mentioned genes are reflected on the microarray to be down-regulated, only LTβR, IRAK1, RAD21, Bid, IL-2R and NF-κB1 down-regulation could be validated by real-time PCR. IRAK1 and Bid were down-regulated across all three cell lines, lymphotoxin β receptor in HCT116 and U937 cells, IL-2R in Jurkat and U937 cells, NF-κB1 in HCT116 and Jurkat cells, and RAD21 was down-regulated only in HCT116 cells (Figure 4.5.1 & 4.5.2). Interestingly, the protein expression of Bid and RAD 21 were found not to be induced nor repressed as assessed by western blot, even though their transcripts were verified to be down-regulated in real-time and RT-PCR, strongly indicating that these 2 genes may be further regulated at the post-translational level.

Figure 4.5.1

A

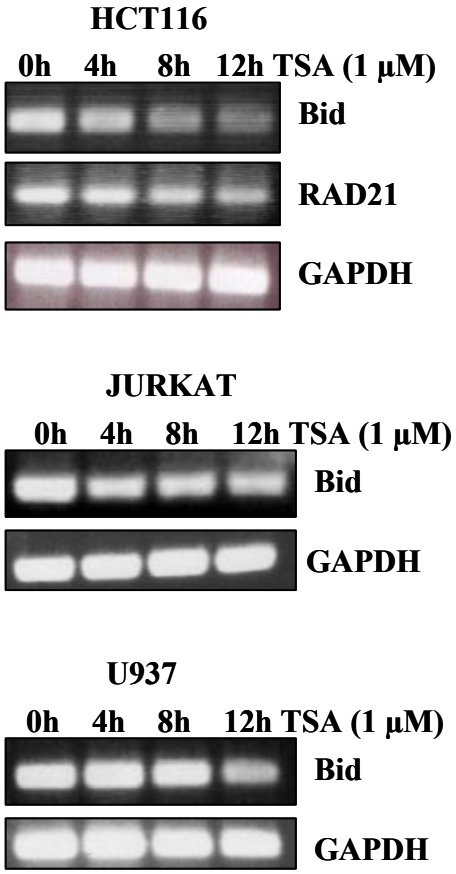
HCT116
0h 4h 8h 12h TSA (1 μM)
Bid
RAD21
GAPDH
JURKAT
0h 4h 8h 12h TSA (1 μM)
Bid
GAPDH
U937
0h 4h 8h 12h TSA (1 μM)
Bid
GAPDH

Figure 4.5.1

B

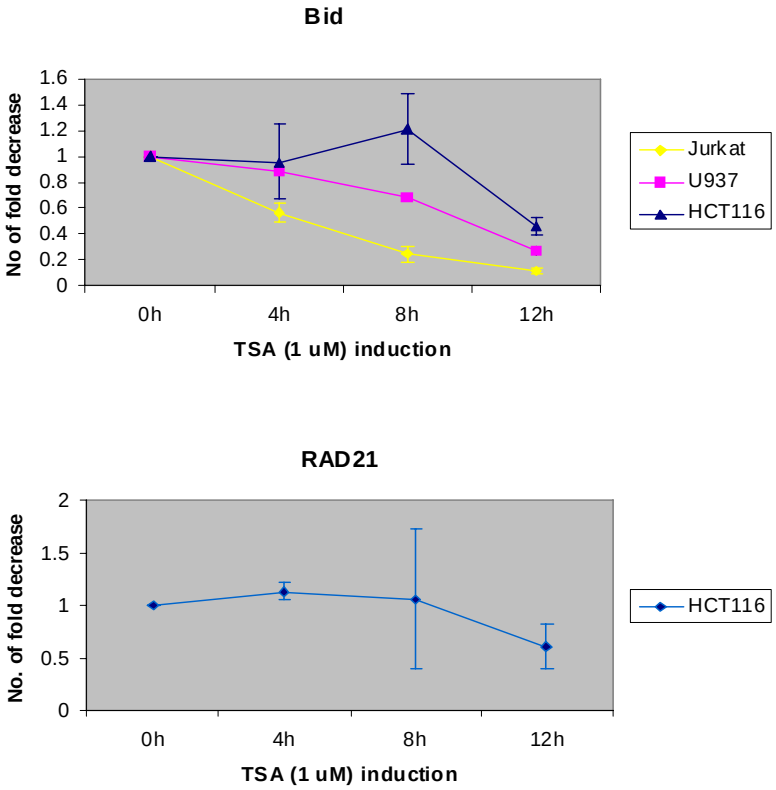

C

Gene	Cell line	Fold decrease
Bid	Jurkat	10.0
	U937	3.0
	HCT116	2.0
RAD21	HCT116	2.0

Figure 4.5.1

D

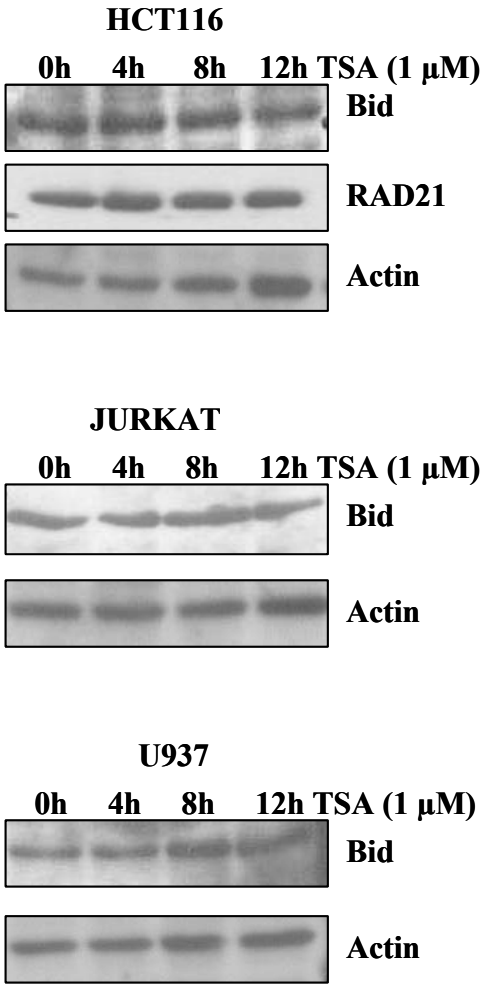
HCT116
0h 4h 8h 12h TSA (1 μM)
Bid
RAD21
Actin
JURKAT
0h 4h 8h 12h TSA (1 μM)
Bid
Actin
U937
0h 4h 8h 12h TSA (1 μM)
Bid
Actin

Figure 4.5.1 TSA repressed genes.

RT-PCR (A), real-time PCR (B) and western blot (D) of TSA repressed genes in the microarray. Actin was used as a loading control in the western blot. RT-PCR and real-time PCR were performed using gene-specific primers and the fold of repression by 12 hours TSA treatment for the real-time results was tabulated (C). In (B), data is the mean S.D. of three samples in one experiment representative of three independent experiments.

Figure 4.5.2

A. Receptors

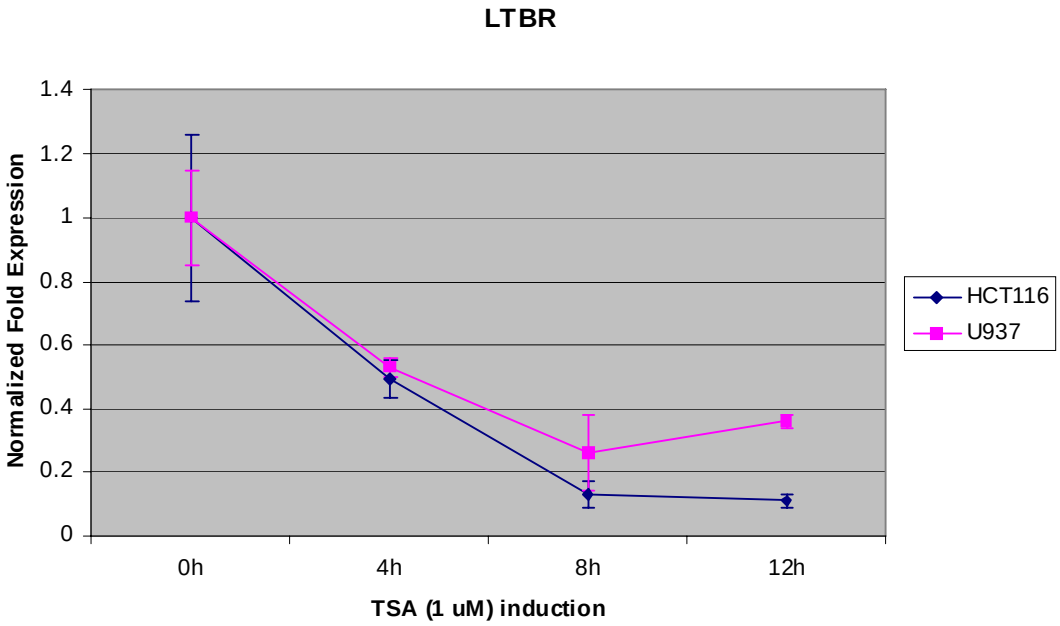

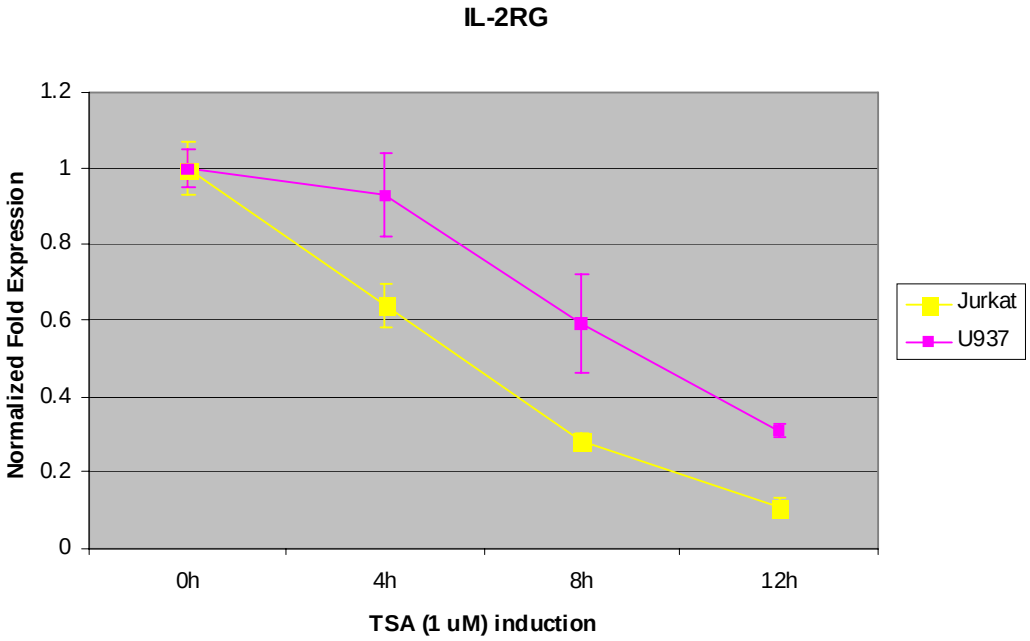

Figure 4.5.2

B. Adaptors

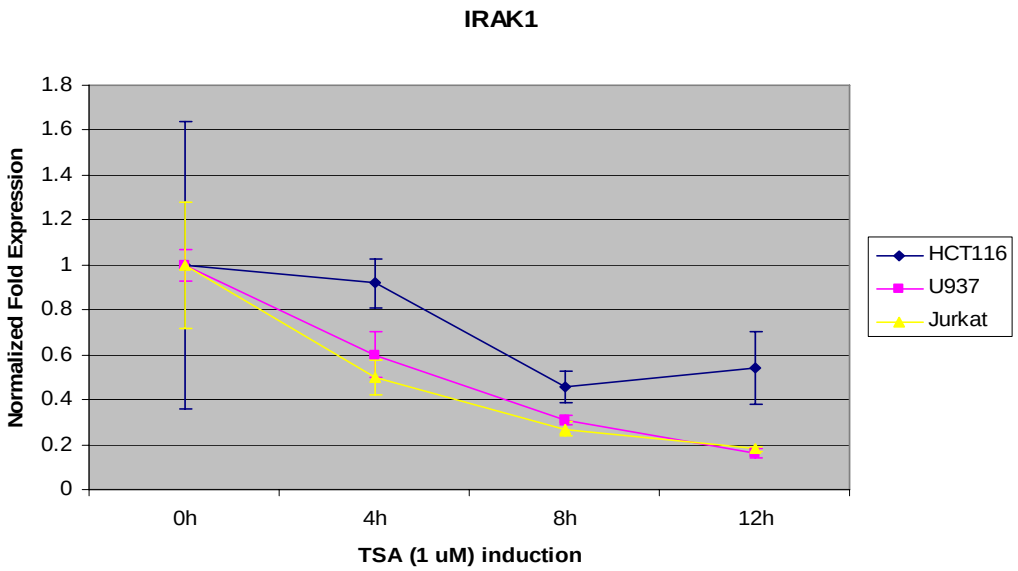

C. Presursors IκBs

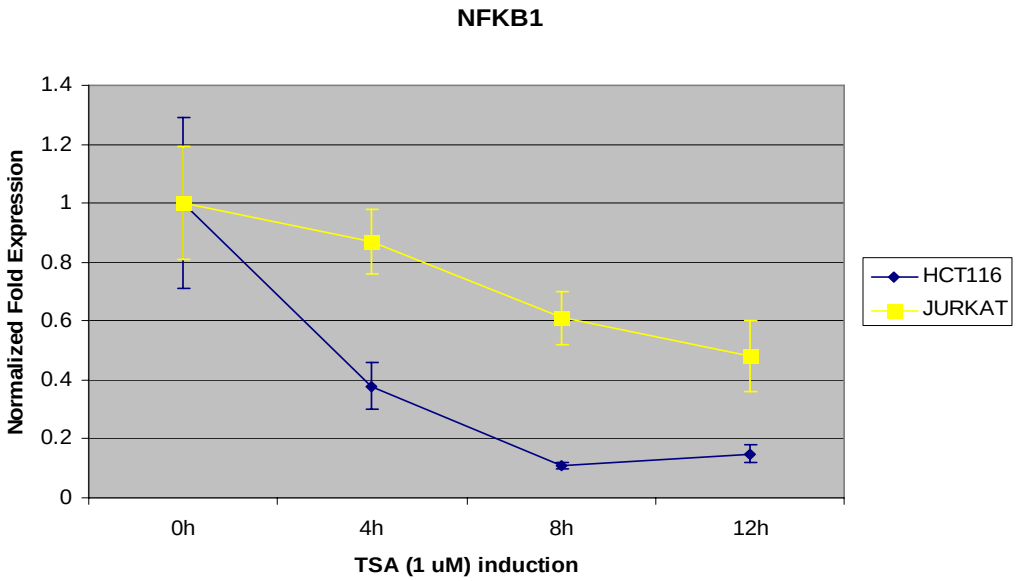

Figure 4.5.2 TSA repressed genes that are in the NF-κB signaling pathway.

Real-time PCR of genes that were repressed are receptors (A), adaptor (B) and precursor IkappaB (C) in the NF-κB signaling pathway in the microarray using gene-specific primers. Data is the mean S.D. of two samples in one experiment representative of two independent experiments.

4.6 Role of Clusterin in TSA induced apoptosis

Clusterin (CLU), also known as apoliprotein J, has been implicated in various physiological processes like carcinogenesis and tumour growth, cell cycle regulation, and apoptotic cell death. Induction of clusterin mRNA and protein levels have been consistently detected in various human malignancies such as bladder, breast, colon, lung, and kidney tumour, and also in cells and tissues undergoing stress. There are two clusterin isoforms in human cells, a secretory form (sCLU) which is believed to be prosurvival and the nuclear form (nCLU) which is proapoptotic (Leskov *et al*., 2003). As seen in Figure 4.4 D, the secreted form of clusterin is a glycosylated protein of 80 kDa, and appears to have two different protein bands of 40 kDa (α and β subunit) and 60 kDa (full-length, uncleaved form) when analyzed on a SDS-PAGE under reducing conditions (Yang *et al*., 1999). In contrast, the 49 kDa nuclear form of clusterin is synthesized from a second AUG start codon resulting in an alternative spliced nCLU mRNA. In response to ionizing radiation (IR), it becomes modified to a 55kDa proapoptotic form, which translocates to the nucleus in MCF-7 cells (Leskov *et al*., 2003).

In our microarray, real-time PCR, RT-PCR and western blot data, we saw a consistent up-regulation of clusterin in all three cell lines. Since clusterin has been implicated in apoptosis, we seeked to investigate if the induction of clusterin by TSA participate in apoptotic events in these cells. Firstly, we investigated the inducibility of the proapoptotic form of nCLU in HCT116, Jurkat, and U937 cells treated with TSA for 12 hours. We extracted the nuclear fraction of these treated cells and analyzed the expression of the nuclear form of clusterin by western blot. As seen in Figure 4.6.1A, there was no accumulation of clusterin in the nucleus when cells were treated with TSA.

Hence, it is highly probable that the induced expression seen resulted in the increased in the secretory form of clusterin. Next, we sought to elucidate if the sCLU is involved in apoptosis of the TSA-treated cell lines. We knocked down the expression of secretory clusterin using pre-designed siRNA oligos from Ambion. We selected siRNA oligonucleotides (ID numbers: 2566, 2568 and 2745) from the Ambion database and tested the efficiency of these oligonucleotides to silent the mRNA of clusterin. As shown in Figure 4.6.1B, oligo ID number 2566 and 2745 efficiently knocked down the expression of clusterin. Subsequently, these two oligo were utilized to elucidate the physiological effect of knocking down clusterin protein, with respect to TSA induced apoptosis. Intriguingly, the reduction in the protein levels of sCLU decreased the proportion of apoptotic cells as determined by sub-G_1 phase of treated cells stained with PI (Figure 4.6.1C). Our results show for the first time, that sCLU, similar to nCLU, also has a proapoptotic function, since the reduction of clusterin levels resulted in lesser cell death. Next, we were interested to find out if the induction of clusterin gene expression upon TSA treatment was a direct effect of inhibiting HDAC or an indirect effect through the regulation of other genes by TSA. This is a relevant question since Tingan Chen *et al.* showed that the induced expression of clusterin in 5-flurouracil (5-FU) and anti-Fas antibody treated HCT116 cells is largely dependent on p21 since cells lacking p21 lacked induction of expression of clusterin upon similar treatment (Chen *et al*., 2004). In addition, they also showed that the treatment of p53-deficient HCT116 cells with 5-FU and anti-Fas antibody resulted in the overexpression of clusterin protein. Since the expression of p21 and p53 could be induced by TSA in cells (Johnstone, 2002), we investigated if clusterin up-regulation in TSA-treated cells was a consequence of p21 and

p53 inducible expression. To answer this question, we used HCT116 cells devoid of p21 and p53, treated the cells with TSA and determined the expression of clusterin in these cells. The expression of clusterin protein was induced and the pattern of induction was similar to those of wildtype HCT116 cells (Figure 4.6.2 A & C). This suggested that clusterin expression in our model was independent of p21 and p53. We next investigated if clusterin-inducible expression required *de novo* protein synthesis. The expression of clusterin both in the basal and TSA-treated levels were sensitive to cyclohexamide treatment (Figure 4.6.2E), indicating that *de novo* protein synthesis is required.

Figure 4.6.1

A

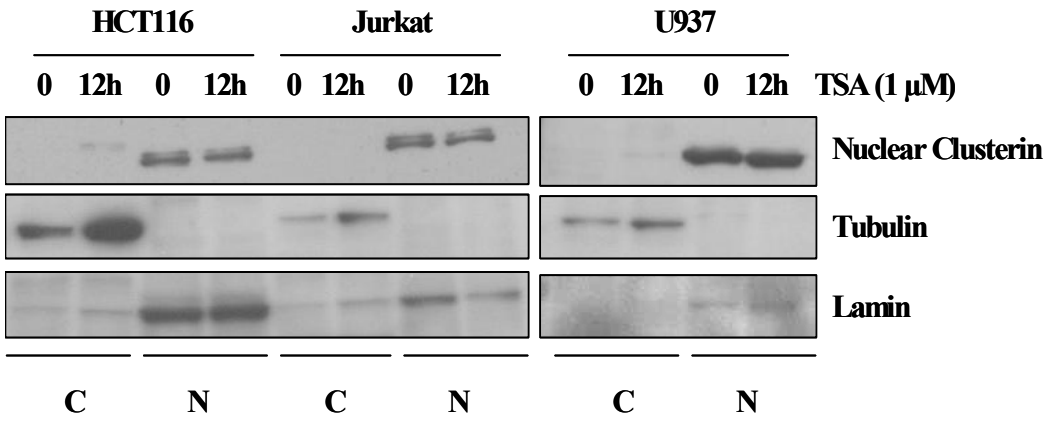

B

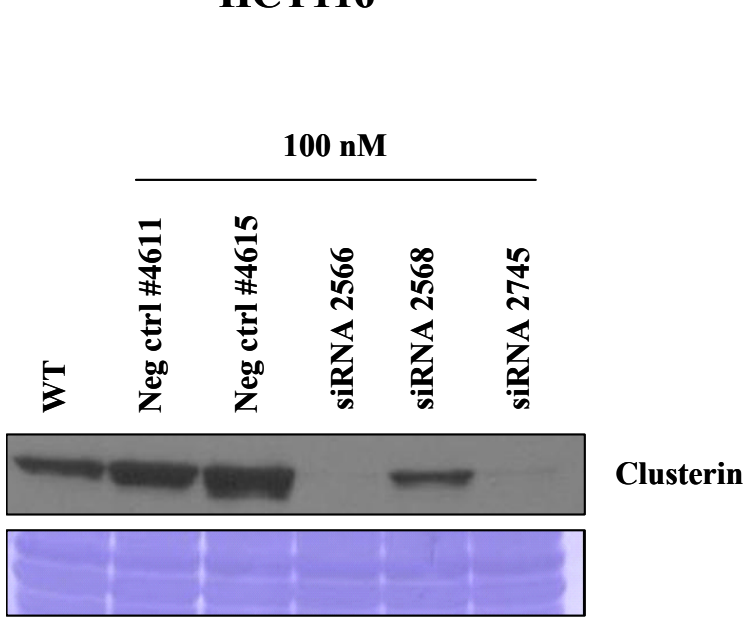

Figure 4.6.1

C

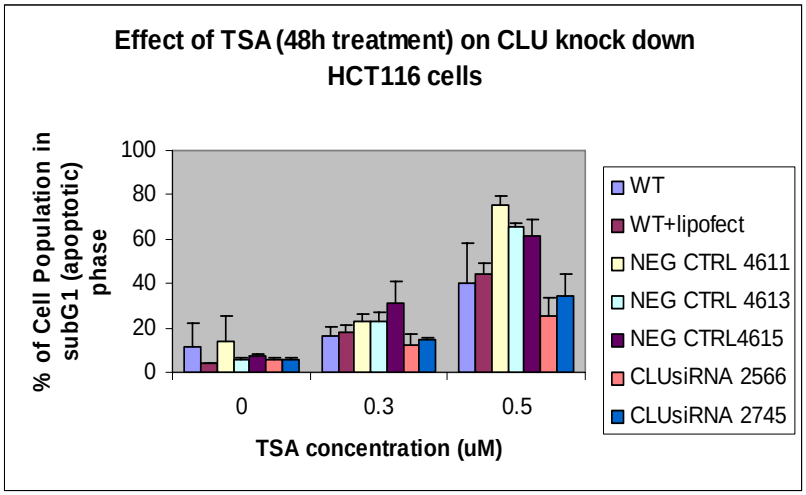
Effect of TSA (48h treatment) on CLU knock down HCT116 cells
% of Cell Population in subG1 (apoptotic) phase
100
80
60
40
20
0
0
0.3
0.5
TSA concentration (uM)
WT
WT+lipofect
NEG CTRL 4611
NEG CTRL 4613
NEG CTRL4615
CLUsiRNA 2566
CLUsiRNA 2745

Figure 4.6.1 Secretory clusterin has a proapoptotic role in TSA induced apoptosis.

A) Nuclear extracts from HCT116, Jurkat and U937 cells either untreated or treated with TSA for 12 hours. Nuclear form of clusterin, purity of cytoplasmic (C) and nuclear (N) extract were analyzed by western blot using anti-clusterin, anti-lamin (nuclear) and anti-tubulin (cytoplamic) antibody. B) Reducing clusterin protein expression in HCT116 cells using pre-designed Ambion siRNA oligonucleotides. The expression of clusterin protein is validated in western blot and the membrane was stained with coomassie blue to show equal loading of protein sample. C) Apoptosis in clusterin siRNA HCT116 cells is measured using PI staining. Data is the mean S.D. of three samples in one experiment representative of two independent experiments.

Figure 4.6.2

A

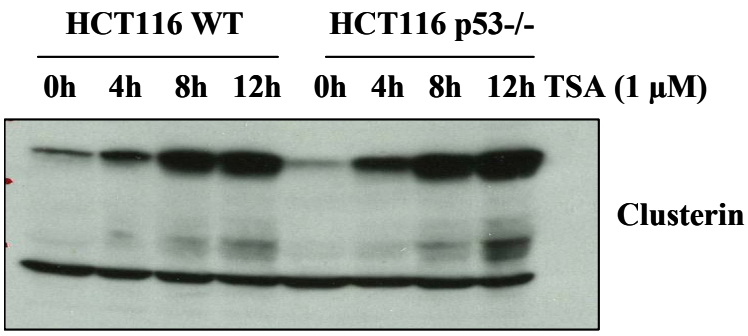

B

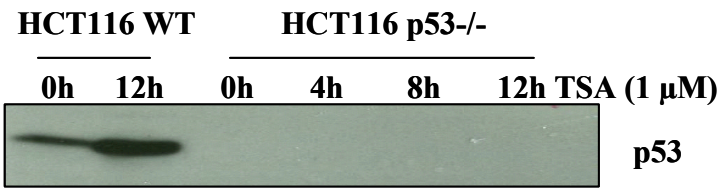

Figure 4.6.2

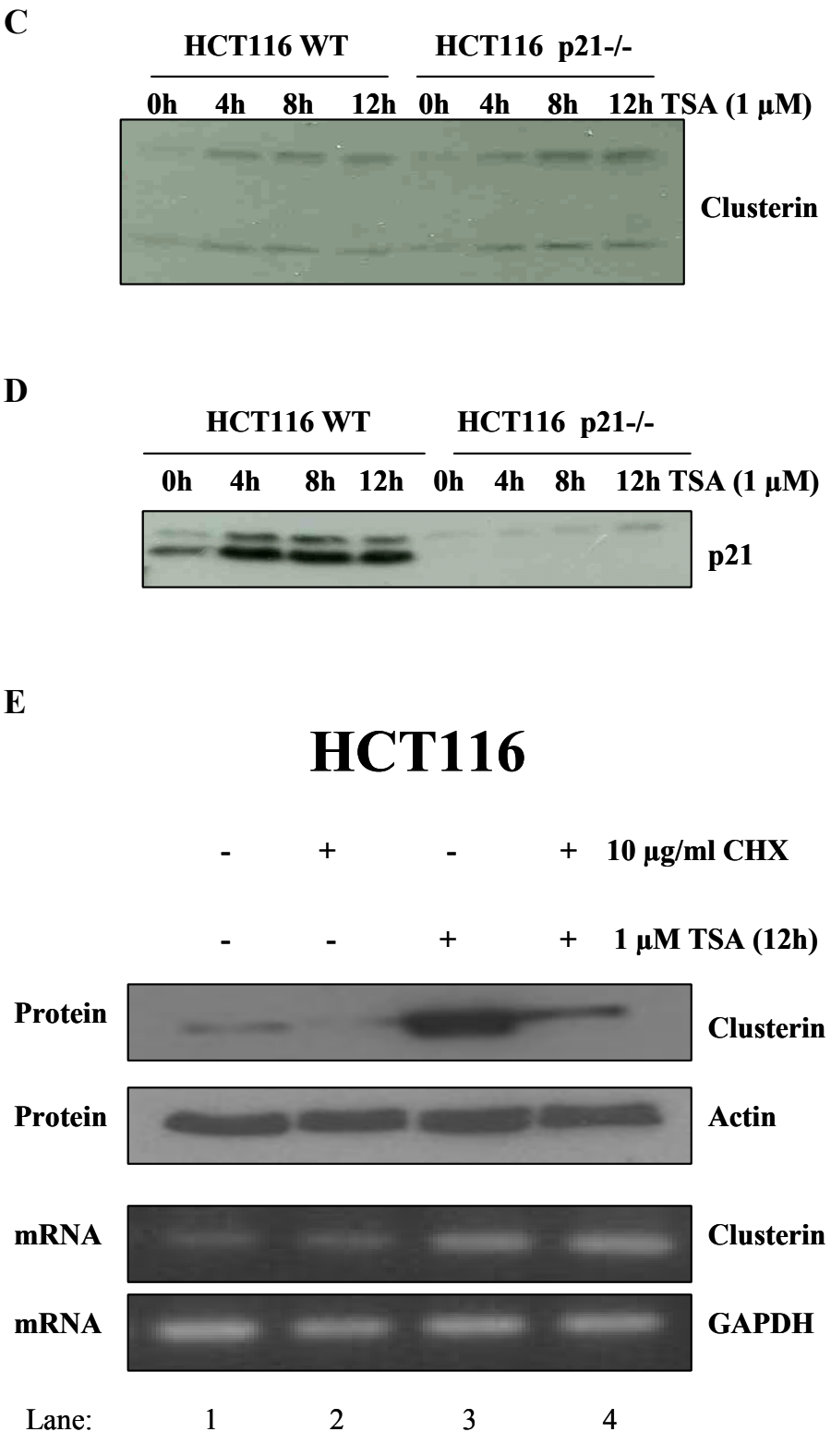
C
HCT116 WT
HCT116 p21-/-
0h 4h 8h 12h 0h 4h 8h 12h TSA (1 µM)
Clusterin
D
HCT116 WT
HCT116 p21-/-
0h 4h 8h 12h 0h 4h 8h 12h TSA (1 µM)
p21
E
HCT116
- + - + 10 µg/ml CHX
- - + + 1 µM TSA (12h)
Protein
Clusterin
Protein
Actin
mRNA
Clusterin
mRNA
GAPDH
Lane: 1 2 3 4

Figure 4.6.2 Increased clusterin expression is dependent on HDAC regulation.

Up-regulation of the clusterin protein by TSA treatment is independent of p53 (A) and p21 (C). Actin was used as a loading control in the western blot. The protein levels of p53 (B) and p21 (D) in HCT116 cells is verified in western blot using p53 and p21 antibody. (E) HCT116 cells were treated with or without cyclohexamide (CHX) and TSA, or both in combination. Clusterin protein and mRNA levels were analyzed in western blot and RT-PCR respectively. GAPDH was used as a loading control in RT-PCR.

4.7 Discussion

Microarray-based gene expression profiling of drug-treated cancer cells is a powerful tool to investigate the mechanism of action of anti-tumour agents, especially HDAC inhibitors which directly target the transcriptional machinery of cancer cells, hence altering the transcription of a subset of genes that control diverse molecular pathways, particularly those important for mediating apoptosis, and tumour growth suppression. In this section, we investigated the genes that are regulated by histone deacetylase and the molecular events involved.

Increase in histone acetylation is often observed in TSA-treated cells resulting in chromatin remodeling, and hence the accessibility of the transcriptional machinery to target genes, generally leading to enhance gene transcription. However, the gene expression profile of TSA-treated cancer cells were not all hallmarked by enhanced global transcription. Rather, we found distinct patterns of coordinated transcriptional changes, including repression of some genes in the microarray data. We identified in the microarray, genes in the apoptotic pathway (CLU, BNIP3L, Bid, Perp, PDCD2), DNA damage inducible signaling pathway (RAD9), cytokinesis (RAD21), mediators of cytokine signaling (STAT3), and genes associated with the transcription factor NF-κB pathway (LTβR, IRAK1, IL-2R and NF-κB1) that exhibited transcriptional changes. We verified selected genes by RT and real-time PCR. Some of these genes such as CLU, BNIP3L, PERP, RAD9 and STAT3 mRNA are reactivated, while Bid and RAD21 mRNA are repressed in response to HDAC inhibition.

HDAC inhibitors cause cell-cycle arrest in G1 and/or G2 phase, apoptosis or differentiation of cultured transformed cells. Normal cells undergo cell cycle checkpoints, and survive TSA treatment, while cancer cells can replicate their DNA and subsequently undergo apoptosis (Marks *et al*., 2001). RAD9 is a member of the family of cell cycle checkpoint RAD genes required for S phase (DNA replication) and G2 (DNA mitosis) checkpoints in response to DNA damage (Rhind and Russell, 1998; Stewart and Enoch, 1996). The induction of RAD9 mRNA and protein in U937 cells by TSA may implicate its importance in the regulation of the cell cycle, and may play a role in cell cycle checkpoint in U937 cells. In addition, RAD9 has also been reported to have a proapoptotic role. RAD9 interacts with antiapoptotic Bcl2 family proteins Bcl2 and Bcl-XL to trigger apoptosis (Komatsu *et al*., 2000). Therefore, RAD9 may promote apoptosis in U937 cells treated with TSA, but confirmation will require further investigation.

It is interesting to observe the induction of STAT3 in TSA-treated HCT116 and U937 cells. STAT3 is a transcription factor regulating cell-growth related genes, enhances transformation, and blocks apoptosis (Bromberg *et al*., 1999). STAT3 is acetylated on Lysine (lys) 685 upon cytokine treatment (Yuan *et al*., 2005). Lys 685 acetylation is required for STAT3 to form stable dimers required for the transcription of its target genes. Hence, the induction and acetylation of STAT3 may be a mechanism of protecting TSA-treated cells against apoptosis.

We were able to verify the repressed RAD21 gene expression in the microarray analysis by RT and real-time PCR. However, the level of RAD21 protein remains unchanged upon TSA treatment. RAD21 is one of the cohesin subunit that holds sister chromatids together and required for appropriate chromosomal adhesion during mitotic

cell cycle and double-strand-break repair after DNA damage (Biggins and Murray, 1999; Nasmyth *et al*., 2000). It is currently unclear as to why the relief of histone deacetylation resulted in the repression of RAD21 transcription and even more intriguing that the RAD21 protein level is unaffected. The decreased gene transcription of RAD21 could be an indirect effect from the enhanced transcription of other transcription factors that regulate RAD21 gene expression. As for the unaltered protein level, it may be explained by the treatment time since the down-regulation of RAD21 transcript was only obvious at the 12 hour TSA treatment. A longer treatment time point may be necessary to see an effect at the protein level especially if the protein is highly stable.

Since TSA can induce apoptosis in cancer cells, one would expect the activation of proapoptotic genes and repression of antiapoptotic genes in cells treated with TSA. It was interesting to note that the transcript for the proapopotic gene, Bid was suppressed in all three cancer cells by TSA but the protein expression remained stable throughout TSA treatment. It is unclear at present the contribution of Bid to TSA induced apoptosis. Perhaps, other proapoptotic Bcl2 family members may play a more dominant role in the apoptotic response of TSA treatment.

We further extended our analysis to establish the role of clusterin in TSA induced apoptosis because of the up-regulation of clusterin observed in the microarray analysis that was validated by RT-PCR, real-time PCR, and western blotting in HCT116, Jurkat and U937 cells. In Figure 4.6.2E, we show sCLU is a target gene of HDAC regulation. Interfering with protein translation of clusterin using cyclohexamide in HCT116 cells led to a dramatic reduction of clusterin protein, and hence strongly suggesting that *de novo* protein synthesis of clusterin is required.

Clusterin is an enigmatic protein with two isoforms (sCLU and nCLU) showing distinct functions and subcellular localization. 1, 25-Dihydroxyvitamin D3 (1, 25 $(OH)_2$ D_3) could inhibit cell proliferation, induce apoptosis in cancer cells, and increased expression of sCLU in benign prostate hyperplastic cells (Crescioli *et al*., 2004). It was speculated that sCLU is a stress-associated cytoprotective protein that is up-regulated in response to various apoptotic triggers. On the flip side, transient expression of clusterin in Myc-transduced clonocytes decreased cell accumulation, and knockdown of clusterin via antisense RNA in neoplastic epidermoid cells enhanced proliferation. In addition, Thomas-Tikhonenko *et al.* showed in a DMBA/TPA induced skin carcinogenesis mouse model that clusterin could inhibit skin tumour development as they observed an increase in the mean number of papilloma in clusterin null mice compared to wild type (Thomas-Tikhonenko *et al*., 2004). Conflicting data exhibiting both proapoptotic and antiapoptotic properties of clusterin are currently present in the field and are dependent on cell type and stimulus (Table 2). Here, we showed that sCLU gene expression is up-regulated upon TSA induced apoptosis, supporting the role of clusterin as a proapoptotic protein in our model (Figure 4.6.1C).

The nuclear form of clusterin is 49 kDa, is synthesized from a second AUG start codon of an alternative spliced CLU mRNA, in cells exposed to ionizing radiation (IR). nCLU then becomes modified to a 55 kDa proapoptotic form and translocate to the nucleus in MCF-7 cells. The mutation of the NLS in the C-terminal of nCLU abrogated nCLU ability to induce apoptosis, thus suggesting that the localization of nCLU in the nucleus is essential for its apoptotic function (Leskov *et al*., 2003). If nCLU plays a part in TSA induced apoptosis, one would expect an increase in the translocation and

subcellular localization of nCLU in the nucleus upon TSA treatment. We showed in Figure 4.6.1A, that basal protein level of nCLU in the nucleus, was not further increased upon TSA treatment. Therefore, our data suggested that nCLU may be redundant, and that sCLU is the dominant player in TSA induced apoptosis in HCT116 cells.

Besides nCLU, ionizing radiation can also induce the expression of sCLU in MCF-7 and HCT116 cells. Since ionizing radiation can induce both isoforms of clusterin, intracellular regulation of the expression of both isoforms may exist for cells to determine if they were to survive or to undergo apoptosis. Criswell *et al* showed that lack of p53 augmented CLU *de novo* synthesis after IR exposure, and further demonstrated that p53 repressed sCLU protein, not nCLU in mediating apoptosis in their study (Criswell *et al*., 2003). In Figure 4.6.2A, we showed that this regimen of p53 repression of sCLU did not occur in TSA-treated HCT116 cells, because cells lacking p53 did not show a decrease or abolishment of sCLU protein levels upon treatment with TSA. This data suggested that the regulation of sCLU and nCLU isoforms by TSA is entirely different from that of IR, and further supported our observation that TSA induced the expression of sCLU to activate apoptosis, independently of nCLU.

The mechanisms that differentially regulate the clusterin isoforms so that sCLU activates apoptosis (or compensates for nCLU) in TSA-treated cells require further investigation. It can be speculated that treating cells with TSA may lead to signal transduction pathways and activation of upstream molecules which can differentially regulate the two isoforms by 1) preventing the induction and processing of the alternatively spliced nCLU, 2) suppressing basal nCLU propapoptotic function in the nucleus, and 3) molecules which inhibit the translocation and accumulation of nCLU in

the nucleus by sequestering nCLU in the cytoplasm upon TSA induction and thus rendering nCLU's redundant role in TSA induced apoptosis.

Cell type/system	Factor inducing PCD	ApoJ function	References
Rat ventral prostate	Castration	Proapoptotic	[116,177]
Thymus/spleen	Glucocorticoids	Proapoptotic	[178]
Dystrophic retinas/intestinal epithelial cells	Developmental signals	Proapoptotic	[179]
A431 epidermoid carcinoma cells	Phthalocyanine 4	Proapoptotic	[141]
Mouse skin tumors	Phthalocyanine 4	Proapoptotic	[141]
MCF-7 breast carcinoma cells	Ionizing radiation	Proapoptotic	[88]
Cultured cortical neurons	Oxygen/glucose-deprivation	Proapoptotic	[107]
ApoJ$^{-/-}$ mice/neurons	Neonatal hypoxic-ischemic brain injury	Proapoptotic	[107]
Prostatic LNCaP, PC3 cells	TNFα	Antiapoptotic	[70,105]
Primary mixed hippocampal cultures	Amyloid-β_{1-40}	Antiapoptotic	[180]
Fibrosarcoma L929 cells	TNFα, TGFβ	Antiapoptotic	[71]
Rat ventral prostate	Castration	Antiapoptotic	[116]
LLC-PK$_1$ tubular cell line	H_2O_2	Antiapoptotic	[181]
Transgenic mice/photoreceptor cells	Developmental signals	Antiapoptotic	[182]
A431 epidermoid carcinoma cells	Heat shock, H_2O_2, superoxide anion, hyperoxia, UVA	Antiapoptotic	[81]
ApoJ$^{-/-}$ mice/heart	Autoimmune myocarditis	Antiapoptotic	[183]
Prostatic LNCaP cells	Adrogen ablation	Antiapoptotic	[142]
Prostatic LNCaP cells	Chemotherapy	Antiapoptotic	[84]
Granulosa cells	Follicular atresia	Antiapoptotic	[184]
ApoJ$^{-/-}$ mice/neurons	Ischemic brain injury	Antiapoptotic	[185]
Renal cells	Chemotherapy	Antiapoptotic	[186]
Osteosarcoma KH OS, U2 OS cells	Chemotherapy	Antiapoptotic	[86]
Primary WI38 fibroblasts	EtOH, t-BHP	Antiapoptotic	[125]
Primary WI38 fibroblasts	H_2O_2	Neutral	[36]

Table 2 Function of clusterin in different cell types

The proapoptotic or antiapoptotic function of clusterin is distinct in different cell types and dependent on the genetic background of the cell type and the nature of the stimulus/factor that induces its expression. (Reproduced with permission from The International Journal of Biochemistry & Cell Biology) (Trougakos and Gonos, 2002)

4.8 Conclusion and future directions

The search for genes that are regulated by the HDAC inhibitors using oligonucleotide microarray is a tedious, yet challenging venture. TSA induces apoptosis in human colon cancer (HCT116), T-cell leukemia (Jurkat) and monocytic U937 cells. We have shown that the relief of HDAC inhibition, and hence chromatin remodeling can bring about changes in the expression of a number of genes, resulting in the induction of genes such as clusterin, STAT3, RAD9, Perp and BNIP3L, and repressed the expression of genes like LTβR, IRAK1, RAD21, Bid, IL-2R and NF-κB1 in human cancer cells. Specifically, TSA up-regulated the expression of the secretory form of clusterin, promoting apoptosis in HCT116 cells.

The pleiotrophic effects of HDAC inhibitors provided an advantage as an anticancer agent because most cancer cells have multiple gene defects, affecting several pathways that regulate cell proliferation and survival. Through genome wide screening, we found several targets belonging to several different signaling pathways to be regulated by the HDAC inhibitor, TSA. Although we have shown that the relief of HDAC inhibition did result in the derepression of the clusterin gene expression, analysis of the clusterin promoter using CHIP assay to show the acetylation of histone in this region, hence the remodeling of chromatin leading to the accessibility of transcription factors and the transcriptional machinery to the clusterin promoter will be necessary to confirm HDAC direct effects on clusterin gene expression. Another possible candidate in inducing a proapoptotic response in TSA-treated cells which is worth investigating is RAD9. Studies involving the overexpression or siRNA knockdown of RAD9 will be necessary to investigate its transcriptional reactivation by TSA, and if such reactivation

represses expression of antiapoptotic protein like Bcl2 and Bcl-XL leading to apoptosis in TSA-treated cells.

HDAC inhibitors are good agents to treat inflammation-associated malignancies because they have been reported to reduce the production of cytokines in various inflammatory diseases, and are able to induce apoptosis in cancer cells. TSA has been observed to inhibit IL-8 expression in colonic epithelial cells which suggest that it is effective in the treatment of ulcerative colitis through increased histone acetylation and reduced production of proinflammatory cytokines by the intestinal epithelium (Yin *et al*., 2001; Huang *et al*., 1997; Gibson *et al*., 1999). TSA and another HDAC inhibitor, suberoylanilide hydroxamic acid (SAHA) also exhibited anti-inflammatory effects *in vivo*, by inhibiting IL-6, IL-10, IL-12 and IFN-γ production in MRL-*lpr/lpr* mice, a model of systemic lupus erythematosis (SLE) (Mishra *et al*., 2003).

TSA has also been reported to affect the functionality of NF-κB, a transcription factor responsible for the expression of many proinflammatory cytokines like TNFα, IL-1, IL-2, IL-6 and IL-8. NF-κB is kept inactive, through interaction with the inhibitor of kappa B (IκBα), as a NF-κB-IκBα complex in the cytoplasm, and prevented from translocation to the nucleus to activate transcription. NF-κB activation is promoted by its disassociation from IκBα when IκBα undergo degradation upon stimulation with NF-κB activating stimuli such as IL-1, LPS and TNFα. TSA has been reported to inhibit constituitive NF-κB activation in a concentration dependent manner by increasing the stability of IκBα protein (Yin *et al*., 2001).

Imre et al. also reported that the treatment of human non-small cell lung cancer (NSCLC) with TSA reduced TNF receptor mRNA and protein expression, and hence resulted in a reduction in IKK phosphorylation and the delayed phosphorylation of IκBα in these cells when further treated with TNFα (Imre *et al*., 2006). These results suggested that HDAC inhibitors can cause TNF receptor down-regulation, triggering the desensitization of the NF-κB pathway. On the contrary, several groups have also reported the opposite effect of HDAC inhibitors in activating NF-κB through either direct acetylation or inhibiting HDACs that physically associate with NF-κB. In our microarray analysis, we reported a down-regulation of the LTβR (NF-κB alternative pathway), IL-2R, adaptor IRAK1, and its precursor p105, NF-κB1 mRNA, all known to be associated with the NF-κB signaling pathway. Due to time constraint, we were not able to perform further analysis to establish the significance of the down-regulation of these genes upon TSA treatment. It will therefore be worthwhile to investigate if these targets are also affected at the protein level and if down-regulation of these genes could lead to the desensitization of the NF-κB pathway.

Clusterin has been reported to negatively regulate NF-κB activity. Ectopic expression of clusterin in human neuroblastoma cells inhibited NF-κB activity through stabilizing IκBα. Absence of clusterin in MEF cause a reduction in IκBα stability, and a TNF-dependent increase in NF-κB activation, and transcription of its target gene cIAP (Santilli *et al*., 2003). It is currently unclear if the induced expression of clusterin by TSA in HCT116 cells resulted in an attenuation of NF-κB activity and if the attenuation is due to an enhanced stability of IκBα. Hence, further experiment could be carried out to determine if the reduction of clusterin protein levels in TSA-treated HCT116 cells will

show a reduced stability of the IκBα proteins, finally leading to increase and activation of NF-κB.

4.9 Perspective

Due to the pleiotrophic effect of HDACs, it is not possible to determine a single pathway to be solely involved in its anti-tumour effect. At the molecular level, we need to improve our understanding of the nature of the selectivity of HDAC inhibitors in alterating gene transcription as to why some genes get activated and some genes get repressed. HDAC inhibitors seem to selectively have an anti-tumourigenic effect on transformed cells while leaving healthy, normal cells intact. One possible reason for tumour cells being more sensitive to HDAC inhibitors than normal cells, perhaps is due to the presence of multiple gene defects. Moreover, SAHA inhibition of HDACs is rapidly reversible, this suggest that normal cells with less genetic defects may be able to compensate for HDAC inhibitors induced changes more effectively than cancer cells, and therefore are more resistant to HDAC inhibitor induced cell death (Marks and Breslow, 2007). Perhaps HDAC inhibitors may offer a major therapeutic effect of targeting different signaling pathways by activating or repressing some gene promoters in tumour cells. The mechanism of healthy normal cells in evading the apoptotic effect of HDAC inhibitors still remains an area of intense research.

The deacetylation process does not occur only on histones. Non-histone protein substrate which may be deacetylated by HDACs includes DNA transcription factors like p53 and NF-κB, steroid receptors such as glucocorticoid receptor, transcription co-regulator such as retinoblastoma protein (Rb), signaling mediators such as STAT3 and Smad7, chaperone protein such as HSP90 and structural protein such as α-tubulin (Xu *et al*., 2007). These HDAC substrates are either directly or indirectly involved in many biological processes such as gene expression, and regulation of cellular pathways of

proliferation, differentiation and cell death. Therefore, the effects of HDAC inhibitors may not only affect chromatin remodeling but tumour cell death may also be induced through the acetylation of non-histone protein substrates. For example, transcription factors such as p53 and p65 can also be acetylated which may result in the regulation of their transcriptional activities, either enhancing or inhibiting expression of their target genes. However, the precise effect of HDAC inhibitors on these two transcription factors, ultimately resulting in the suppression of cell growth and apoptosis is also unclear and worth investigating.

HDAC inhibitors exhibited synergistic anti-tumour effects with chemotherapeutic agents such as VP-16 (etopside), ellipticine, camptothecin, doxorubicin, cisplatin, 5-fluorouracil, cyclophomamide (Kim *et al*., 2003), and TRAIL through the simultaneous activation of both the intrinsic and extrinsic apoptotic pathways (Rosato and Grant, 2004), suggesting that the combination of HDAC inhibitors together with other chemotherapeutic agents can be attractive strategies in combating cancer. However, just like any other anti-tumour therapy, whereby resistance to apoptotic cell death occurs, resistance to the effect of HDAC inhibitor induced cell death have also been observed in prostate cancer cells (PC3) (Xu *et al*., 2006). Several candidate proteins that may confer resistance to HDAC inhibitor induced apoptosis includes the overexpression of Bcl2 (Mitsiades *et al*., 2003), and peroxiredoxins that reduce ROS generation (Kang *et al*., 1998).

While the activation of anti-tumour pathways, and the mechanisms of the resistance to HDAC inhibitors is not entirely clear, SAHA (vorinostat), which belongs to the hydroxamate family of HDAC inhibitor as with TSA, is the first HDAC inhibitor to

be approved by the Food and Drug Adminstration (FDA) for the treatment of cutaneous T-cell lymphoma (CTCL) (Carew *et al*., 2008). Understanding the molecular events and mechanisms underlying the resistance and sensitivity to HDAC inhibitors will therefore be beneficial to improving the efficacy of HDAC inhibitors, and in understanding the long-term use, as well as the side effects that may accompany the use of these promising drugs in the treatment of cancer.

References

References

Anest, V., Hanson, J.L., Cogswell, P.C., Steinbrecher, K.A., Strahl, B.D. and Baldwin, A.S. 2003. A nucleosomal function for IkappaB kinase-alpha in NF-kappaB-dependent gene expression. *Nature* 423:659-663.

Ben Neriah, Y. 2002. Regulatory functions of ubiquitination in the immune system. *Nat Immunol* 3:20-26.

Beyaert, R., Cuenda, A., Vanden Berghe, W., Plaisance, S., Lee, J.C., Haegeman, G., Cohen, P. and Fiers, W. 1996. The p38/RK mitogen-activated protein kinase pathway regulates interleukin-6 synthesis response to tumor necrosis factor. *EMBO J* 15:1914-1923.

Biggins, S. and Murray, A.W. 1999. Sister chromatid cohesion in mitosis. *Curr Opin Genet. Dev* 9:230-236.

Birbach, A., Gold, P., Binder, B.R., Hofer, E., De Martin, R. and Schmid, J.A. 2002. Signaling molecules of the NF-kappa B pathway shuttle constitutively between cytoplasm and nucleus. *J Biol Chem* 277:10842-10851.

Bird, T.A., Schooley, K., Dower, S.K., Hagen, H. and Virca, G.D. 1997. Activation of nuclear transcription factor NF-kappaB by interleukin-1 is accompanied by casein kinase II-mediated phosphorylation of the p65 subunit. *J Biol Chem* 272:32606-32612.

Blander, G. and Guarente, L. 2004. The Sir2 family of protein deacetylases. *Annu Rev Biochem* 73:417-435.

Bohuslav, J., Chen, L.F., Kwon, H., Mu, Y. and Greene, W.C. 2004. p53 induces NF-kappaB activation by an IkappaB kinase-independent mechanism involving phosphorylation of p65 by ribosomal S6 kinase 1. *J Biol Chem* 279:26115-26125.

Bolden, J.E., Peart, M.J. and Johnstone, R.W. 2006. Anticancer activities of histone deacetylase inhibitors. *Nat Rev Drug Discov.* 5:769-784.

Bonizzi, G. and Karin, M. 2004. The two NF-kappaB activation pathways and their role in innate and adaptive immunity. *Trends Immunol* 25:280-288.

Bradley, J.R. and Pober, J.S. 2001. Tumor necrosis factor receptor-associated factors (TRAFs). *Oncogene* 20:6482-6491.

Bromberg, J.F., Wrzeszczynska, M.H., Devgan, G., Zhao, Y., Pestell, R.G., Albanese, C. and Darnell Jr, J.E. 1999. Stat3 as an oncogene. *Cell* 98:295-303.

Bulavin, D.V., Demidov, O.N., Saito, S., Kauraniemi, P., Phillips, C., Amundson, S.A., Ambrosino, C., Sauter, G., Nebreda, A.R., Anderson, C.W., Kallioniemi, A., Fornace Jr., A.J. and Appella, E. 2002. Amplification of PPM1D in human tumors abrogates p53 tumor-suppressor activity. *Nat Genet.* 31:210-215.

Campbell, J., Ciesielski, C.J., Hunt, A.E., Horwood, N.J., Beech, J.T., Hayes, L.A., Denys, A., Feldmann, M., Brennan, F.M. and Foxwell, B.M. 2004a. A novel mechanism for TNF-alpha regulation by p38 MAPK: involvement of NF-kappa B with implications for therapy in rheumatoid arthritis. *J Immunol* 173:6928-6937.

Campbell, K.J., Rocha, S. and Perkins, N.D. 2004b. Active repression of antiapoptotic gene expression by RelA(p65) NF-kappa B. *Mol Cell* 13:853-865.

Carew, J.S., Giles, F.J. and Nawrocki, S.T. 2008. Histone deacetylase inhibitors: Mechanisms of cell death and promise in combination cancer therapy. *Cancer Lett.* 269:7-17.

Chen, L.F., Williams, S.A., Mu, Y., Nakano, H., Duerr, J.M., Buckbinder, L. and Greene, W.C. 2005. NF-kappaB Rel A phosphorylation regulates Rel A acetylation. *Mol Cell Biol* 25:7966-7975.

Chen, L.F. and Greene, W.C. 2004. Shaping the nuclear action of NF-kappaB. *Nat Rev Mol Cell Biol* 5:392-401.

Chen, L.F., Mu, Y. and Greene, W.C. 2002. Acetylation of RelA at discrete sites regulates distinct nuclear functions of NF-kappaB. *EMBO J* 21:6539-6548.

Chen, L., Fischle, W., Verdin, E. and Greene, W.C. 2001. Duration of nuclear NF-kappaB action regulated by reversible acetylation. *Science* 293:1653-1657.

Chen, T., Turner, J., McCarthy, S., Scaltriti, M., Bettuzzi, S. and Yeatman, T.J. 2004. Clusterin-mediated apoptosis is regulated by adenomatous polyposis coli and is p21 dependent but p53 independent. *Cancer Res* 64:7412-7419.

Chen, Z.J., Parent, L. and Maniatis, T. 1996. Site-specific phosphorylation of IkappaBalpha by a novel ubiquitination-dependent protein kinase activity. *Cell* 84:853-862.

Chew, J., Biswas, S., Sheeram, S., Humaidi, M., Wong, E.T., Dhillion, M.K., Teo, H., Hazra, A., Fang, C.C., Lopez-Collazo, E., Bulavin, D.V. and Tergaonkar, V. 2009. WIP1 phosphatase is a negative regulator of NF-kappaB signaling. *Nat Cell Biol* 11:659-666.

Choi, J., Nannenga, B., Demidov, O.N., Bulavin, D.V., Cooney, A., Brayton, C., Zhang, Y.X., Mbawuike, I.N., Bradley, A., Appella, E. and Donehower, L.A. 2002. Mice deficient for the wild-type p53-induced phosphatase gene (Wip1) exhibit defects in reproductive organs, immune function, and cell cycle control. *Mol Cell Biol* 22:1094-1105.

Cohen, P. 1997. The search for physiological substrates of MAP and SAP kinases in mammalian cells. *Trends Cell Biol* 7:353-361.

Crescioli, C., Ferruzzi, P., Caporali, A., Scaltriti, M., Bettuzzi, S., Mancin, R., Gelmini, S., Serio, M., Villari, D., Vannelli, G.B., Colli, E., Adorini, L. and Maggi, M. 2004. Inhibition of prostate cell growth by BXL-628, a calcitriol analogue selected for a phase

II clinical trial in patients with benign prostate hyperplasia. *Eur. J Endocrinol* 150:591-603.

Criswell, T., Klokov, D., Beman, M., Lavik, J.P. and Boothman, D.A. 2003. Repression of IR-inducible clusterin expression by the p53 tumor suppressor protein. *Cancer Biol Ther*. 2:372-380.

Cuenda, A. and Rousseau, S. 2007. p38 MAP-kinases pathway regulation, function and role in human diseases. *Biochim. Biophys. Acta* 1773:1358-1375.

Dhordain, P., Lin, R.J., Quief, S., Lantoine, D., Kerckaert, J.P., Evans, R.M. and Albagli, O. 1998. The LAZ3(BCL-6) oncoprotein recruits a SMRT/mSIN3A/histone deacetylase containing complex to mediate transcriptional repression. *Nucleic Acids Res* 26:4645-4651.

Dmitrieva, N.I., Bulavin, D.V., Fornace Jr., A.J. and Burg, M.B. 2002. Rapid activation of G_2/M checkpoint after hypertonic stress in renal inner medullary epithelial (IME) cells is protective and requires p38 kinase. *Proc Natl Acad Sci* 99:184-189.

Duran, A., Diaz-Meco, M.T. and Moscat. J. 2003. Essential role of RelA Ser311 phosphorylation by zetaPKC in NF-kappaB transcriptional activation. *EMBO J* 22:3910-3918.

Eisen, M.B., Spellman, P.T., Brown, P.O. and Botstein, D. 1998. Cluster analysis and display of genome-wide expression patterns. *Proc Natl Acad Sci U S A* 95:14863-14868.

El Omar, E.M., Carrington, M., Chow, W.H., McColl, K.E., Bream, J.H., Young, H.A., Herrera, J., Lissowska, J., Yuan, C.C., Rothman, N., Lanyon, G., Martin, M., Fraumeni Jr., J.F. and Rabkin, C.S. 2000. Interleukin-1 polymorphisms associated with increased risk of gastric cancer. *Nature* 404:398-402.

Fiscella, M., Zhang, H. Fan, S., Sakaguchi, K., Shen, S., Mercer, W.E., Vande Woude, G.F., O'Connor, P.M. and Appella, E. 1997. Wip1, a novel human protein phosphatase that is induced in response to ionizing radiation in a p53-dependent manner. *Proc Natl Acad Sci U S A* 94:6048-6053.

Flaus, A. and Owen-Hughes, T. 2001. Mechanisms for ATP-dependent chromatin remodelling. *Curr Opin Genet. Dev* 11:148-154.

Fu, D.X., Kuo, Y.L. Liu, B.Y., Jeang, K.T. and Giam, C.Z. 2003. Human T-lymphotropic virus type I tax activates I-kappa B kinase by inhibiting I-kappa B kinase-associated serine/threonine protein phosphatase 2A. *J Biol Chem* 278:1487-1493.

Fujimoto, H., Onishi, N., Kato, N., Takekawa, M., Xu, X.Z., Kosugi, A., Kondo, T., Imamura, M., Oishi , I., Yoda, A. and Minami, Y. 2006. Regulation of the antioncogenic Chk2 kinase by the oncogenic Wip1 phosphatase. *Cell Death. Differ.* 13:1170-1180.

Gao, L., Cueto, M.A., Asselbergs, F. and Atadja, P. 2002. Cloning and functional characterization of HDAC11, a novel member of the human histone deacetylase family. *J Biol Chem* 277:25748-25755.

Gibson, P.R., Rosella, O., Wilson, A.J., Mariadason, J.M., Rickard, K., Byron, K. and Barkla, D.H. 1999. Colonic epithelial cell activation and the paradoxical effects of butyrate. *Carcinogenesis* 20:539-544.

Gloire, G., Horion, J., El Mjiyad, N., Bex, F., Chariot, A., Dejardin, E. and Piette, J. 2007. Promoter-dependent effect of IKKalpha on NF-kappaB/p65 DNA binding. *J Biol Chem* 282:21308-21318.

Guo, Y.L., Baysal, K., Kang, B., Yang, L.J. and Williamson, J.R. 1998. Correlation between sustained c-Jun N-terminal protein kinase activation and apoptosis induced by tumor necrosis factor-alpha in rat mesangial cells. *J Biol Chem* 273:4027-4034.

Hacker, H. and Karin, M. 2006. Regulation and function of IKK and IKK-related kinases. *Sci STKE*. 2006:re13.

Han, J., Lee, J.D., Bibbs, L. and Ulevitch, R.J. 1994. A MAP kinase targeted by endotoxin and hyperosmolarity in mammalian cells. *Science* 265:808-811.

Hayden, M.S. and Ghosh, S. 2004. Signaling to NF-kappaB. *Genes Dev* 18:2195-2224.

Hayden, M.S. and Ghosh, S. 2008. Shared principles in NF-kappaB signaling. *Cell* 132:344-362.

Hirasawa, A., Saito-Ohara, F., Inoue, J., Aoki, D., Susumu, N., Yokoyama, T., Nozawa, S., Inazawa, J. and Imoto, I. 2003. Association of 17q21-q24 gain in ovarian clear cell adenocarcinomas with poor prognosis and identification of PPM1D and APPBP2 as likely amplification targets. *Clin Cancer Res* 9:1995-2004.

Hsu, H., Shu, H.B., Pan, M.G. and Goeddel, D.V. 1996. TRADD-TRAF2 and TRADD-FADD interactions define two distinct TNF receptor 1 signal transduction pathways. *Cell* 84:299-308.

Huang, N., Katz, J.P., Martin, D.R. and Wu, G.D. 1997. Inhibition of IL-8 gene expression in Caco-2 cells by compounds which induce histone hyperacetylation. *Cytokine* 9:27-36.

Huxford, T., Huang, D.B., Malek, S. and Ghosh, G. 1998. The crystal structure of the IkappaBalpha/NF-kappaB complex reveals mechanisms of NF-kappaB inactivation. *Cell* 95:759-770.

Hwang, D., Jang, B.C., Yu, G. and Boudreau, M. 1997. Expression of mitogen-inducible cyclooxygenase induced by lipopolysaccharide: mediation through both mitogen-activated protein kinase and NF-kappaB signaling pathways in macrophages. *Biochem Pharmacol.* 54:87-96.

Ichijo, H., Nishida, E., Irie, K., ten Dijke, P., Saitoh, M., Moriguchi, T., Takagi, M., Matsumoto, K., Miyazono, K. and Gotoh, Y. 1997. Induction of apoptosis by ASK1, a mammalian MAPKKK that activates SAPK/JNK and p38 signaling pathways. *Science* 275:90-94.

Imre, G., Gekeler, V., Leja, A., Beckers, T. and Boehm, M. 2006. Histone deacetylase inhibitors suppress the inducibility of nuclear factor-kappaB by tumor necrosis factor-alpha receptor-1 down-regulation. *Cancer Res* 66:5409-5418.

Insinga, A., Monestiroli, S., Ronzoni, S., Gelmetti, V., Marchesi, F., Viale, A., Altucci, L., Nervi, C., Minucci, S. and Pelicci, P.G. 2005. Inhibitors of histone deacetylases induce tumor-selective apoptosis through activation of the death receptor pathway. *Nat Med.* 11:71-76.

Janssens, S. and Beyaert, R. 2003. Functional diversity and regulation of different interleukin-1 receptor-associated kinase (IRAK) family members. *Mol Cell* 11:293-302.

Jenuwein, T. and Allis, C.D. 2001. Translating the histone code. *Science* 293:1074-1080.

Jiang, Y., Chen, C., Li, Z., Guo, W., Gegner, J.A., Lin, S. and Han, J. 1996. Characterization of the structure and function of a new mitogen-activated protein kinase (p38beta). *J Biol Chem* 271:17920-17926.

Jiang, Y., Gram, H., Zhao, M., New, L., Gu, J., Feng, L., Di Padova, F., Ulevitch, R.J. and Han, J. 1997. Characterization of the structure and function of the fourth member of p38 group mitogen-activated protein kinases, p38delta. *J Biol Chem* 272:30122-30128.

Jiang, Y., Woronicz, J.D., Liu, W. and Goeddel, D.V. 1999. Prevention of constitutive TNF receptor 1 signaling by silencer of death domains. *Science* 283:543-546.

Johnstone, R.W. 2002. Histone-deacetylase inhibitors: novel drugs for the treatment of cancer. *Nat Rev Drug Discov.* 1:287-299.

Kang, S.W., Chae, H.Z., Seo, M.S., Kim, K., Baines, I.C. and Rhee, S.G. 1998. Mammalian peroxiredoxin isoforms can reduce hydrogen peroxide generated in response to growth factors and tumor necrosis factor-alpha. *J Biol Chem* 273:6297-6302.

Karin, M. 2006. Nuclear factor-kappaB in cancer development and progression. *Nature* 441:431-436.

Karin, M. and Ben Neriah, Y. 2000. Phosphorylation meets ubiquitination: the control of NF-[kappa]B activity. *Annu Rev Immunol* 18:621-663.

Karin, M. and Greten, F.R. 2005. NF-kappaB: linking inflammation and immunity to cancer development and progression. *Nat Rev Immunol* 5:749-759.

Kato T., Jr., Delhase, M., Hoffmann, A. and Karin, M. 2003. CK2 Is a C-Terminal IkappaB Kinase Responsible for NF-kappaB Activation during the UV Response. *Mol Cell* 12:829-839.

Kim, M.S., Blake, M., Baek, J.H., Kohlhagen, G., Pommier, Y. and Carrier, F. 2003. Inhibition of histone deacetylase increases cytotoxicity to anticancer drugs targeting DNA. *Cancer Res* 63:7291-7300.

Kinjyo, I., Hanada, T., Inagaki-Ohara, K., Mori, H., Aki, D., Ohishi, M., Yoshida, H., Kubo, M. and Yoshimura, A. 2002. SOCS1/JAB is a negative regulator of LPS-induced macrophage activation. *Immunity.* 17:583-591.

Komatsu, K., Miyashita, T., Hang, H., Hopkins, K.M., Zheng, W., Cuddeback, S., Yamada, M., Lieberman, H.B. and Wang, H.G. 2000. Human homologue of S. pombe Rad9 interacts with BCL-2/BCL-xL and promotes apoptosis. *Nat Cell Biol* 2:1-6.

Kopp, E. and Medzhitov, R. 2003. Recognition of microbial infection by Toll-like receptors. *Curr Opin Immunol* 15:396-401.

Kopp, E., Medzhitov, R., Carothers, J., Xiao, C., Douglas, I., Janeway, C.A. and Ghosh, S. 1999. ECSIT is an evolutionarily conserved intermediate in the Toll/IL-1 signal transduction pathway. *Genes Dev* 13:2059-2071.

Kyriakis, J.M. and Avruch, J. 2001. Mammalian mitogen-activated protein kinase signal transduction pathways activated by stress and inflammation. *Physiol Rev* 81:807-869.

Lamb, J.A., Ventura, J.J., Hess, P., Flavell, R.A. and Davis, R.J. 2003. JunD mediates survival signaling by the JNK signal transduction pathway. *Mol Cell* 11:1479-1489.

Landesman-Bollag, E., Channavajhala, P.L., Cardiff, R.D. and Seldin, D.C. 1998. p53 deficiency and misexpression of protein kinase CK2alpha collaborate in the development of thymic lymphomas in mice. *Oncogene* 16:2965-2974.

Lane, D.P. 2005. Exploiting the p53 pathway for the diagnosis and therapy of human cancer. *Cold Spring Harb. Symp. Quant. Biol* 70:489-497.

Lawrence, T., Bebien, M., Liu, G.Y., Nizet, V. and Karin, M. 2005. IKKalpha limits macrophage NF-kappaB activation and contributes to the resolution of inflammation. *Nature* 434:1138-1143.

Lechner, C., Zahalka, M.A., Giot, J.F., Moller, N.P. and Ullrich, A. 1996. ERK6, a mitogen-activated protein kinase involved in C2C12 myoblast differentiation. *Proc Natl Acad Sci U S A* 93:4355-4359.

Lee, J.C., Laydon, J.T., McDonnell, P.C., Gallagher, T.F., Kumar, S., Green, D., McNulty, D., Blumenthal, M.J., Heys, J.R. and Landvatter, S.W. 1994. A protein kinase involved in the regulation of inflammatory cytokine biosynthesis. *Nature* 372:739-746.

Lee, S.H. and Hannink, M. 2002. Characterization of the nuclear import and export functions of Ikappa B(epsilon). *J Biol Chem* 277:23358-23366.

Leskov, K.S., Klokov, D.Y., Li, J., Kinsella, T.J. and Boothman, D.A. 2003. Synthesis and functional analyses of nuclear clusterin, a cell death protein. *J Biol Chem* 278:11590-11600.

Letai, A., Bassik, M.C., Walensky, L.D., Sorcinelli, M.D., Weiler, S. and Korsmeyer, S.J. 2002. Distinct BH3 domains either sensitize or activate mitochondrial apoptosis, serving as prototype cancer therapeutics. *Cancer Cell* 2:183-192.

Li, H.Y., Liu, H., Wang, C.H., Zhang, J.Y., Man, J.H., Gao, Y.F., Zhang, P.J., Li, W.H., Zhao, J., Pan, X., Zhou, T., Gong, W.L., Li, A.L. and Zhang, X.M. 2008. Deactivation of the kinase IKK by CUEDC2 through recruitment of the phosphatase PP1. *Nat Immunol* 9:533-541.

Li, J., Yang, Y., Peng, Y., Austin, R.J., G.van Eyndhoven, W., Nguyen, K.C., Gabriele, T., McCurrach, M.E., Marks, J.R., Hoey, T., Lowe, S.W. and Powers, S. 2002. Oncogenic properties of PPM1D located within a breast cancer amplification epicenter at 17q23. *Nat Genet.* 31:133-134.

Li, N., Banin, S., Ouyang, H., Li, G.C., Courtois, G., Shiloh, Y., Karin, M. and Rotman, G. 2001. ATM is required for IkappaB kinase (IKKk) activation in response to DNA double strand breaks. *J Biol Chem* 276:8898-8903.

Li, N. and Karin, M. 1998. Ionizing radiation and short wavelength UV activate NF-kappaB through two distinct mechanisms. *Proc Natl Acad Sci U S A* 95:13012-13017.

Li, P., Nijhawan, D., Budihardjo, I., Srinivasula, S.M., Ahmad, M., Alnemri, E.S. and Wang, X. 1997. Cytochrome c and dATP-dependent formation of Apaf-1/caspase-9 complex initiates an apoptotic protease cascade. *Cell* 91:479-489.

Li, Q., Estepa, G., Memet, S., Israel, A. and Verma, I.M. 2000. Complete lack of NF-kappaB activity in IKK1 and IKK2 double-deficient mice: additional defect in neurulation. *Genes Dev* 14:1729-1733.

Li, Q., Lu, Q., Bottero, V., Estepa, G., Morrison, L., Mercurio, F. and Verma, I.M. 2005. Enhanced NF-kappaB activation and cellular function in macrophages lacking IkappaB kinase 1 (IKK1). *Proc Natl Acad Sci U S A* 102:12425-12430.

Li, Q. and Verma, I.M. 2002. NF-kappaB regulation in the immune system. *Nat Rev Immunol* 2:725-734.

Li, S., Wang, L., Berman, M.A., Zhang, Y. and Dorf, M.E. 2006. RNAi screen in mouse astrocytes identifies phosphatases that regulate NF-kappaB signaling. *Mol Cell* 24:497-509.

Lin, L., DeMartino, G.N. and Greene, W.C. 1998. Cotranslational biogenesis of NF-kappaB p50 by the 26S proteasome. *Cell* 92:819-828.

Lin, R., Beauparlant, P., Makris, C., Meloche, S. and Hiscott, J. 1996. Phosphorylation of IkappaBalpha in the C-terminal PEST domain by casein kinase II affects intrinsic protein stability. *Mol Cell Biol* 16:1401-1409.

Lind, M.H., Rozell, B., Wallin, R.P., van Hogerlinden, M., Ljunggren, H.G., Toftgard, R. and Sur, I. 2004. Tumor necrosis factor receptor 1-mediated signaling is required for skin cancer development induced by NF-kappaB inhibition. *Proc Natl Acad Sci U S A* 101:4972-4977.

Lomaga, M.A., Yeh, W.C., Sarosi, I., Duncan, G.S., Furlonger, C., Ho, A., Morony, S., Capparelli, C., Van, G., Kaufman, S., van der, H.A., Itie, A., Wakeham, A., Khoo, W., Sasaki, T., Cao, Z., Penninger, J.M., Paige, C.J., Lacey, D.L., Dunstan, C.R., Boyle, W.J., Goeddel, D.V. and Mak, T.W. 1999. TRAF6 deficiency results in osteopetrosis and defective interleukin-1, CD40, and LPS signaling. *Genes Dev* 13:1015-1024.

Lowe, S.W. and Lin, A.W. 2000. Apoptosis in cancer. *Carcinogenesis* 21:485-495.

Lowe, S.W., Schmitt, E.M., Smith, S.W., Osborne, B.A. and Jacks, T. 1993. p53 is required for radiation-induced apoptosis in mouse thymocytes. *Nature* 362:847-849.

Lu, X., Ma, O., Nguyen, T.A., Jones, S.N., Oren, M. and Donehower, L.A. 2007. The Wip1 Phosphatase acts as a gatekeeper in the p53-Mdm2 autoregulatory loop. *Cancer Cell* 12:342-354.

Lu, X., Nannenga, B. and Donehower, L.A. 2005. PPM1D dephosphorylates Chk1 and p53 and abrogates cell cycle checkpoints. *Genes Dev* 19:1162-1174.

Luthi, A.U. and Martin, S.J. 2007. The CASBAH: a searchable database of caspase substrates. *Cell Death. Differ.* 14:641-650.

Madrid, L.V., Mayo, M.W., Reuther, J.Y. and Baldwin Jr., A.S. 2001. Akt stimulates the transactivation potential of the RelA/p65 Subunit of NF-kappa B through utilization of the Ikappa B kinase and activation of the mitogen-activated protein kinase p38. *J Biol Chem* 276:18934-18940.

Malek, S., Chen, Y., Huxford, T. and Ghosh, G. 2001. IkappaBbeta, but not IkappaBalpha, functions as a classical cytoplasmic inhibitor of NF-kappaB dimers by masking both NF-kappaB nuclear localization sequences in resting cells. *J Biol Chem* 276:45225-45235.

Marks, P., Rifkind, R.A., Richon, V.M., Breslow, R., Miller, T. and Kelly, W.K. 2001. Histone deacetylases and cancer: causes and therapies. *Nat Rev Cancer* 1:194-202.

Marks, P.A. and Breslow, R. 2007. Dimethyl sulfoxide to vorinostat: development of this histone deacetylase inhibitor as an anticancer drug. *Nat Biotechnol.* 25:84-90.

McDonnell, T.J., Deane, N., Platt, F.M., Nunez, G., Jaeger, U., McKearn, J.P. and Korsmeyer, S.J. 1989. bcl-2-immunoglobulin transgenic mice demonstrate extended B cell survival and follicular lymphoproliferation. *Cell* 57:79-88.

Mishra, N., Reilly, C.M., Brown, D.R., Ruiz, P. and Gilkeson, G.S. 2003. Histone deacetylase inhibitors modulate renal disease in the MRL-lpr/lpr mouse. *J Clin Invest* 111:539-552.

Mitsiades, N., Mitsiades, C.S., Richardson, P.G., McMullan, C., Poulaki, V., Fanourakis, G., Schlossman, R., Chauhan, D., Munshi, N.C., Hideshima, T., Richon, V.M., Marks, P.A. and Anderson, K.C. 2003. Molecular sequelae of histone deacetylase inhibition in human malignant B cells. *Blood* 101:4055-4062.

Nakagawa, R., Naka, T., Tsutsui, H., Fujimoto, M., Kimura, A., Abe, T., Seki, E., Sato, S., Takeuchi, O., Takeda, K., Akira, S., Yamanishi, K., Kawase, I., Nakanishi, K. and Kishimoto, T. 2002. SOCS-1 participates in negative regulation of LPS responses. *Immunity.* 17:677-687.

Nasmyth, K., Peters, J.M. and Uhlmann, F. 2000. Splitting the chromosome: cutting the ties that bind sister chromatids. *Science* 288:1379-1385.

Naumann, M. and Scheidereit, C. 1994. Activation of NF-kappa B in vivo is regulated by multiple phosphorylations. *EMBO J* 13:4597-4607.

Olson, C.M., Hedrick, M.N., Izadi, H., Bates, T.C., Olivera, E.R. and Anguita, J. 2007 p38 mitogen-activated protein kinase controls NF-kappaB transcriptional activation and tumor necrosis factor alpha production through RelA phosphorylation mediated by mitogen- and stress-activated protein kinase 1 in response to Borrelia burgdorferi antigens. *Infect. Immun.* 75:270-277.

Oshima, M., Oshima, H., Matsunaga, A. and Taketo, M.M. 2005. Hyperplastic gastric tumors with spasmolytic polypeptide-expressing metaplasia caused by tumor necrosis factor-alpha-dependent inflammation in cyclooxygenase-2/microsomal prostaglandin E synthase-1 transgenic mice. *Cancer Res* 65:9147-9151.

Ozaki, A., Morimoto, H., Tanaka, H., Okamura, H., Yoshida, K., Amorim, B.R. and Haneji, T. 2006. Okadaic acid induces phosphorylation of p65NF-kappaB on serine 536 and activates NF-kappaB transcriptional activity in human osteoblastic MG63 cells. *J Cell Biochem* 99:1275-1284.

Pahl, H.L. 1999. Activators and target genes of Rel/NF-kappaB transcription factors. *Oncogene* 18:6853-6866.

Pearson, G., Robinson, F., Beers, G.T., Xu, B.E., Karandikar, M., Berman, K. and Cobb, M.H. 2001. Mitogen-activated protein (MAP) kinase pathways: regulation and physiological functions. *Endocr. Rev* 22:153-183.

Perkins, N.D. 2006. Post-translational modifications regulating the activity and function of the nuclear factor kappa B pathway. *Oncogene* 25:6717-6730.

Pons, S. and Torres-Aleman, I. 2000. Insulin-like growth factor-I stimulates dephosphorylation of ikappa B through the serine phosphatase calcineurin (protein phosphatase 2B). *J Biol Chem* 275:38620-38625.

Poyet, J.L., Srinivasula, S.M., Lin, J.H., Fernandes-Alnemri, T., Yamaoka, S., Tsichlis, P.N. and Alnemri, E.S. 2000. Activation of the Ikappa B kinases by RIP via IKKgamma /NEMO-mediated oligomerization. *J Biol Chem* 275:37966-37977.

Prajapati, S., Verma, U., Yamamoto, Y., Kwak, Y.T. and Gaynor, R.B. 2004. Protein phosphatase 2Cbeta association with the IkappaB kinase complex is involved in regulating NF-kappaB activity. *J Biol Chem* 279:1739-1746.

Rhind, N. and Russell, P. 1998. Mitotic DNA damage and replication checkpoints in yeast. *Curr Opin Cell Biol* 10:749-758.

Rosato, R.R. and Grant, S. 2004. Histone deacetylase inhibitors in clinical development. *Expert. Opin Investig. Drugs* 13:21-38.

Rosato, R.R., Maggio, S.C., Almenara, J.A., Payne, S.G., Atadja, P., Spiegel, S., Dent, P. and Grant, S. 2006. The histone deacetylase inhibitor LAQ824 induces human leukemia

cell death through a process involving XIAP down-regulation, oxidative injury, and the acid sphingomyelinase-dependent generation of ceramide. *Mol Pharmacol.* 69:216-225.

Rudolph, D., Yeh, W.C., Wakeham, A., Rudolph, B., Nallainathan, D., Potter, J., Elia, A.J. and Mak, T.W. 2000. Severe liver degeneration and lack of NF-kappaB activation in NEMO/IKKgamma-deficient mice. *Genes Dev* 14:854-862.

Ruefli, A.A., Ausserlechner, M.J., Bernhard, D., Sutton, V.R., Tainton, K.M., Kofler, R., Smyth, M.J. and Johnstone, R.W. 2001. The histone deacetylase inhibitor and chemotherapeutic agent suberoylanilide hydroxamic acid (SAHA) induces a cell-death pathway characterized by cleavage of Bid and production of reactive oxygen species. *Proc Natl Acad Sci U S A* 98:10833-10838.

Saccani, S. and Natoli, G. 2002. Dynamic changes in histone H3 Lys 9 methylation occurring at tightly regulated inducible inflammatory genes. *Genes Dev* 16:2219-2224.

Saccani, S., Pantano, S. and Natoli, G. 2001. Two waves of nuclear factor kappaB recruitment to target promoters. *J Exp Med.* 193:1351-1359.

Saccani, S., Pantano, S. and Natoli, G. 2002. p38-Dependent marking of inflammatory genes for increased NF-kappa B recruitment. *Nat Immunol* 3:69-75.

Saito-Ohara, F., Imoto, I., Inoue, J., Hosoi, H., Nakagawara, A., Sugimoto, T. and Inazawa, J. 2003. PPM1D is a potential target for 17q gain in neuroblastoma. *Cancer Res* 63:1876-1883.

Sakurai, H., Chiba, H., Miyoshi, H., Sugita, T. and Toriumi, W. 1999. IkappaB kinases phosphorylate NF-kappaB p65 subunit on serine 536 in the transactivation domain. *J Biol Chem* 274:30353-30356.

Sanjo, H., Takeda, K., Tsujimura, T., Ninomiya-Tsuji, J., Matsumoto, K. and Akira, S. 2003. TAB2 is essential for prevention of apoptosis in fetal liver but not for interleukin-1 signaling. *Mol Cell Biol* 23:1231-1238.

Santilli, G., Aronow, B.J. and Sala, A. 2003. Essential requirement of apolipoprotein J (clusterin) signaling for IkappaB expression and regulation of NF-kappaB activity. *J Biol Chem* 278:38214-38219.

Scherer, D.C., Brockman, J.A., Chen, Z., Maniatis, T. and Ballard, D.W. 1995. Signal-induced degradation of I kappa B alpha requires site-specific ubiquitination. *Proc Natl Acad Sci U S A* 92:11259-11263.

Sen, R. and Baltimore, D. 1986. Multiple nuclear factors interact with the immunoglobulin enhancer sequences. *Cell* 46:705-716.

Shapiro, L. and Dinarello, C.A. 1995. Osmotic regulation of cytokine synthesis in vitro. *Proc Natl Acad Sci U S A* 92:12230-12234.

Shreeram, S., Demidov, O.N., Hee, W.K., Yamaguchi, H., Onishi, N., Kek, C., Timofeev, O.N., Dudgeon, C., Fornace, A.J., Anderson, C.W., Minami, Y., Appella, E. and Bulavin, D.V. 2006. Wip1 phosphatase modulates ATM-dependent signaling pathways. *Mol Cell* 23:757-764.

Silke, J., Hawkins, C.J., Ekert, P.G., Chew, J., Day, C.L., Pakusch, M., Verhagen, A.M. and Vaux, D.L. 2002. The anti-apoptotic activity of XIAP is retained upon mutation of both the caspase 3- and caspase 9-interacting sites. *J Cell Biol* 157:115-124.

Songyang, Z., Lu, K.P., Kwon, Y.T., Tsai, L.H., Filhol, O., Cochet, C., Brickey, D.A.. Soderling, T.R., Bartleson, C., Graves, D.J., DeMaggio, A.J., Hoekstra, M.F., Blenis, J., Hunter, T. and Cantley, L.C. 1996. A structural basis for substrate specificities of protein Ser/Thr kinases: primary sequence preference of casein kinases I and II, NIMA, phosphorylase kinase, calmodulin-dependent kinase II, CDK5, and Erk1. *Mol Cell Biol* 16:6486-6493.

Steed, P.M., Tansey, M.G., Zalevsky, J., Zhukovsky, E.A., Desjarlais, J.R., Szymkowski, D.E., Abbott, C., Carmichael, D., Chan, C., Cherry, L., Cheung, P., Chirino, A.J., Chung, H.H., Doberstein, S.K., Eivazi, A., Filikov, A.V., Gao, S.X., Hubert, R.S., Hwang, M., Hyun, L., Kashi, S., Kim, A., Kim, E., Kung, J., Martinez, S.P., Muchhal, U.S., Nguyen, D.H., O'Brien, C., O'Keefe, D., Singer, K., Vafa, O., Vielmetter, J., Yoder, S.C. and

Dahiyat, B.I. 2003. Inactivation of TNF signaling by rationally designed dominant-negative TNF variants. *Science* 301:1895-1898.

Stewart, E. and Enoch, T. 1996. S-phase and DNA-damage checkpoints: a tale of two yeasts. *Curr Opin Cell Biol* 8:781-787.

Sun, J., Wiklund, F., Zheng, S.L., Chang, B., Balter, K., Li, L., Johansson, J.E., Li, G., Adami, H.O., Liu, W., Tolin, A., Turner, A.R., Meyers, D.A., Isaacs, W.B., Xu, J. and Gronberg, H. 2005. Sequence variants in Toll-like receptor gene cluster (TLR6-TLR1-TLR10) and prostate cancer risk. *J Natl Cancer Inst.* 97:525-532.

Sun, L., Stoecklin, G., Van Way, S., Hinkovska-Galcheva, V., Guo, R.F., Anderson, P. and Shanley, T.P. 2007. Tristetraprolin (TTP)-14-3-3 complex formation protects TTP from dephosphorylation by protein phosphatase 2a and stabilizes tumor necrosis factor-alpha mRNA. *J Biol Chem* 282:3766-3777.

Suzuki, H., Chiba, T., Kobayashi, M., Takeuchi, M., Suzuki, T., Ichiyama, A., Ikenoue, T., Omata, M., Furuichi, K. and Tanaka, K. 1999. IkappaBalpha ubiquitination is catalyzed by an SCF-like complex containing Skp1, cullin-1, and two F-box/WD40-repeat proteins, betaTrCP1 and betaTrCP2. *Biochem Biophys. Res Commun.* 256:127-132.

Suzuki, N., Suzuki, S., Duncan, G.S., Millar, D.G., Wada, T., Mirtsos, C., Takada, H., Wakeham, A., Itie, A., Li, S., Penninger, J.M., Wesche, H., Ohashi, P.S., Mak, T.W. and

Yeh, W.C. 2002. Severe impairment of interleukin-1 and Toll-like receptor signalling in mice lacking IRAK-4. *Nature* 416:750-756.

Takaesu, G., Surabhi, R.M., Park, K.J., Ninomiya-Tsuji, J., Matsumoto, K. and Gaynor, R.B. 2003. TAK1 is critical for IkappaB kinase-mediated activation of the NF-kappaB pathway. *J Mol Biol* 326:105-115.

Takekawa, M., Adachi, M., Nakahata, A., Nakayama, I., Itoh, F., Tsukuda, H., Taya, Y. and Imai, K. 2000. p53-inducible wip1 phosphatase mediates a negative feedback regulation of p38 MAPK-p53 signaling in response to UV radiation. *EMBO J* 19:6517-6526.

Tang, G., Minemoto, Y., Dibling, B., Purcell, N.H., Li, Z., Karin, M. and Lin, A. 2001. Inhibition of JNK activation through NF-kappaB target genes. *Nature* 414:313-317.

Tergaonkar, V., Bottero, V., Ikawa, M., Li, Q. and Verma, I.M. 2003. IkappaB kinase-independent IkappaBalpha degradation pathway: functional NF-kappaB activity and implications for cancer therapy. *Mol Cell Biol* 23:8070-8083.

Tergaonkar, V., Correa, R.G., Ikawa, M. and Verma, I.M. 2005. Distinct roles of IkappaB proteins in regulating constitutive NF-kappaB activity. *Nat Cell Biol* 7:921-923.

Tergaonkar, V. and Perkins, N.D. 2007. p53 and NF-kappaB crosstalk: IKKalpha tips the balance. *Mol Cell* 26:158-159.

Thomas-Tikhonenko, A., Viard-Leveugle, I., Dews, M., Wehrli, P., Sevignani, C., Yu, D., Ricci, S., el Deiry, W., Aronow, B., Kaya, G., Saurat, J.H. and French, L.E. 2004. Myc-transformed epithelial cells down-regulate clusterin, which inhibits their growth in vitro and carcinogenesis in vivo. *Cancer Res* 64:3126-3136.

Trougakos, I.P. and Gonos, E.S. 2002. Clusterin/apolipoprotein J in human aging and cancer. *Int. J Biochem Cell Biol* 34:1430-1448.

Ungerstedt, J.S., Sowa, Y., Xu, W.S., Shao, Y., Dokmanovic, M., Perez, G., Ngo, L., Holmgren, A., Jiang, X. and Marks, P.A. 2005. Role of thioredoxin in the response of normal and transformed cells to histone deacetylase inhibitors. *Proc Natl Acad Sci U S A* 102:673-678.

Ventura, J.J., Kennedy, N.J., Lamb, J.A., Flavell, R.A. and Davis, R.J. 2003. c-Jun NH(2)-terminal kinase is essential for the regulation of AP-1 by tumor necrosis factor. *Mol Cell Biol* 23:2871-2882.

Verhagen, A.M., Ekert, P.G., Pakusch, M., Silke, J., Connolly, L.M., Reid, G.E., Moritz, R.L., Simpson, R.J. and Vaux, D.L. 2000. Identification of DIABLO, a mammalian protein that promotes apoptosis by binding to and antagonizing IAP proteins. *Cell* 102:43-53.

Vermeulen, L., De Wilde, G., Van Damme, P., Vanden Berghe, W. and Haegeman, G. 2003. Transcriptional activation of the NF-kappaB p65 subunit by mitogen- and stress-activated protein kinase-1 (MSK1). *EMBO J* 22:1313-1324.

Vilk, G., Saulnier, R.B., St Pierre, R. and Litchfield, D.W. 1999. Inducible expression of protein kinase CK2 in mammalian cells. Evidence for functional specialization of CK2 isoforms. *J Biol Chem* 274:14406-14414.

Villunger, A., Michalak, E.M., Coultas, L., Mullauer, F., Bock, G., Ausserlechner, M.J., Adams, J.M. and Strasser, A. 2003. p53- and drug-induced apoptotic responses mediated by BH3-only proteins puma and noxa. *Science* 302:1036-1038.

Wang, C., Deng, L., Hong, M., Akkaraju, G.R., Inoue, J. and Chen, Z.J. 2001. TAK1 is a ubiquitin-dependent kinase of MKK and IKK. *Nature* 412:346-351.

Wang, D., Westerheide, S.D., Hanson, J.L. and Baldwin Jr., A.S. 2000. Tumor necrosis factor alpha-induced phosphorylation of RelA/p65 on Ser529 is controlled by casein kinase II. *J Biol Chem* 275:32592-32597.

Willis, S.N., Fletcher, J.I., Kaufmann, T., van Delft, M.F., Chen, L., Czabotar, P.E., Ierino, H., Lee, E.F., Fairlie, W.D., Bouillet, P., Strasser, A., Kluck, R.M., Adams, J.M. and Huang, D.C. 2007. Apoptosis initiated when BH3 ligands engage multiple Bcl-2 homologs, not Bax or Bak. *Science* 315:856-859.

Wu, J. and Grunstein, M. 2000. 25 years after the nucleosome model: chromatin modifications. *Trends Biochem Sci* 25:619-623.

Wyllie, A.H., Kerr, J.F. and Currie, A.R. 1980. Cell death: the significance of apoptosis. *Int. Rev Cytol.* 68:251-306.

Xiao, G., Fong, A. and Sun, S.C. 2004. Induction of p100 processing by NF-kappaB-inducing kinase involves docking IkappaB kinase alpha (IKKalpha) to p100 and IKKalpha-mediated phosphorylation. *J Biol Chem* 279:30099-30105.

Xiao, G., Harhaj, E.W. and Sun, S.C. 2001. NF-kappaB-inducing kinase regulates the processing of NF-kappaB2 p100. *Mol Cell* 7:401-409.

Xu, W., Ngo, L., Perez, G., Dokmanovic, M. and Marks, P.A. 2006. Intrinsic apoptotic and thioredoxin pathways in human prostate cancer cell response to histone deacetylase inhibitor. *Proc Natl Acad Sci U S A* 103:15540-15545.

Xu, W.S., Parmigiani, R.B. and Marks, P.A. 2007. Histone deacetylase inhibitors: molecular mechanisms of action. *Oncogene* 26:5541-5552.

Yamaguchi, H., Durell, S.R., Chatterjee, D.K., Anderson, C.W. and Appella, E. 2007. The Wip1 phosphatase PPM1D dephosphorylates SQ/TQ motifs in checkpoint substrates phosphorylated by PI3K-like kinases. *Biochemistry* 46:12594-12603.

Yamamoto, M., Yamazaki, S., Uematsu, S., Sato, S., Hemmi, H., Hoshino, K., Kaisho, T., Kuwata, H., Takeuchi, O., Takeshige, K., Saitoh, T., Yamaoka, S., Yamamoto, N., Yamamoto, S., Muta, T., Takeda, K. and Akira, S. 2004. Regulation of Toll/IL-1-receptor-mediated gene expression by the inducible nuclear protein IkappaBzeta. *Nature* 430:218-222.

Yamamoto, Y., Verma, U.N., Prajapati, S., Kwak, Y.T. and Gaynor, R.B. 2003. Histone H3 phosphorylation by IKK-alpha is critical for cytokine-induced gene expression. *Nature* 423:655-659.

Yang, C.R., Yeh, S., Leskov, K., Odegaard, E., Hsu, H.L., Chang, C., Kinsella, T.J., Chen, D.J. and Boothman, D.J. 1999. Isolation of Ku70-binding proteins (KUBs). *Nucleic Acids Res* 27:2165-2174.

Yang, J., Liu, X., Bhalla, K., Kim, C.N., Ibrado, A.M., Cai, J., Peng, T.I., Jones, D.P. and Wang, X. 1997. Prevention of apoptosis by Bcl-2: release of cytochrome c from mitochondria blocked. *Science* 275:1129-1132.

Yin, L., Laevsky, G. and Giardina, C. 2001. Butyrate suppression of colonocyte NF-kappa B activation and cellular proteasome activity. *J Biol Chem* 276:44641-44646.

Yuan, Z.L., Guan, Y.J., Chatterjee, D. and Chin, Y.E. 2005. Stat3 dimerization regulated by reversible acetylation of a single lysine residue. *Science* 307:269-273.

Zhong, H., May, M.J., Jimi, E. and Ghosh, S. 2002. The phosphorylation status of nuclear NF-kappa B determines its association with CBP/p300 or HDAC-1. *Mol Cell* 9:625-636.

Zhong, H., SuYang, H., Erdjument-Bromage, H., Tempst, P. and Ghosh, S. 1997. The transcriptional activity of NF-kappaB is regulated by the IkappaB-associated PKAc subunit through a cyclic AMP-independent mechanism. *Cell* 89:413-424.

Publication List

Silke, J., Ekert, P.G., Day, C.L., Hawkins, C.J., Baca, M., **Chew, J.**, Pakusch, M., Verhagen, A.M. and Vaux, D.L. 2001. Direct inhibition of caspase 3 is dispensable for the anti-apoptotic activity of XIAP. *EMBO J.* 20:3114-3123.

Silke, J., Hawkins, C.J., Ekert, P.G., **Chew, J.**, Day, C.L., Pakusch, M., Verhagen, A.M.and Vaux, D.L. 2002. The anti-apoptotic activity of XIAP is retained upon mutation of both the caspase 3- and caspase 9-interacting sites. *J Cell Biol.*157:115-124.

Chew, J., Biswas, S., Sheeram, S., Humaidi, M., Wong, E.T., Dhillion, M.K., Teo, H., Hazra, A., Fang, C.C., Lopez-Collazo, E., Bulavin, D.V. and Tergaonkar, V. 2009. WIP1 phosphatase is a negative regulator of NF-kappaB signaling. *Nat Cell Biol* 11:659-666. (This paper was published after the original submission of the thesis and included after the amendment of the thesis).